

**Glycomic profiles of Interferon-gamma (IFN- γ)
treated melanoma cells may indicate patient
response to immunotherapy**

Janine Sleiman



MACQUARIE
University
SYDNEY · AUSTRALIA

A thesis submitted in fulfilment of the requirements for the degree of Master of Research, in the
Department of Biomedical Sciences, Faculty of Medicine and Health Sciences, Macquarie
University.

October 2018

Declaration of originality

This work has not previously been submitted for a degree or diploma in any university. To the best of my knowledge and belief, the thesis contains no material previously published or written by another person except where due reference is made in the thesis itself.

Janine

Date: 18/10/2018

Janine Sleiman

Supervisor: Dr. Esther Lim

Co-supervisors: Prof. Helen Rizos & Prof. Nicki Packer

Student number: 43714218

Precision Cancer Therapy

Department of Biomedical Sciences

Faculty of Medicine and Health Sciences

Macquarie University

Date of submission: 18/10/2018

Acknowledgments

Firstly, I'd like to thank Prof. Helen Rizos for giving me an opportunity to work in her research group, I have always had an interest in cancer research and this group was just perfect for me. Despite being the Head of Department, and juggling so many different roles and being super busy, thank you for always making the time to meet up and always looking for ways to allow me to learn something new, I really appreciate that. I'd also like to thank everyone on the team for being so welcoming and making this a pleasant experience. To those that helped me a whole heap and those that only helped with small things, all your help was most appreciated, you know who you are. Thanks to Prof. Nicki Packer (my co-supervisor) from the Faculty of Molecular Sciences who took me on board and allowed me to discover the world of glycans. Thanks to Dr. Edward Moh who helped me immensely in learning and understanding Mass Spectrometry, an extremely complicated technique, however with your help, it was possible to (almost) master it.

I'd like to thank my mum and dad for supporting me everything I do and always being there for me from day one. You guys are the best. A BIG thanks to my sisters, Alana, Angie and Nour for always listening to me complain about all my problems, but for also keeping me sane when I was stressing out hard. Thanks to my little brother Ali, who had to deal with me saying 'no' every time he asked me to play with him because I was busy, I promise to play with you after this is finished. I love you guys.

Finally, last but not least the biggest thanks goes to Dr. Esther Lim, Esther you are the BEST supervisor anyone can ask for. You are amazing at what you do, I admire the way you instantly come up with solutions to answer any question, the graceful way you explain things and your patience and kindness. Thanks for always helping me and being patient with me when I don't understand a concept or when I'm learning a new experimental technique. Thanks for always understanding what I'm trying to say, even when I'm not quite sure how to say it and thanks for being with me every step of the way and watching this project unfold with me. Thank you. Thank you. Thank you.

Abstract

Immunotherapy has shown favourable results in prolonging survival of melanoma patients. Response to immunotherapy is partly dependent on interferon gamma (IFN- γ) a cytokine that mediates immune activity by inducing antigen presentation (i.e. HLA-ABC) and immune checkpoint molecules (i.e. programmed death ligand-1 and -2, PD-L1 and PD-L2). A recent study has shown that PD-L1 glycosylation promotes its stabilisation and immunosuppressive activity. Protein glycosylation regulates its structure, function and interaction. In this research project, we investigated the effects of IFN- γ treatment on the expression of immune activity molecules HLA-ABC, PD-L1 and PD-L2, and the level of cell surface glycosylation on 16 melanoma cell lines, using flow cytometry and liquid chromatography-mass spectrometry. We hypothesize that glycosylation profiles may influence response to immunotherapy. Our results indicated that IFN- γ induced expression of immune molecules PD-L2 and HLA-ABC on the majority of melanoma cells. This study also showed that glycosylation levels were not affected by IFN- γ treatment, however the levels of glycosylation differed between melanoma cell lines. Differences in the extent and type of glycosylation in each melanoma cell line may be associated with tumour progression and immunotherapy response.

Table of Contents

Declaration of originality	ii
Acknowledgments	iii
Abstract	iv
1. Introduction	1
1.1 Melanoma incidence and prevalence	1
1.2 Treatments for melanoma.....	2
1.3 Immune checkpoint inhibition	5
1.4 Immune checkpoint inhibitors targeting the PD-1 and PD-L1/L2 interaction	6
1.4.1 Downregulation of interferon gamma (IFN- γ) response	7
1.4.2 Loss of Major Histocompatibility Complex Class I (MHC I) expression.....	8
1.4.3 Altered expression of PD-L1 and PD-L2	9
1.5 Glycosylation	10
1.5.1 Biological role of <i>N</i> -glycosylation	10
1.5.2 <i>N</i> -glycosylation in cancer.....	11
1.6 Aims	12
2. Materials and Methods	13
2.1 Cell lines.....	13
2.2 Cell culture	13
2.3. Analysis of cell proliferation using the Incucyte Zoom live cell system.	14
2.4 Flow cytometry	15
2.4.1 Flow cytometry analysis.....	15
2.5 Determining protein concentration using the BCA assay	16
2.6 SDS-PAGE gel electrophoresis and Western blotting	16
2.7 Mass spectrometry of PNGaseF released <i>N</i> -glycans; composition and abundance in melanoma cell lines	17
2.7.1 Membrane enrichment.....	17
2.7.2 <i>N</i> -Glycan release of membrane proteins	17
2.7.3 Reduction of <i>N</i> -glycans	18
2.7.4 Desalting of reduced glycans	18
2.7.5 Carbon clean-up of glycans.....	18
2.7.6 Porous graphitised carbon-liquid chromatography- electrospray ionization-mass spectrometry (PGC-LC-ESI-MS/MS).....	18
2.7.6 Data analysis	19
3. Effects of IFN-γ on melanoma cell growth and expression of immune effector molecules	19
3.1 Introduction.....	19

3.2 Results	20
3.2.1 Selection of melanoma cell models.....	20
3.2.2 The impact of IFN- γ on melanoma cell proliferation.....	21
3.2.3 IFN- γ mediated regulation of immune cell markers.....	23
3.3 Discussion	29
4. Post-translational modifications of immune effector molecules	31
4.1 Introduction	31
4.2 Results	33
4.2.1 PD-L1 detection by western blotting.....	33
4.2.2 PD-L2 detection by western blotting.....	35
4.2.3 Effect of PNGaseF treatment on PD-L1 detection	38
4.3 Discussion	39
5. Mass spectrometry of released <i>N</i>-glycans from melanoma cells.....	43
5.1 Introduction	43
5.2 Results	44
5.2.1 Liquid Chromatography – mass spectrometry (LC-MS) spectral analysis of released glycans.....	44
5.2.2 Glycan composition and abundance of released glycans	46
5.2.3 Comparison of glycan abundance after treatment and across melanoma cell lines	48
5.3 Discussion	53
6. General Discussion & Future Directions.....	57
6.1 Conclusion.....	62
7. References	63
8. Appendix	72

1. Introduction

1.1 Melanoma incidence and prevalence

Melanoma is a disease characterised by the uncontrolled proliferation of melanocytes. Melanocytes are pigment producing cells, responsible for hair colour and skin colour. They are primarily found in the epidermis of the skin, as well as the uvea of the eye, the meninges and the inside of the ear. Melanocytes produce the pigment melanin which absorbs ultra violet B (UVB) rays to protect against UV induced damage (Li et al., 2018; Li et al., 2016; Queen, 2017). The abnormal proliferation of melanocytes upon transformation into malignant melanoma cells is due to acquired mutations induced by UV exposure (Godar et al., 2017).

Excessive UV exposure is a risk factor contributing towards the increased diagnosis of melanoma. Tanning beds, which are popular amongst young adults, utilize UV radiation to mimic the sun and result in proliferation of melanocytes putting users at risk of melanoma (Queen, 2017). The ability of UV to penetrate through windows and sunscreens also leads to UV induced damage of DNA and therefore melanoma (Godar et al., 2017). However, a decrease in vitamin D, due to increased indoor jobs, is another risk factor of melanoma, as calcitriol, a hormone involved in the Vitamin D production pathway inhibits melanoma growth (COLSTON et al., 1981; Feldman et al., 2014). Other risk factors include Human Papilloma Virus (HPV) infection, fair skin, light hair, red-hair and family history (Godar et al., 2017; Queen, 2017; Rastrelli et al., 2014).

Melanoma can metastasize to distant organs and lymph nodes, making it one of the leading causes of deaths among individuals of all ages, especially young adults (Hyde, 2017). It is more prevalent in men than women, with men having an increased 1.5 chance of developing melanoma compared to women (Arrangoiz et al., 2016). Age and gender also play a role, as women under forty years of age are more likely to develop melanoma, with the highest incidence rate occurring in women aged 25 to 29 years old. Males, on the other hand, are more likely to get melanoma if they are aged over 40, with 65 being the age group with the highest incidence rate (Arrangoiz et al., 2016; Erickson and Driscoll, 2010). Unlike other highly prevalent cancers, the incidence of melanoma is still increasing rather than decreasing over time (Geller et al., 2015). Although melanoma only accounts for 4% of all skin cancers, it is responsible for 75% of skin cancer related deaths (Arrangoiz et al., 2016). Australia and New Zealand have the highest melanoma incidence, with New Zealand having the highest skin cancer related death rate, followed by Australia (Goyal and Jain, 2018). It is estimated that out of the 14,320 Australians that will be diagnosed with melanoma in 2018 there will be approximately 1,905 deaths (Cancer Australia, 2017).

1.2 Treatments for melanoma

There are a variety of treatments available for melanoma patients, with surgery being one of the oldest approaches, involving the excision of the tumour mass. The most well-known surgical technique is known as Mohs micrographic surgery; this technique involves microscopic observation of the tumour during surgery to ensure that all involved tissues are removed, thus leaving no traces of the tumour to limit the chance of recurrence. This treatment has been used for many years and often results in good prognosis with increased survival rates for cutaneous melanoma (Zitelli et al., 1997). However, this treatment is limited to patients with early stage disease as it is much more difficult to treat melanoma after it has metastasized to multiple organs.

Compared to patients with early stage disease (stage I-II), patients with advanced metastatic melanoma (stage IV) have a poor prognosis, with less than 12 months median survival rate (Marzuka et al., 2015). Chemotherapy and radiotherapy were previously used as conventional treatments for melanoma, but melanoma patients treated with the most common forms of chemotherapy including carboplatin, dacarbazine and paclitaxel had low response rates with no effects on the overall median survival rates compared to untreated patients (Elliott et al., 2017; Marzuka et al., 2015).

Radiotherapy, another well-known therapy, works by exposing the area affected by the tumour to radiation, which damages the DNA to cause cell death (Escorcía et al., 2017). Radiotherapy is most commonly used to treat melanoma brain metastasis, and is often paired with surgery, and increases the overall survival from approximately 3 months with radiotherapy alone to around 9 months when paired with surgery (Ajithkumar et al., 2015; Fonkem et al., 2012; Franceschini et al., 2016). Recent studies have also shown that radiotherapy activates the immune system by increasing recruitment of CD8⁺ T-cells and upregulating major histocompatibility (MHC) class I protein expression, which lead to anti-tumour responses (Kroon et al., 2016). Thus, combination of radiotherapy with immunotherapy has shown improved patient outcomes, with median overall survival increasing to 19 months and median progression free survival increasing to 5 months (Koller et al., 2017).

The idea of harnessing the immune system to combat cancer as a form of therapy was first proposed by William Coley in 1893 (Coley, 1893) however, this proposal was largely ignored because conventional treatments such as chemotherapy and radiotherapy were more common (Sharma et al., 2017). It wasn't until early 2000s that immunotherapy and targeted therapy started gaining interest, and today, these two types of treatments have shown outstanding results in improving melanoma patient survival (Elliott et al., 2017).

Treatment with targeted therapies produced a 13.6-month median overall survival, which is a significant increase compared to treatment with chemotherapy that had a median overall survival of 9.7 months (Table 1). Targeted therapies in melanoma are drugs that selectively bind to kinases, to suppress oncogenic signalling pathways, such as the mitogen-activated protein kinase (MAPK) pathway. Activation of the MAPK pathway promotes melanoma cell proliferation, survival and metastasis (Dhomen and Marais, 2009). Around 70% of melanomas show activating mutations affecting the BRAF kinase or NRAS GTPase, which promote the constitutive activation of the MAPK pathway (Davies et al., 2002; Gray-Schopfer et al., 2007). The most common mutation in melanoma is the *BRAF*^{V600E}; this is an activating mutation that induces the phosphorylation and activity of the downstream kinase MEK1/2 and ERK1/2. Activation of this MAPK cascade enhances the proliferative activity of melanoma cells (Konieczkowski et al., 2014). Selective inhibitors of mutant *BRAF* including vemurafenib and dabrafenib have improved the progression-free and overall survival of patients with advanced *BRAF*-mutant melanoma (Maio et al., 2015).

Another targeted treatment is trametinib, which targets the downstream kinase MEK1/2 (Maio et al., 2015). Combination BRAF and MEK inhibition produces response in around 80% of patients, but most patients will develop resistance and progress within the first year of therapy (Chapman et al., 2011; Flaherty et al., 2012; Konieczkowski et al., 2014).

Immunotherapy in the form of immune checkpoint inhibitors was first approved for the treatment of advanced melanoma in 2011, and these inhibitors include ipilimumab, pembrolizumab and nivolumab (Michielin and Hoeller, 2015). The mechanism of action and effects of these treatments on melanoma are described in more detail in the subsequent section.

Table 1: Types of melanoma treatments

	Chemotherapy	Targeted therapy	Immunotherapy	Surgery
Mechanism of action	Targets and kills fast-growing cells in the body (Michielin and Hoeller, 2015).	Targets and inhibits signaling pathways, specifically the MAPK pathway (Elliott et al., 2017).	Activates anti-tumour immune response by targeting immune inhibitory checkpoints (Maio et al., 2015).	Excision of tumour. Often performed when melanoma is localised or after loco-regional recurrence (Veness et al., 2005).
Median overall 5-year survival (months)	9.7 months (for dacarbazine) (Marzuka et al., 2015).	13.6 months (for vemurafenib) (Marzuka et al., 2015).	10.1 months (for ipilimumab) (Michielin and Hoeller, 2015).	93% using Mohs micrographic surgery. ^a (Zitelli et al., 1997)
Median Progression free survival (months)	1.6 months (for dacarbazine) (Marzuka et al., 2015).	6.8 months (for vemurafenib) (Marzuka et al., 2015).	2.9 months (for ipilimumab) (Michielin and Hoeller, 2015).	8 months (Veness et al., 2005).
Common side effects	Nausea, vomiting, fatigue, neutropenia (Marzuka et al., 2015).	Arthralgia, rash, photosensitivity, fatigue, alopecia (Marzuka et al., 2015).	Colitis, endocrinopathies, pneumonitis, immune-related adverse events (Marzuka et al., 2015).	Wound pain, however wound heals overtime (Zitelli et al., 1997).
Commonly used therapeutic agents.	Carboplatin, Dacarbazine, Paclitaxel (Maio et al., 2015).	Vemurafenib, Trametinib, Dabrafenib (Maio et al., 2015).	Ipilimumab, Pembrolizumab, Nivolumab (Michielin and Hoeller, 2015).	-

^aResult corresponds to early stage disease whilst the others were treating late stage patients, therefore making comparison not equal (Zitelli et al., 1997).

1.3 Immune checkpoint inhibition

The main role of the immune system is to identify and fight against microbial infections and other foreign pathogens within the host (Abbas et al., 2014). To regulate the extent and duration of the immune response, the adaptive immune system utilizes multiple receptors known as immune checkpoints. These immune checkpoints can either be co-stimulatory, sending activation signals when bound to their respective ligands, or co-inhibitory, sending inhibitory or suppressive signals upon ligand binding (Hamanishi et al., 2007). For example, binding of CD28 receptor expressed on CD4+ and CD8+ T-cells to the B7-1 and B7-2 proteins found on antigen presenting cells is a co-stimulatory response (Marzuka et al., 2015). This stimulus is important as it enables the complete activation of naive T-cells, allowing them to grow and survive, until they are ready to initiate an immune response (Chen and Flies, 2013).

On the other hand, interaction between the programmed death receptor 1 (PD-1) and the cytotoxic T lymphocyte-associated protein 4 (CTLA4) on T-cells with their respective ligands, programmed death ligand 1 or 2 (PD-L1 or PD-L2), and B7-1 or B7-2, illicit an immune-suppressive response by sending inhibitory signals to dampen T-cell activity (Marzuka et al., 2015). This helps maintain and regulate self-tolerance and prevents excessive stimulation or overactivation of the immune response. However, tumour cells have been shown to express the PD-L1 and PD-L2 ligands in order to suppress immune response and evade immune attack (Hamanishi et al., 2007; Ma et al., 2016; Marzuka et al., 2015).

Many monoclonal antibodies have been developed to block the inhibitory interaction between PD-L1 and PD-L2 with the PD-1 receptor on T-cells. These antibodies, known as immune checkpoint inhibitors, include anti-CTLA-4, anti-PD-L1 and anti-PD-1 antibodies. Use of immune checkpoint inhibitors have been tested in many clinical trials and have revolutionised the treatment of advanced melanoma (Marzuka et al., 2015). Table 2 shows a summary of the three commonly used immune checkpoint inhibitors, ipilimumab (anti-CTLA-4), pembrolizumab (anti-PD-1), and nivolumab (anti-PD-1).

Although these drugs have shown positive outcomes, Table 2 also highlights the low response rates of these drugs. There is now interest in combining these checkpoint inhibitors in order to improve response rates, but combination treatments often lead to increased toxicities. For example, when nivolumab is administered alone, 11.7% of patients experienced treatment-associated toxicities and a 3.7 months progression free survival (Table 2). In contrast, when nivolumab is combined with ipilimumab, toxicity rate increased to 55% and progression free survival increased to 11.5 months (Larkin et al., 2015). Combination therapy is still being investigated as it produces

best patient outcomes, and interest is now focused on selecting the patients that require combination treatment (Robert et al., 2015a).

Table 2: Summary of three immune checkpoint inhibitors used as monotherapy and their effects.

Agent	Target	Overall response rate	Median PFS (months)	Median OS (months)	Grade 3 to 4 toxicity
Ipilimumab (Phase III)	CTLA-4 (Michielin and Hoeller, 2015)	11% (Michielin and Hoeller, 2015)	2.9 (Michielin and Hoeller, 2015)	10.1 (Michielin and Hoeller, 2015)	20% (Robert et al., 2015b)
Pembrolizumab (Phase III)	PD-1 (Michielin and Hoeller, 2015)	36% (Robert et al., 2015b)	4.1 (Robert et al., 2015b)	-	17% (Robert et al., 2015b)
Nivolumab (Phase III)	PD-1 (Larkin et al., 2017)	27% (Larkin et al., 2017)	3.1 (Larkin et al., 2017)	16 (Larkin et al., 2017)	11.7% (Robert et al., 2015a)

1.4 Immune checkpoint inhibitors targeting the PD-1 and PD-L1/L2 interaction

PD-L1 and PD-L2 ligands which bind to the PD-1 receptor, typically play an important role in immune homeostasis, by preventing excessive immune activation and auto-immune attack. PD-1 is expressed on the majority of T-cells including CD4+, CD8+ and natural killer T-cells and functions to prevent auto-immune attack when bound to its ligands PD-L1 and PD-L2 (Sharpe et al., 2007). However, in the context of cancer, PD-L1 and PD-L2 are over expressed by tumour cells to suppress T-cell activity and evade immune defence (Figure 1) (Hamanishi et al., 2007). In a study by Hino et. al (2010), it was found that patients with higher stage of melanoma had higher levels of PD-1 expression on CD8+ and CD4+ cells compared to the levels found on healthy individuals (Hino et al., 2010). This suggests that cancer progression is directly correlated with increased PD-1 expression.

Blocking of the PD-1 receptor on T-cells using the anti-PD-1 antibodies nivolumab and pembrolizumab mitigate the suppressive effects. Although PD-1 blockade has shown success in extending the life of patients, only 40% of patients will respond initially to treatment (innate resistance) (Postow et al., 2015; Sharma et al., 2017), and acquired resistance, whereby patients progress on treatment after an initial response, is also emerging (Zaretsky et al., 2016). Several

mechanisms of resistance to PD-1 inhibition have been identified, including downregulation of interferon gamma (IFN- γ) response, altered expression of PD-L1 and PD-L2, and loss of MHC class I expression (Zaretsky et al., 2016).

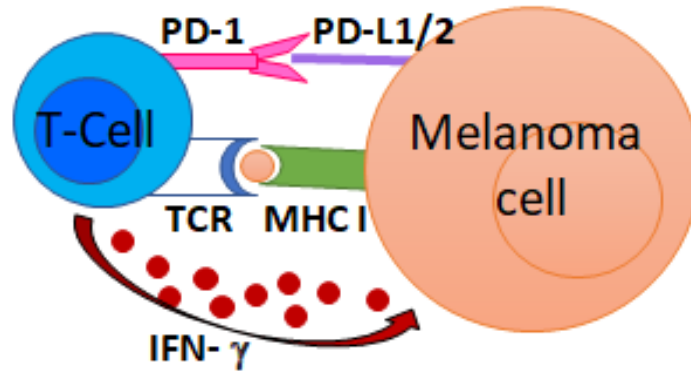


Figure 1. Simplified diagram of T-cell interaction with a melanoma cell. Major histocompatibility complex I (MHC I) on the surface of the melanoma cell presents the antigen, which is recognised by the T-cell receptor (TCR) on the T-cell. This leads to production of the IFN- γ cytokine, which is required for immune response regulation. However, IFN- γ also induces expression of PD-L1 and PD-L2 on the melanoma cell, which bind to the programmed cell death-1 (PD-1) receptor on T-cells. Once bound, this suppresses T-cell activity and as a result, dampens the anti-tumour immune response (Sharma et al., 2017).

1.4.1 Downregulation of interferon gamma (IFN- γ) response

Interferon gamma (IFN- γ), also known as interferon type II, is a cytokine produced by CD8⁺ T-cells, CD4⁺ helper T-cells and natural killer cells (Young and Hardy, 1995). It plays an important role in immunity as it is involved in regulating immune and inflammatory responses. For example, IFN- γ is produced and released by CD8⁺ T-cells upon cell activation, triggered by T-cell receptor binding to antigen presenting MHC class I receptor. IFN- γ directly binds to the IFN- γ receptor 1 (IFNGR1), which then recruits IFNGR2 subunits (Garcia-Diaz et al., 2017). The dimerization of the interferon receptor allows the Janus kinase (JAK) 1 and 2 kinases to phosphorylate the receptor and the downstream signal transducer and activator of transcription (STAT) 1 and 3 in order to initiate STAT-mediated transcription of genes containing the gamma activated sequence (GAS) (Garcia-Diaz et al., 2017; Gough et al., 2008). This signalling cascade leads to the transcription of immune regulatory factors including the major histocompatibility complex (MHC) molecules such as HLA-ABC that display peptide fragments for recognition by immune cells (Parker et al., 2016; Sharma et al., 2017) (Figure 2). Consequently, IFN- γ also upregulates expression of PD-L1 or PD-L2 on the tumour cells in order to evade the immune system (Shin et al., 2017).

However, mutations in the interferon pathway abolish anti-tumour responses and can contribute to resistance to immunotherapy (Zaretsky et al., 2016). Inactivating mutations in the JAK1 and

JAK2 genes, or in beta 2-microglobulin (B2M) (structural component of HLA-ABC) cause resistance to PD-1 blockade therapy in melanoma (Shin et al., 2017; Zaretsky et al., 2016). Thus efficacy of PD-1 inhibitors relies on an intact IFN- γ signalling pathway and functional antigen presentation machinery (Garcia-Diaz et al., 2017).

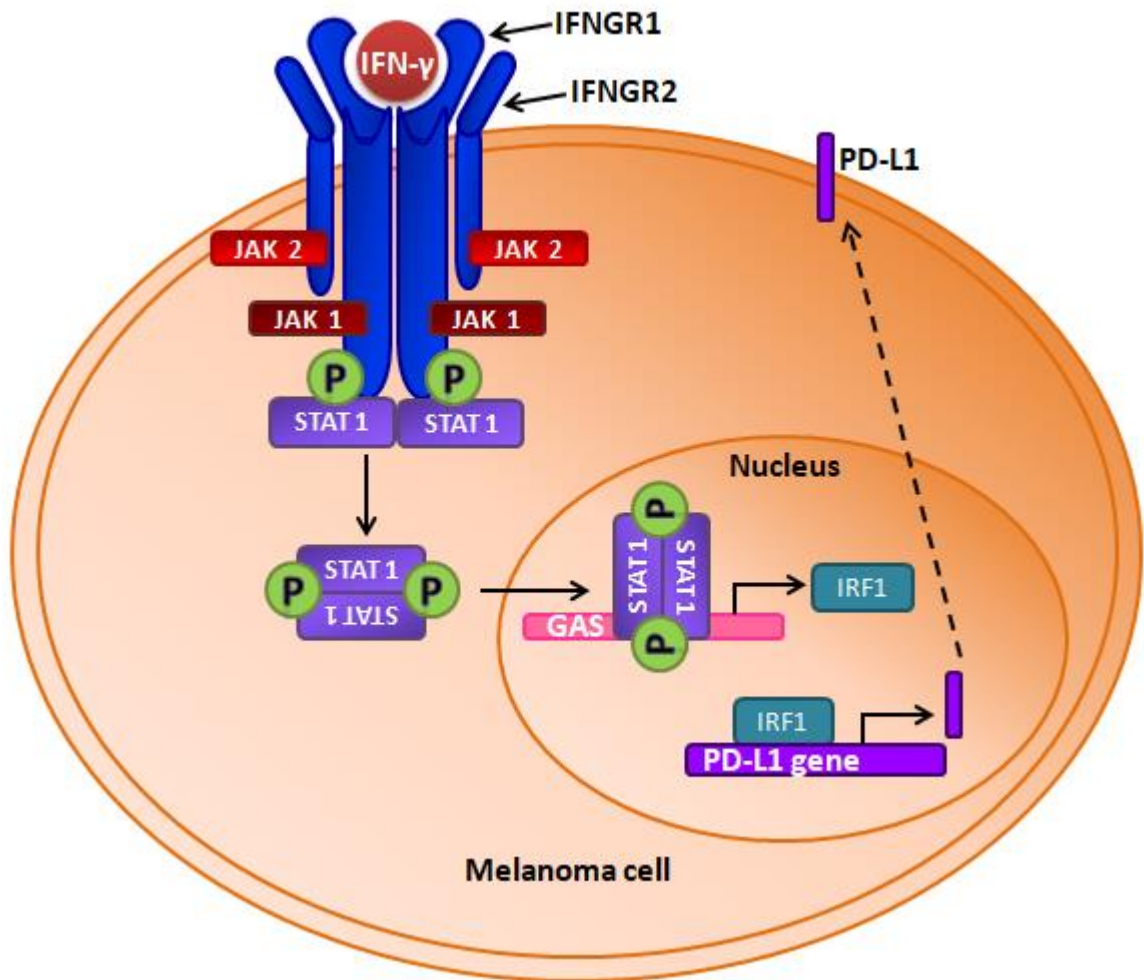


Figure 2. JAK/STAT pathway induced by IFN- γ . The binding of IFN- γ to its receptor IFNGR1 occurs extracellularly and recruits IFNGR2 causing dimerisation. This configuration allows JAK 1 and 2 to auto-phosphorylate following phosphorylation of the receptor. The signal transducer and activator of transcription (STAT1) are then phosphorylated forming a homodimer, and dissociate from IFNGR1 in an antiparallel arrangement. This STAT complex enters the nucleus of the cell via nuclear translocation and binds to gamma activated sequence (GAS) elements which initiate transcription of factors such as interferon regulatory factor (IRF-1). IRF-1 then leads to transcription of other regulatory genes such as PD-L1, PD-L2 and MHC (Garcia-Diaz et al., 2017; Gough et al., 2008; Johnson et al., 2013; Zaidi and Merlino, 2011).

1.4.2 Loss of Major Histocompatibility Complex Class I (MHC I) expression

MHC Class I molecules are expressed on the surface of all epithelial cells and function to present antigens for T-cell recognition (Rock et al., 2016). In humans, the MHC class I genes encode the main types of MHC classes called human leukocyte antigens (HLA), the most common comprising of HLA-A, HLA-B and HLA-C (Rossjohn et al., 2015). The MHC class I complex is comprised of β 2 microglobulin (β 2m) and α microglobulins. The α 3 microglobulin is

noncovalently bound to $\beta 2m$, which is further connected to 2 antiparallel alpha helices microglobulins, $\alpha 1$ and $\alpha 2$ (Saper et al., 1991). The $\alpha 1$ and $\alpha 2$ proteins form a groove which acts as the peptide binding site. The antigenic peptide is usually made up of around 8–12 amino acids, and is presented to the CD8+ T-cell (Figure 3) (Cole et al., 2007; Pamer and Cresswell, 1998). The T-cell receptor, also called the $\alpha\beta$ TCR, due to the α and β chains, has a strong affinity for the MHC protein complex as it has complementarity-determining regions 1, 2 and 3 which interact with the MHC to send a signal cascade needed to elicit an immune response (Adams et al., 2016; Rossjohn et al., 2015).

However, loss of the MHC class I protein or change in the protein structure can prevent the T-cell receptor from properly binding, thus not sending a signal or eliciting an immune response. Loss of MHC class I expression has been found in tumours of patients with acquired resistance to immune checkpoint blockade, and has been proposed as a way of escaping immune recognition (Cabrera et al., 2003). The downregulation of HLA has been attributed to mutations on HLA-A or HLA-B alleles or mutations in specific domains such as $\beta 2m$, which has been reported in melanoma cells (Garrido and Algarra, 2001).

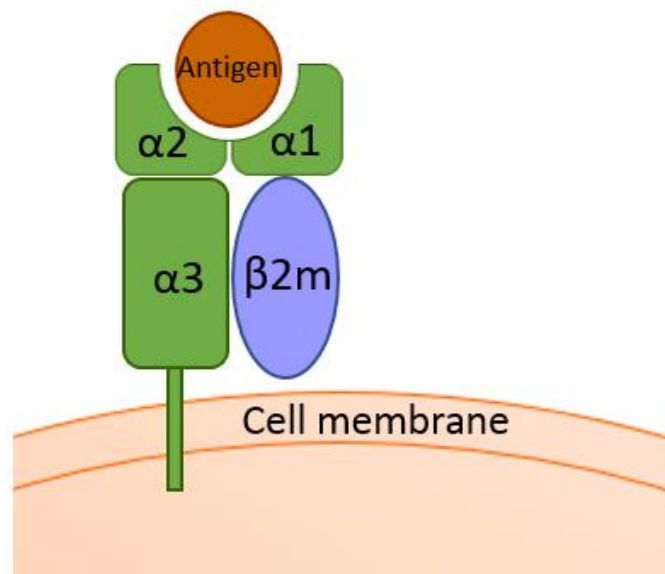


Figure 3. The Major Histocompatibility Complex Class I protein. $\beta 2$ microglobulin ($\beta 2m$), $\alpha 3$ protein and two antiparallel alpha helices, $\alpha 1$ and $\alpha 2$ make up the MHC class I complex which is required for T-cell receptor binding. The groove between $\alpha 1$ and $\alpha 2$ forms the peptide binding site which presents the antigen to the CD8+ T-cell (Cole et al., 2007).

1.4.3 Altered expression of PD-L1 and PD-L2

PD-L1 also known as B7-H1, is found on T-cells and B cells, mast cells, macrophages and dendritic cells. It is also found on many different types of cells, such as pancreatic islet-cells, hepatocytes, brain astrocytes, vascular endothelial cells, cells in the placenta, epithelial cells,

muscle cells, mesenchymal stem cells and eye cells (Patel and Kurzrock, 2015; Sharpe et al., 2007). PD-L1 expression, which leads to immune evasion when bound to PD-1, is also expressed in melanoma, ovarian cancer, colorectal cancer, renal cell carcinoma, and non-small cell lung cancer (Patel and Kurzrock, 2015).

Although immune checkpoint therapies blocking PD-L1 or PD-1 have shown positive results in patients with different types of cancer, it was initially reported that patients with PD-L1 overexpression have poorer prognosis (Hamanishi et al., 2007; Hino et al., 2010; Patel and Kurzrock, 2015; Thompson et al., 2006). However, more recent findings suggest that cancer cells treated with anti PD-L1 therapy or anti-PD-1 therapy have a better response when expression of PD-L1 is high (Topalian et al., 2015). In a clinical trial using nivolumab, the response rate for patients with a higher expression of PD-L1 was 44% compared to the 17% response rate in patients with low expression. The overall survival was 21.1 months, and the progression-free survival was 9.1 months in PD-L1 high patients compared to 12.5 months and 2 months in patients with PD-L1 negative tumours i.e. have low PD-L1 expression (Grosso et al., 2013; Patel and Kurzrock, 2015). The correlation of high PD-L1 expression and better treatment results was also found using other PD-1/PD-L1 targeting agents, such as pembrolizumab (Kefford et al., 2014) and ipilimumab (Wolchok et al., 2013). However, PD-L1 levels cannot be used as a predictive biomarker of therapy, as the levels of PD-L1 range from 45% to 75% (Patel and Kurzrock, 2015), and while majority of patients do benefit, patients with low PD-L1 still show anti-tumour activity when treated with PD-1 inhibitors (Kefford et al., 2014).

PD-L2 also known as B7-DC, is another ligand for the PD-1 receptor, and similar to PD-L1, when bound to its receptor, PD-L2 also decreases T-cell activity by sending inhibitory signals (Hino et al., 2010). Unlike PD-L1, PD-L2 is not expressed on a large variety of cells and is mainly found on mast-cells, dendritic cells and macrophages (Patel and Kurzrock, 2015). Expression of PD-L1 and PD-L2 is induced by IFN- γ , however PD-L2 is also induced by interleukin 4 (IL-4) (Topalian et al., 2015). PD-L2 binding to the PD-1 receptor and the ensuing suppressive activity was only identified in 2001 (Latchman et al., 2001). Therefore, PD-L2 is not as well researched or understood and is a topic of interest for this project.

1.5 Glycosylation

1.5.1 Biological role of *N*-glycosylation

N-glycosylation is a post translational modification that modulates protein interactions, structure, function, folding, expression and trafficking (Li et al., 2018; Li et al., 2016). The importance of *N*-glycans depends on the biological environment of the glycan as a range of glycans

can be found in a range of different tissues (Varki and Lowe, 2009). All *N*-glycans have a common core consisting of sugars in a particular sequence; this sequence contains three mannose sugar residues, attached to two *N*-Acetylglucosamine (GlcNAc) sugar residues which is attach to the protein. The sugar residues are attached to the amide nitrogen present on an asparagine (Asn) side chain in an Asparagine-X-Serine/Threonine sequence on the protein, where the 'X' residue cannot be a proline (Cheung and Reithmeier, 2007; Wang, 2005). Other sugars bind to the ends of the mannose residues, and these include addition of more mannose structures thus forming an oligomannose type *N*-glycan (oligomannose), or addition of deoxyhexose, *N*-Acetyl-neuraminic Acid (NeuAc) or antennary *N*-acetylhexoseamine (HexNAc) to form more complex structures (Stanley et al., 2009).

The biosynthesis of these sugars occurs with the aid of glycotransferases, glycan building enzymes, and the sugars are then modified by glycosidases, sugar degrading enzymes. This process and the attachment and degradation of the glycans to the protein occur in the endoplasmic reticulum (Stanley et al., 2009). These complexes then move to the Golgi apparatus where they are further modified, thus conferring a range of *N*-glycans structures on proteins (Hang et al., 2015).

1.5.2 *N*-glycosylation in cancer

Altered expression of *N*-glycans have been associated with tumour proliferation and metastasis (Christiansen et al., 2014). This could be attributed to defective enzyme activity and transcription of genes involved in glycosylation, thus affecting the cell surface *N*-glycans structure and abundance, and causing signal alterations which lead to tumour proliferation (Christiansen et al., 2014; Pocheć et al., 2003).

N-glycans found on cancer cells are often mutated or have specific characteristics. For example *N*-glycans display more glycan branches or undergo altered processing during the modification process (Zhao et al., 2008), or have higher levels of a specific glycan such as deoxyhexose, which has been found to be elevated in a range of cancers (Guo et al., 2018; Miyoshi et al., 2008). Expression of these *N*-glycans on tumour tissues have been a point of interest for investigating glycan biomarkers or potential drug targets (Christiansen et al., 2014).

Although failure to respond to immune checkpoint inhibitors has been attributed, in a subset of patients, to altered expression of PD-L1, PD-L2 and/or HLA-ABC (Sharma et al., 2017), recent studies have also shown that post-translational modifications of PD-L1 and PD-L2 may affect immunotherapy response (Li et al., 2018). A recent study by Li et al (2016) showed that PD-L1 on cancer cells is *N*-glycosylated (Li et al., 2016). Li et al. (2016) reported that the glycosylation

of PD-L1 confers higher protein stability compared to unglycosylated PD-L1 which is rapidly degraded. It has been proposed that the glycogen synthase kinase 3b (GSK3b) which induces protein degradation, cannot interact with glycosylated PD-L1, therefore preventing protein degradation and in turn stabilizing PD-L1 (Li et al., 2018; Li et al., 2016). Cells that express non-glycosylated PD-L1 are more sensitive to activated T-cells and have a higher apoptosis rate. In contrast, cells expressing glycosylated PD-L1 are less sensitive to cytotoxic T-cell killing, and are associated with reduced CD8⁺ T-cell numbers and decreased IFN- γ expression (Li et al., 2016).

1.6 Aims

Although immune checkpoint blockade has shown promising results benefitting around 40% of patients with advanced melanoma, there are some patients who do not respond to this treatment. Failure to respond to immune checkpoint inhibitors has been attributed to loss of the MHC class I protein or change in the protein structure, such as mutations affecting HLA-A, HLA-B or β 2m expression (Cabrera et al., 2003; Garrido and Algarra, 2001), and altered expression of PD-L1 and PD-L2. Moreover, due to the heterogeneous nature of cancer cells, not all cancer cells will express or induce these molecules in a similar manner (Sharma et al., 2017). Therefore, the first aim of this project is to explore the expression of HLA-ABC and PD-L2, at baseline and following IFN- γ treatment, in a panel of melanoma cell lines derived from patients who failed immune checkpoint inhibitor therapy.

Response to immune checkpoint inhibitors may also be affected by glycosylation of proteins on cancer cells. A recent study showed that glycosylation of PD-L1 promotes its stability (Li et al., 2016). Therefore, our second aim is to investigate post-translational modification of PD-L1 and PD-L2 in the melanoma cell lines. Because the type and extent of protein glycosylation may influence response to PD-1 inhibition, our third aim is to investigate the glycosylation profiles of the melanoma cell lines at baseline and following IFN- γ treatment. By doing this study and further understanding how glycans play a role in tumour immunity, it opens up the possibility of elucidating novel biomarkers and development of improved immunotherapies to help increase patient response rate and prevent resistance and recurrence.

2. Materials and Methods

2.1 Cell lines

A total of 16 short-term melanoma cell lines (referred to as PD-1 PROG cells) were included in this study. The PD-1 PROG cell lines were derived from surgically excised, enzymatically-processed melanoma lesions of patients who have failed immunotherapy. These patients had unresectable stage III and IV melanoma and were treated with either anti-PD-1 monotherapy (pembrolizumab or nivolumab), or anti-PD-1 in combination with anti-CTLA-4 (ipilimumab) according to the schedule in the NCT02374242, NCT02089685, NCT02905266, NCT02599402, NCT02714218 and NCT02977052 clinical trials. Written consent was obtained from all patients under approved Human Research Ethics Committee protocols from the Royal Prince Alfred Hospital (Protocol X15-0454 & HREC/11/RPAH/444). Cell line name, biopsy date and mutation status are summarised in Table 3.

2.2 Cell culture

Melanoma cells were cultured in Dulbecco's Modified Eagle Medium (DMEM) (Gibco, Thermo Fisher Scientific, Waltham, MA) supplemented with 10% fetal bovine serum (FBS; Sigma-Aldrich, St Louis, MO), 11.25 mM glutamine (Gibco, Thermo Fisher Scientific, Waltham, MA) and 10 mM HEPES (Gibco, Thermo Fisher Scientific, Waltham, MA) and incubated at 37°C in 5% CO₂. Each of the 16 melanoma cell lines were treated with 1000 U/ml IFN- γ (Peprotech, Rocky Hill, NJ) or with 0.1% bovine serum albumin (BSA) as the control, for 24 hours at 37°C and 5% CO₂ conditions in T75 flasks seeded with 1x10⁵ cells. The following day, cells were washed in pre-warmed PBS, trypsinised and collected by centrifugation at 1,200 rpm for 5 min for flow cytometry analysis. The experiment for each cell line was repeated three times to obtain biological triplicates. For liquid chromatography-mass spectrometry (LC-MS) and western blotting, cells were treated as described above, except that cell harvesting was performed by incubating cells with 2 mM EDTA for 10 min, the cells were collected and the EDTA treatment repeated followed by gentle scraping to retrieve any remaining adhered cells. The collected cells were centrifuged at 1,200 rpm for 5 min and each cell pellet stored at -80°C for western blotting and mass spectrometry (MS) analysis. Figure 4 illustrates the workflow used for each cell line in this thesis.

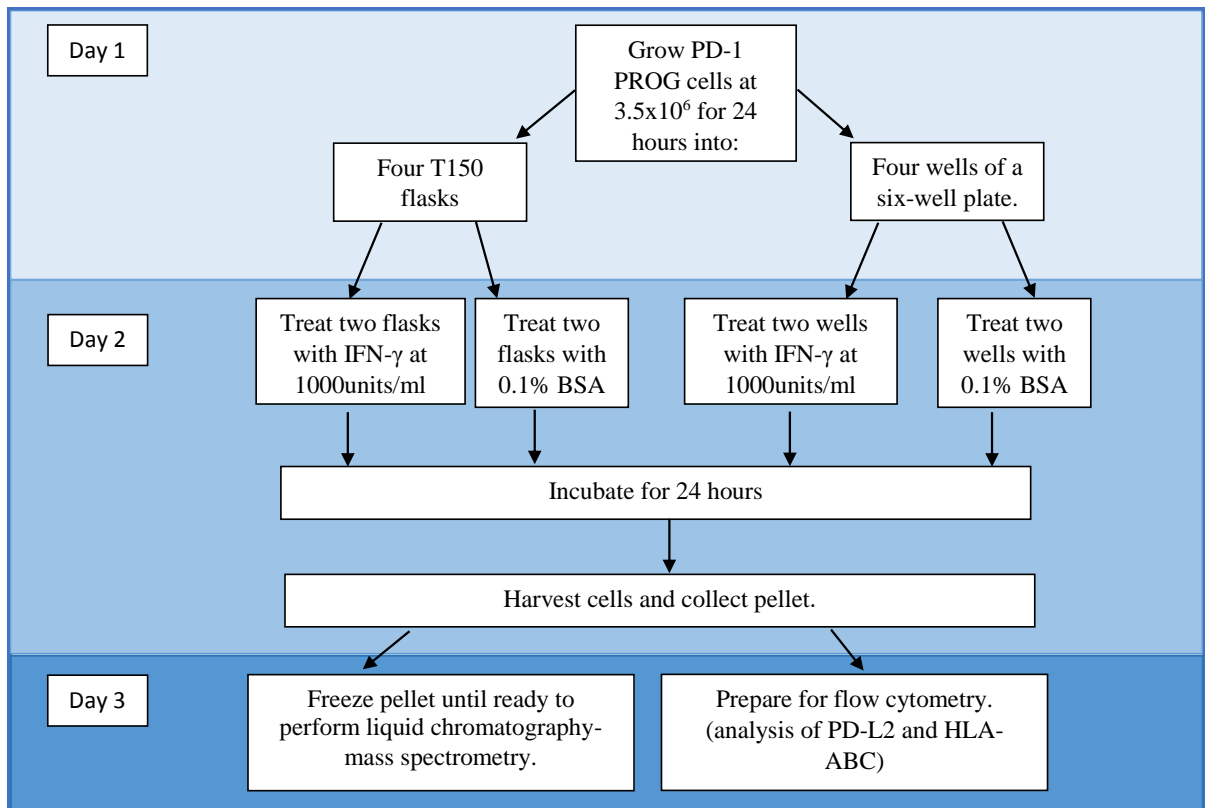


Figure 4. Simplified diagram of the study workflow. Flow diagram showing cell analysis process. Three biological repeats experiments were performed for each cell line.

2.3. Analysis of cell proliferation using the Incucyte Zoom live cell system.

To determine the effect of IFN- γ on cell growth, cells were cultured in the same conditions as described in section 2.2, in DMEM supplemented with 10% FBS, 11.25 mM glutamine and 10 mM HEPES and incubated at 37°C in 5% CO₂. The following day, cells were trypsinised, counted, and 2.5x10⁵ cells/well seeded in a Corning Costar 96-well cell culture plate (MERK, Darmstadt, Germany), with IFN- γ or 0.1% BSA as the control for 24 hours. Four wells were prepared for each condition, and each cell line was repeated for a total of three times. The 96-well cell culture plate was placed in an Incucyte Zoom live cell analysis system (Essen Bioscience, Michigan, USA) at 37°C for 72 hours, images of each well were taken every 4 hours to monitor growth. Images of the cells were masked using the processing definition on the Incucyte ZOOM software; parameters were set at 1.3 for background correction and 400 μ m for minimum area. Percentage of phase object confluence was calculated to determine the area occupied by the cells as a measure of cell confluence (Figure 5). Percentage confluence for each cell lines was plotted over time in the GraphPad Prism software to generate a growth curve (Figure 6).

2.4 Flow cytometry

Melanoma cells collected after treatment (described in section 2.2) were resuspended in PBS and counted using a haemocytometer. For each sample, the control (0.1% BSA treated) cells and IFN- γ treated cells (2×10^5 cells in 100 μ l PBS) were added into each well of a 96 well plate in duplicates (two wells for controls and two wells for IFN- γ treatment). One control and one IFN- γ treatment well was stained with 100 μ l PD-L2-APC antibody (Clone 24F.10C12; 1:50 dilution) (BioLegend, San Diego, CA), and 100 μ l HLA-ABC-PE (Clone W6/32; 1:100 dilution) (BioLegend) with Fc block buffer (BD Biosciences, Franklin Lakes, NJ) at a 1:400 dilution to prevent non-specific binding of the antibodies to the Fc receptors. The remaining wells (one well for control and one well for IFN- γ treated) were left unstained. Cells were incubated for 30 min on ice then washed twice with 170 μ l FACS wash (5% FCS in PBS, with 10 μ l EDTA and 0.05% sodium azide) to remove any unbound antibodies, then centrifuging the sample at 1,500 rpm for 4 min. Cells were then transferred into flow cytometry tubes and 5 mM DAPI (Invitrogen, Thermo Fisher Scientific) was added to each sample to determine cell viability.

Stained cells were acquired using the BD LSRFortessa X20 flow cytometer (BD Biosciences) used alongside with the FACSDiva software (BD Biosciences), and 10,000 live events were acquired and recorded for each sample.

2.4.1 Flow cytometry analysis

Data was analysed using the FlowJo software (TreeStar, Ashland, OR). Cells were gated around the main population based on forward and side scatter area (FSC-A and SSC-A), viable cells were identified using DAPI, and single cells were selected using FSC-A against forward scatter height (FSC-H).

The geometric mean fluorescence intensity (MFI) for each sample was obtained from FlowJo analysis, and the control stained MFI was divided by the control unstained MFI to obtain the baseline fold change for HLA-ABC and PD-L2. The same was done for the IFN- γ treated stained and unstained samples. The fold change MFI values were then divided against each other (IFN- γ fold change/baseline fold change) to determine the level of IFN- γ induction of HLA-ABC or PD-L2. The mean MFI was calculated from three biological replicates and cell lines with mean MFI value lower than 1.5 were considered to have no expression or induction of PD-L2 or HLA-ABC.

2.5 Determining protein concentration using the BCA assay

Cell pellets (obtained as described in section 2.2) were lysed on ice in radioimmunoprecipitation assay (RIPA) lysis buffer containing protease inhibitors and phosphatase inhibitors (Roche, Basel, Switzerland). The extracted total cellular proteins were quantified by a bicinchoninic acid assay (BCA) using a Bio-Rad Protein Assay Kit (BioRad DC, Hercules, CA, USA). Bovine serum albumin was used as a standard to create a standard curve, and samples were diluted at 1:5 or 1:10 in PBS before adding 100 μ l to each well of a 96 well plate, each sample was performed in triplicates. As per manufacturer's instructions (Bio-Rad), 20 μ l of reagent S was prepared for every 1 ml of reagent A, and 25 μ l of this mixture was added to each well. Samples were then incubated with 200 μ l of reagent B (Bio-Rad) for 15 min. After 15 min the absorbance was read on the PHERAstar FS microplate reader (BMG-LABTECH, Guelph, ON, Canada) at 750nm wavelength. Protein concentration was determined by plotting the standard curve in GraphPad Prism and extrapolating the sample absorbance values.

2.6 SDS-PAGE gel electrophoresis and Western blotting

To detect PD-L1 expression, 40 μ g of total proteins extracted from control and IFN- γ treated cells were resolved on 5% stacking and 10% separating SDS-polyacrylamide gels (40% Acrylamide/Bis Solution, 29:1 (Cat#1610146; Biorad)), to look at PD-L1 expression, while 80 μ g total proteins were used to detect PD-L2 expression. 2x Laemmli dye containing β -mercaptoethanol (2% v/v) was added to each sample prior to loading. The gels were run at 120 V for around 1.5 hours and then transferred to Immobilon-P membranes (Millipore, Bedford, MA), in a transfer unit at 0.3 Amps for 2 hours. The membranes were then blocked in 5% skim milk made in tris-buffered saline with 0.5% tween (TTBS) for 50 to 60 min, at room temperature on a rocker. Membranes were probed with primary antibodies against PD-L1 (Clone E13N; Cat#13684) or PD-L2 (clone D7U8C; Cat#82723) (Cell Signalling Technology, Danvers, MA) both used at 1:1000 dilution in TTBS and incubated overnight, rocking at 4°C. The next day the membrane was washed 4 x 5 min in with TTBS, and the membrane was probed with anti-rabbit conjugated with Horseradish Peroxidase (HRP) (DAKO, North America) as the secondary antibody, made up at a 1:6000 dilution with TTBS, and incubated for 50 min at room temperature. Membranes were imaged on the Bio-Rad ChemiDoc Imaging System (BioRad DC- Hercules, CA, USA) using the chemiluminescence setting and adjusting it to take images at a range of different exposures. Membranes were stripped after imaging, by washing with TTBS for 50 to 60 min, while rocking at room temperature. The membranes were probed with antibodies against β -actin (Cat#A5316; 1:6000dilution) (Sigma-Aldrich) for 1 hour, on a rocker at room temperature. The membrane was

then washed 4 x 5 min with TTBS to remove any non-specific bound actin. This was followed by 1-hour incubation with the secondary antibody anti-mouse HRP (DAKO, North America) diluted at 1:6000 in TTBS. After washing 4 x 5 min, the membranes were imaged on the Bio-Rad ChemiDoc Imaging System (BioRad DC- Hercules, CA, USA) and images were exported for analysis.

2.7 Mass spectrometry of PNGaseF released *N*-glycans; composition and abundance in melanoma cell lines

2.7.1 Membrane enrichment

Pellets containing 5×10^5 melanoma cells were prepared as detailed in section 2.2 and Figure 4 were stored at -20°C . Samples were thawed on ice and prepared for membrane extraction using an ultracentrifugation method. Briefly, the cells were lysed by sonication using a Sonic Ruptor 250 sonicator (OMNI International, Kennesaw, GA, USA) (2 x 15s pulses, with 1 min interval on ice at 40% power) in lysis buffer containing 50 mM Tris-HCl (pH 7.4), 1 mM EDTA, 0.1 M NaCl and protease inhibitor cocktail (Roche Diagnostics, Mannheim, Germany). Cell debris was removed by centrifugation at 4°C at $2,000 \times g$ for 20 min and the supernatant was collected subsequent ultracentrifugation. The supernatant was brought up to 3ml using 20 mM Tris-HCl, and 0.1 M NaCl (pH 7.4), balanced, and centrifuged at $120,000 \times g$ for 80 min at 4°C using the Optima MAX-XP Ultracentrifuge (Beckman Coulter, California, United States). The supernatant was discarded, and the pellets containing the membrane proteins were resuspended in 100 μl of 20 mM Tris-HCl, and 0.1 M NaCl (pH 7.4), and precipitated by adding 9 volumes of cold acetone, incubating overnight at -20°C . The acetone precipitate was collected by centrifugation at $10,000 \times g$ for 5 min, supernatant discarded, and the dried pellets were resolubilised in 20 μl of 4 M urea.

2.7.2 *N*-Glycan release of membrane proteins

Approximately 30% of the proteins in the sample were dot blotted (6 μl) onto ethanol activated polyvinylidene difluoride (PVDF) membranes (Millipore, Sydney, Australia), and stained with 0.1% Direct Blue stain in 40% (v/v) ethanol, 10% (v/v) acetic acid (Sigma-Aldrich) to visualise the protein dot. Each dot blot was excised and separately placed in a flat bottom polypropylene 96-well plate (Corning Incorporated, NY) and blocked with 100 μl of 1% (w/v) polyvinylpyrrolidone (PVPP) in methanol for 5 min, on a microplate mixer (500 rpm). PVPP was discarded and the wells containing the membrane were washed twice with 150 μl MilliQ water for 5 min each time on the mixer. *N*-glycans were enzymatically removed from the membrane proteins by PNGaseF. 5 μl of RapidPNGaseF (Promega), diluted to 1 x concentration according to manufacturer protocol was added to each sample. An additional 10 μl of 100mM ammonium bicarbonate was added to prevent the liquid from drying out and the wells were sealed with parafilm, placed in a humidity chamber and incubated overnight at 37°C .

Released glycans were obtained by sonicating the plate for 5 min in an ultrasonic water bath at 40 kHz, and each well washed twice with 20 μ l water. After pooling the washes, 10 μ l of 100mM ammonium acetate pH 5 was added for 1 hour at room temperature to deaminate the glycans to form the reducing end before drying under reduced pressure.

2.7.3 Reduction of *N*-glycans

The dried *N*-glycans were reduced using 20 μ l of 1M sodium borohydride in 50 mM Potassium hydroxide (KOH) and incubated at 50 °C for 3 hours. To neutralize the reaction, 2 μ l glacial acetic acid was then added to stop the reduction and neutralise the basic pH for clean up using strong cation exchange.

2.7.4 Desalting of reduced glycans

Cation exchange columns were prepared by packing cationic resin (Dowex AG 50W X8) onto a 10 μ l pipette tip, blocked with a C18 disc (3M Empore, Maplewood, MN, U.S). The columns were washed by centrifugation three times with 50 μ l of 1 M HCl and three times with 50 μ l of methanol and equilibrated thrice with water prior to sample addition. Glycans, which are either neutral or anionic in charge, do not interact with the cationic resin and were collected in the flow through. The column was washed twice with 50 μ l of deionised water, flow through pooled with the samples and dried under reduced pressure. Excess borate ions were removed by addition of methanol to form methylborate and removed by evaporation.

2.7.5 Carbon clean-up of glycans

After desalting, the dried glycans were resuspended in 20 μ l water and cleaned once more by a Porous Graphitized Carbon (PGC) column, packed in a 10 μ l pipette as described previously. The PGC packing was cleaned with 30 μ l 90% Acetonitrile (ACN) and 0.05% (v/v) Trifluoroic acid (TFA) and equilibrated twice with 20 μ l water prior to sample addition. The glycans were washed twice with 20 μ l of deionised water before elution from the column with 20 μ l of 40% ACN and 0.05% TFA and dried under reduced pressure.

2.7.6 Porous graphitised carbon-liquid chromatography- electrospray ionization-mass spectrometry (PGC-LC-ESI-MS/MS)

The samples were reconstituted with 10 μ l MilliQ water and 3 μ l was injected onto the online PGC-LC-MS, comprising of a Dionex UltiMate3000 high-performance liquid chromatography (HPLC) system (Dionex, Sunnyvale, CA, USA) and a Linear Trap Quadrupole (LTQ) Velos Pro ion trap (Thermo Scientific, San Jose, CA, USA). Separation of the samples was performed on a PGC column (3 μ m, 100 mm \times 0.18 mm, Hypercarb, Thermo Scientific) at 50°C. The mobile phases used were 10 mM ammonium bicarbonate aqueous solution (buffer A) and 10 mM ammonium bicarbonate aqueous solution with 70% acetonitrile (buffer B). The flow rate programmed was 4 μ L/min, the gradient was set at 0 min, 2.6% B, followed by a linear increase

up to 35%B for 53 min, then another linear increase up to 98% B for 20 min and held constant for 5 min. Finally, it was equilibrated at 2.6% B for 5 min and ready for the subsequent sample injection. The MS spectra were acquired in the negative ion mode over the mass range of 580–2000 m/z with a tandem MS acquisition of the top 5 abundant ions. MS parameters were mirrored as described by Ashwood et al., 2018 (Ashwood et al., 2018).

2.7.6 Data analysis

The data was analysed on the Thermo Xcalibur Qual Browser, where the peaks were annotated and identified manually. The deconvoluted mass lists were entered into the Glycomod tool by ExPasy (<http://www.expasy.ch/tools/glycomod>), to calculate the potential glycan composition. The composition information was used to produce an image of the potential glycan structure using GlycoWorkBench v2.1 (<https://code.google.com/archive/p/glycoworkbench/>). A list of the potential glycan compositions, including their mass and retention time was created and input into Sky-line (MacCoss Lab Software, Seattle, WA) to find the area under curve for each peak for relative abundance quantitation.

3. Effects of IFN- γ on melanoma cell growth and expression of immune effector molecules

3.1 Introduction

Interferon gamma (IFN- γ) is a well-studied cytokine, known for its pleiotropic activity, and is especially important in host immunity (Chawla-Sarkar et al., 2003). The importance of IFN- γ in cancer development and progression was first demonstrated in 1994 by Dighe and Richards, who found that administration of IFN- γ led to tumour rejection in mice, likely because of immune activation (Dighe et al., 1994). This anti-tumour activity is attributed to the fact that IFN- γ induces expression of MHC class I, a surface receptor that presents antigens and enables immune cell recognition and immune response against the tumour (Beatty and Paterson, 2001; Mojic et al., 2017). Increased MHC class I expression contributes to enhanced Th1 helper T-cell signalling and cytotoxic T lymphocyte activation (Ivashkiv, 2018). Studies have shown that mice with abnormalities in IFN- γ or the IFN- γ receptor, leading to diminished IFN- γ response, have diminished immunity and are more susceptible to tumour formation when exposed to chemical carcinogens (Kaplan et al., 1998). This phenomenon has also been observed in humans. Reduced IFN- γ sensitivity or loss of function of IFN- γ related genes such as interferon regulatory factor-1 (IRF-1) is associated with increased incidence of gastric cancer, leukemia, lung adenocarcinoma and melanoma (Beatty and Paterson, 2001; Kaplan et al., 1998; Nozawa et al., 1998).

The anti-tumour effects of IFN- γ have made it a propitious agent that can be used as a form of immunotherapy for cancer patients (Mojic et al., 2017). Clinical trials using IFN- γ as an immunotherapy agent have had mixed success, however, and in some cancers such as melanoma, patients treated with IFN- γ showed worse outcomes (Mojic et al., 2017) (Meyskens et al., 1990; Meyskens et al., 1995). This may be due to the emergence of resistance to IFN- γ , thereby allowing tumour cells to escape detection by immune cells (Ivashkiv, 2018; Parker et al., 2016).

IFN- γ is also capable of promoting tumour growth (Mojic et al., 2017). Although IFN- γ upregulates MHC class I molecules, including HLA-A, -B and -C, it also upregulates PD-L1 and PD-L2 expression on tumour cells, via activation of the JAK/STAT signalling pathway. Expression of these ligands is heavily associated with immune suppression (Mojic et al., 2017). Both PD-L1 and PD-L2 bind the same PD-1 receptor on activated immune cells and binding leads to inhibition of immune activity. Although PD-L1 has been well studied, much less is known regarding the role of PD-L2 in cancer. In particular, PD-L1 is used as a biomarker for immunotherapy response; patients with PD-L1 expression on tumour and immune cells display better responses to immune checkpoint blockade, with a response rate ranging from 36% to 100%, compared to patients with no or little PD-L1 expression (response rate of 0% to 17%) (Karachaliou et al., 2018).

In this chapter, the expression of immune regulatory markers HLA-ABC and PD-L2 on melanoma cells following treatment with IFN- γ was evaluated using flow cytometry. IFN- γ also regulates proliferation, growth and survival, and the effect of IFN- γ on melanoma cell proliferation was also examined.

3.2 Results

3.2.1 Selection of melanoma cell models

Sixteen short-term melanoma cell lines were selected for this study (Table 3). These tumour cells are derived from melanoma patients that failed immunotherapy. Patients were treated with anti-PD-1 monotherapy (pembrolizumab or nivolumab), or anti-PD-1 in combination with anti-CTLA-4 (ipilimumab) using doses approved by the FDA (Lee et al., 2017). The biopsied melanoma lesions were enzymatically dissociated and established as melanoma cell lines. The majority of these melanoma cells were also exome sequenced and driver mutations affecting BRAF and NRAS are also summarised in Table 3.

Table 3: Summary of melanoma cell lines used in this study

Cell line	Driver mutation ^a	Site of biopsy	Immunotherapy
SCC15-0111	n/a	Brain	anti-PD-1
WMD15-083	NRAS ^{Q61K}	Large colon	anti-CTLA-4 and anti-PD-1
SCC15-0534	NRAS ^{Q61K}	Neck	anti-PD-1
SMU13-0183 M3	BRAF ^{V600E}	Brain	anti-PD-1
SMU13-0183 M7	BRAF ^{V600E}	Brain	anti-PD-1
WMD-084	NRAS ^{Q61K}	Other	anti-PD-1
SMU16-0150	BRAF ^{V600K}	Scalp	anti-CTLA-4 and anti-PD-1
SMU-092	n/a	Abdomen	anti-CTLA-4 and anti-PD-1
SMU11-0376 M4	BRAF ^{V600E}	Brain	anti-PD-1
SMU11-0376 M2	BRAF ^{V600E}	Brain	anti-PD-1
SCC16-0016	NRAS ^{Q61E/K (b)}	Pancreas	anti-PD-1
SMU15-0404	BRAF ^{G469R/S}	Arm	anti-PD-1
SMU059	NRAS ^{Q61L/R/P}	Flank	anti-PD-1
SCC13-0156	BRAF ^{V600E}	Retroperitoneal LN	anti-PD-1
SCC11-0270	BRAF ^{V600E}	Brain	anti-PD-1
WMD-084 Resistant	NRAS ^{Q61K}	Other	anti-PD-1

n/a, not available; ^aMutation data were analysed using the Oncofocus test, (<https://www.oncologica.com/oncofocus/>);

^bDetermined status of this mutation is E or K; LN, lymph node.

3.2.2 The impact of IFN- γ on melanoma cell proliferation

We assessed the impact of IFN- γ on melanoma cell proliferation using the incucyte ZOOM system for live cell analysis. Three melanoma cell lines, SMU15-0404, SCC16-0016 and SCC13-0156 were treated with IFN- γ (1000U/ml) for 24 hours or vehicle-control (BSA) treated. Growth was monitored in real-time for 72 hours and cell images were taken every 4 hours. Representative images are shown in Figure 5. To determine cell growth, the Confluence Processing analysis tool was applied to each image to generate masks that define the area occupied by the cells (Figure 5B and D). This masking process is applied to all the images and used to calculate percentage of confluent area.

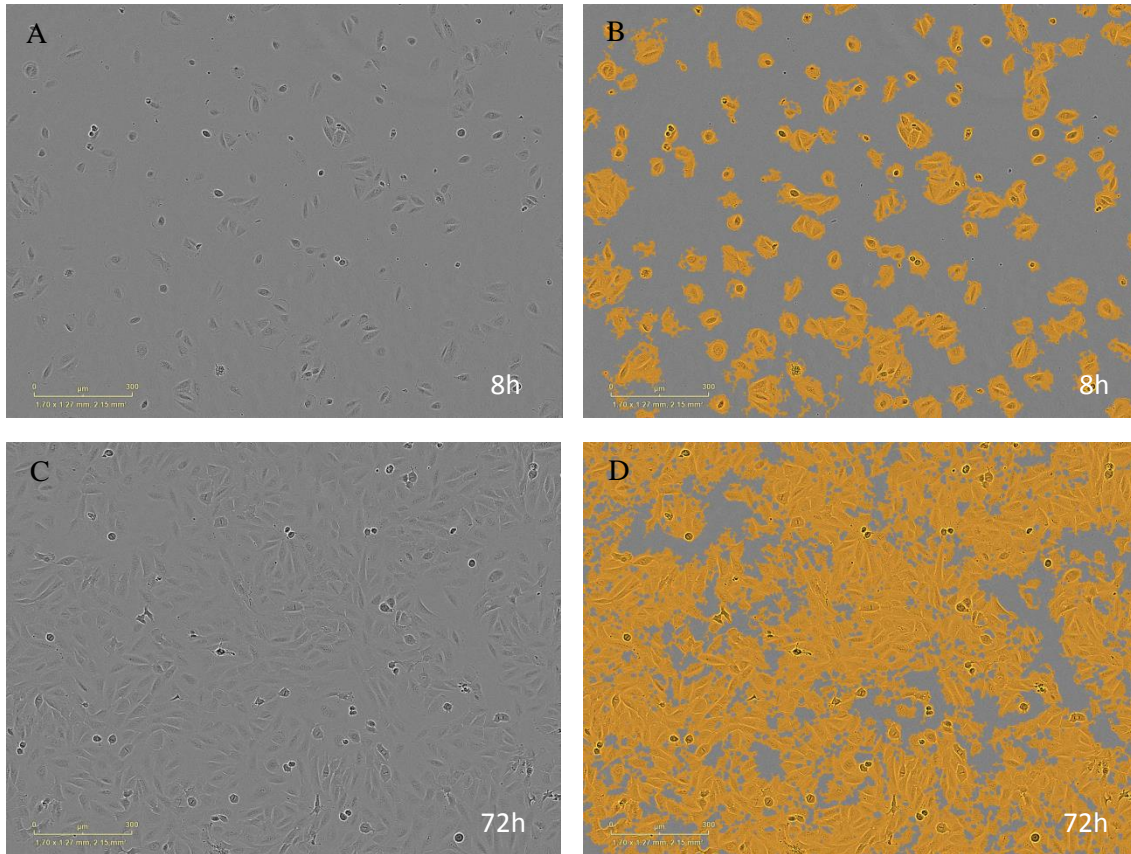


Figure 5. Representative images from IncuCyte ZOOM and the masking process of control cell line SMU15-0404. The SMU15-0404 cell line was treated with 0.1% BSA (as control) and growth was monitored A) shows cells in DMEM media + 0.1% BSA at 8 hours, B) is a replicate image of A) however it shows the cells ‘masked’ with yellow to calculate the area they occupy to calculate growth. C) shows the same cells but after 72 hours and D) shows the same image as C) except ‘masked’ with yellow to calculate the area the cells occupy.

The percentage confluence reflects cell proliferation and no differences were found in the IFN- γ treated versus control-treated cells in all three cell lines tested. These results indicate that IFN- γ had no effect on proliferation of these melanoma cells. We did note that each of these cell lines showed varying proliferation rates after 72 hours. The SMU15-0404 cell line had reached 60% confluency, while the SCC16-0016 and SCC13-0156 cell lines both did not even reach 50% confluency, reaching almost 20% in both cell lines after 72 hours.

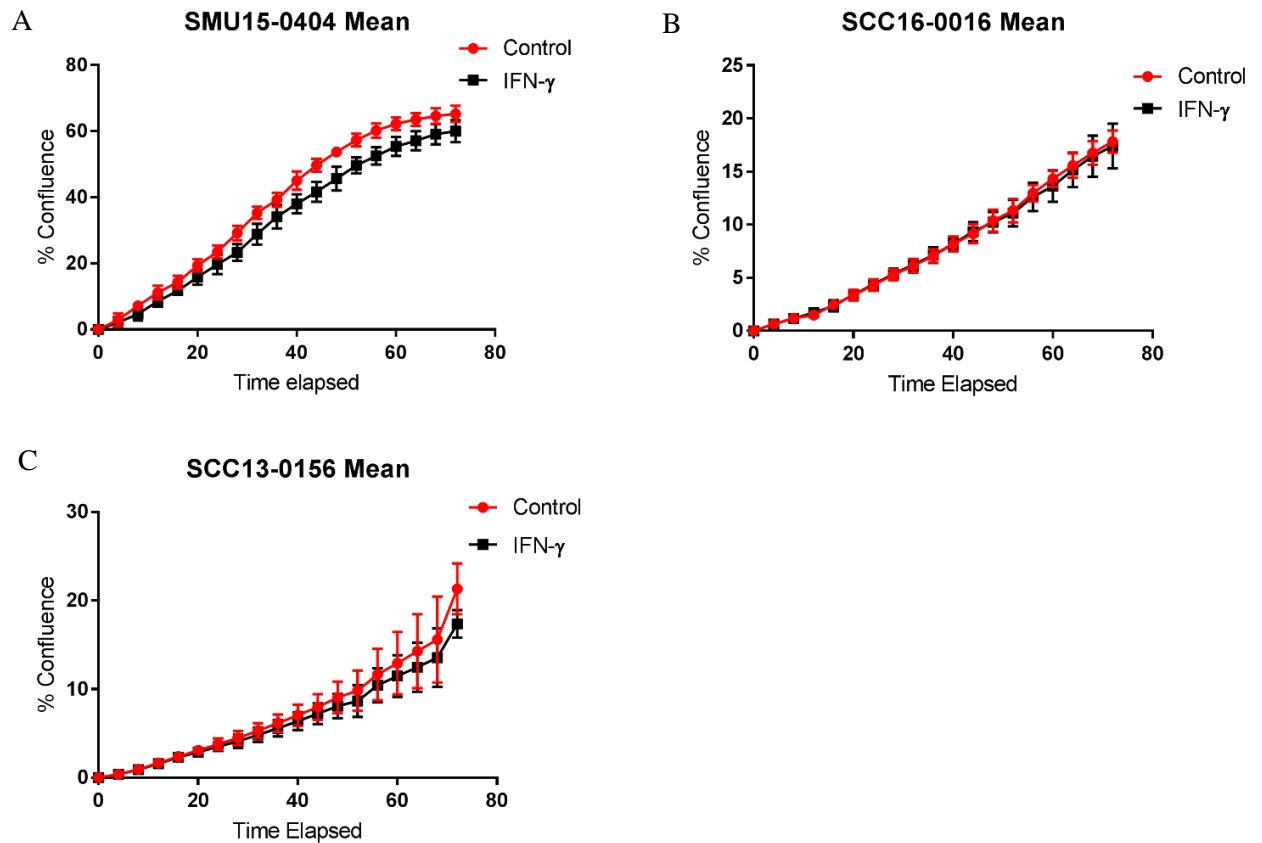


Figure 6. Effects of IFN- γ on growth of melanoma cells. Melanoma cells were treated with 1000U/ml IFN- γ (black line) or with 0.1% BSA (as control, red line) and growth monitored for up to 72 hours using the IncuCyte ZOOM system. Percentage of confluent area was calculated from the Confluence Processing analysis tool and used to assess melanoma growth. Each experiment was done in three biological replicates and data shown represent mean \pm standard deviation of all three experiments. A) B) C) show cell lines SMU15-0404, SCC16-0016 and SCC13-0156, respectively.

3.2.3 IFN- γ mediated regulation of immune cell markers

The effects of IFN- γ on melanoma cell expression of immune markers PD-L2 and HLA-ABC was investigated in all 16 PD-1 PROG cell lines (Table 3). Cells were treated with IFN- γ (1000U/ml) or 0.1% BSA (control) and expression of the two markers analysed by flow cytometer and assessed using the FlowJo software. Viable populations of melanoma cells were selected with the following gates: i. forward and side scatter area (FSC-A and SSC-A) (Figure 7A), ii. cells negative for the DNA-binding dye DAPI (Figure 7B), and iii. single cells were selected using FSC-A against forward scatter height (FSC-H) as these would show proportional peak area and peak height (Figure 7C). Expression of PD-L2 and HLA-ABC was then determined on the gated melanoma cell population (Figure 7D) by comparing expression and setting up quadrant gates to an unstained control.

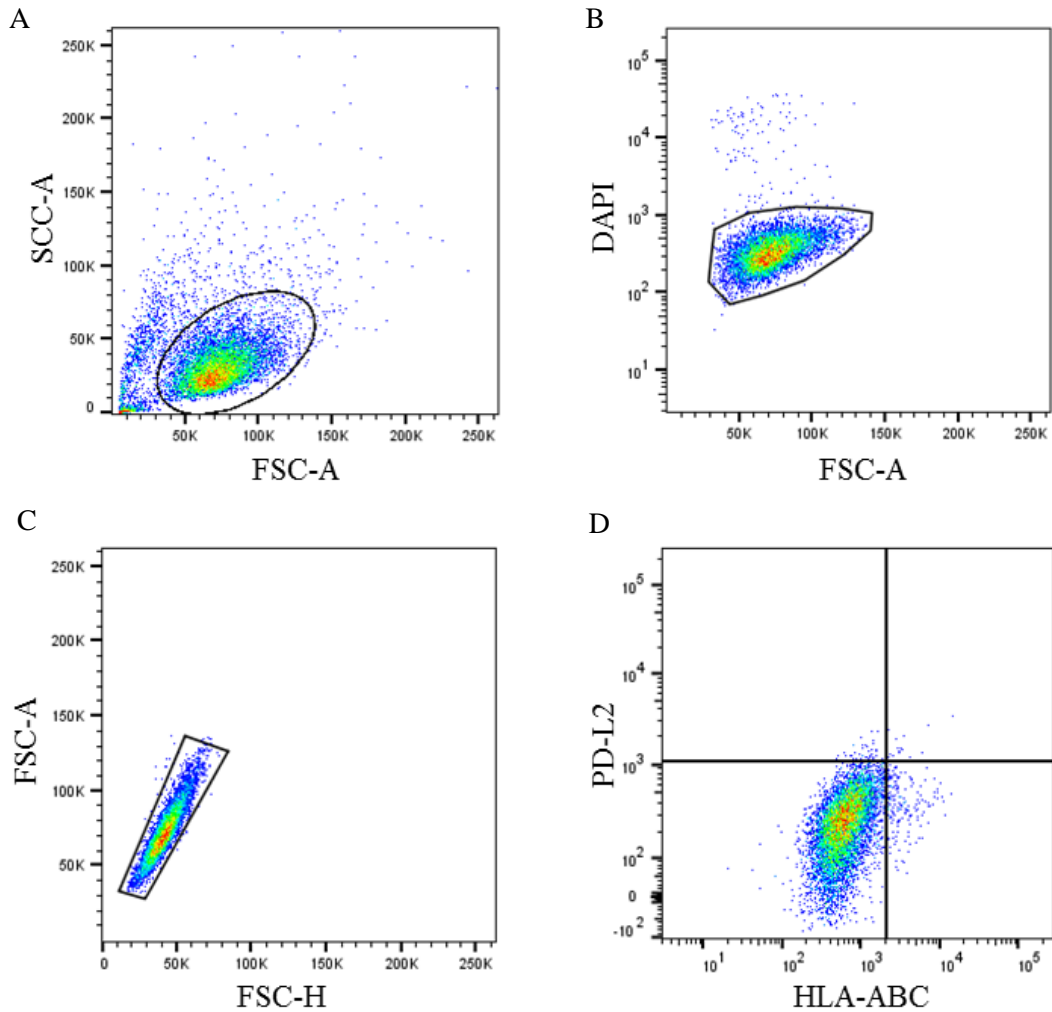


Figure 7. Melanoma cells were gated and analysed using the FlowJo software (TreeStar, Ashland, OR). Scatterplots showing the gating strategy for A) melanoma cells based on forward and side scatter area (FSC-A and SSC-A), B) Viable cells identified and gated based on DAPI staining, C) Single cells selected using a FSC-A against forward scatter height (FSC-H) gate, and D) A quadrant gate set based on unstained controls to determine positive expression of PD-L2 and HLA-ABC.

In all flow cytometry experiments, unstained controls were used to determine non-specific background expression of the markers and to set the gate for positive expression. For example, in the SMU15-0404 cell line, the quadrant gate was set to exclude the majority of the unstained control cells (Figure 8) and the same gate was applied to both the stained control and IFN- γ treated cells. Compared to the unstained control, the stained control cells had a much higher geometric mean (shown in bold in each scatterplot, Figure 8) for both PD-L2 and HLA-ABC, at 9231 and 4151 respectively. This suggests that the SMU15-0404 cell line expressed both PD-L2 and HLA-ABC at baseline in the absence of IFN- γ . The stained IFN- γ treated cells were also compared to its unstained control (data not shown in Figure 8), which had similar geometric mean values as the unstained control cells. When treated with IFN- γ , the SMU15-0404 cell line showed slight increase in HLA-ABC expression (geometric mean of 5907) but a more predominantly increased in PD-L2

expression (geometric mean of 28767). This indicates that IFN- γ treatment induced PD-L2 expression but had minimal effects on HLA-ABC expression in this cell line.

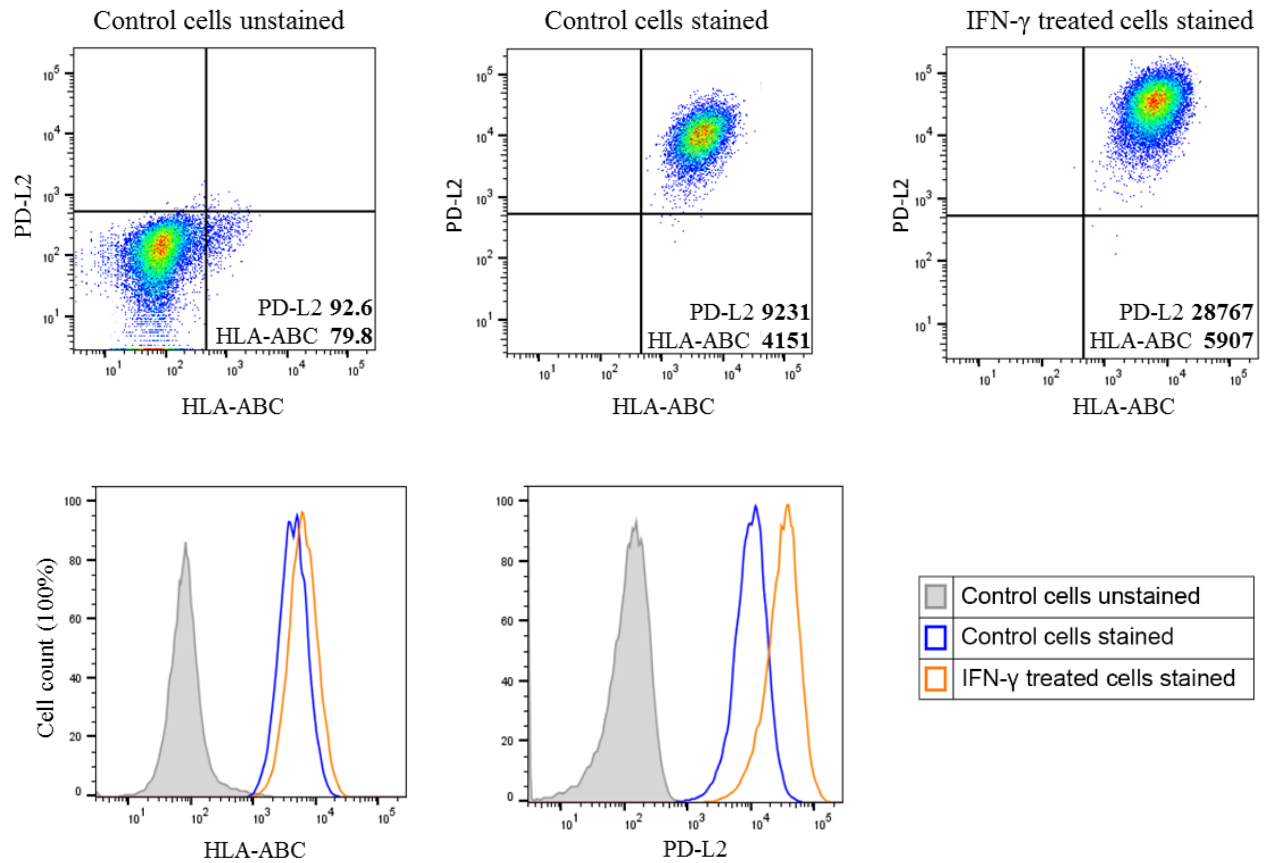


Figure 8. Expression of HLA-ABC and PD-L2 on SMU15-0404 cell line. Top, Scatterplots showing geometric mean expression of HLA-ABC and PD-L2 (values provided in bold) in unstained control cells, stained control cells and stained IFN- γ treated cells. Bottom, Histograms showing the geometric mean expression of HLA-ABC and PD-L2 in stained control cells (blue line) and IFN- γ treated cells (orange line) compared to the unstained control cells (coloured grey).

However, in the SMU-092 cell line, the geometric mean expression levels of PD-L2 and HLA-ABC were similar in the stained control and IFN- γ treated cell when compared to the unstained cells. There was only a slight increase in PD-L2 expression after IFN- γ treatment (geometric mean of 70.3 compared to control cells with a geometric mean of 55.3). HLA-ABC expression showed no change (Figure 9).

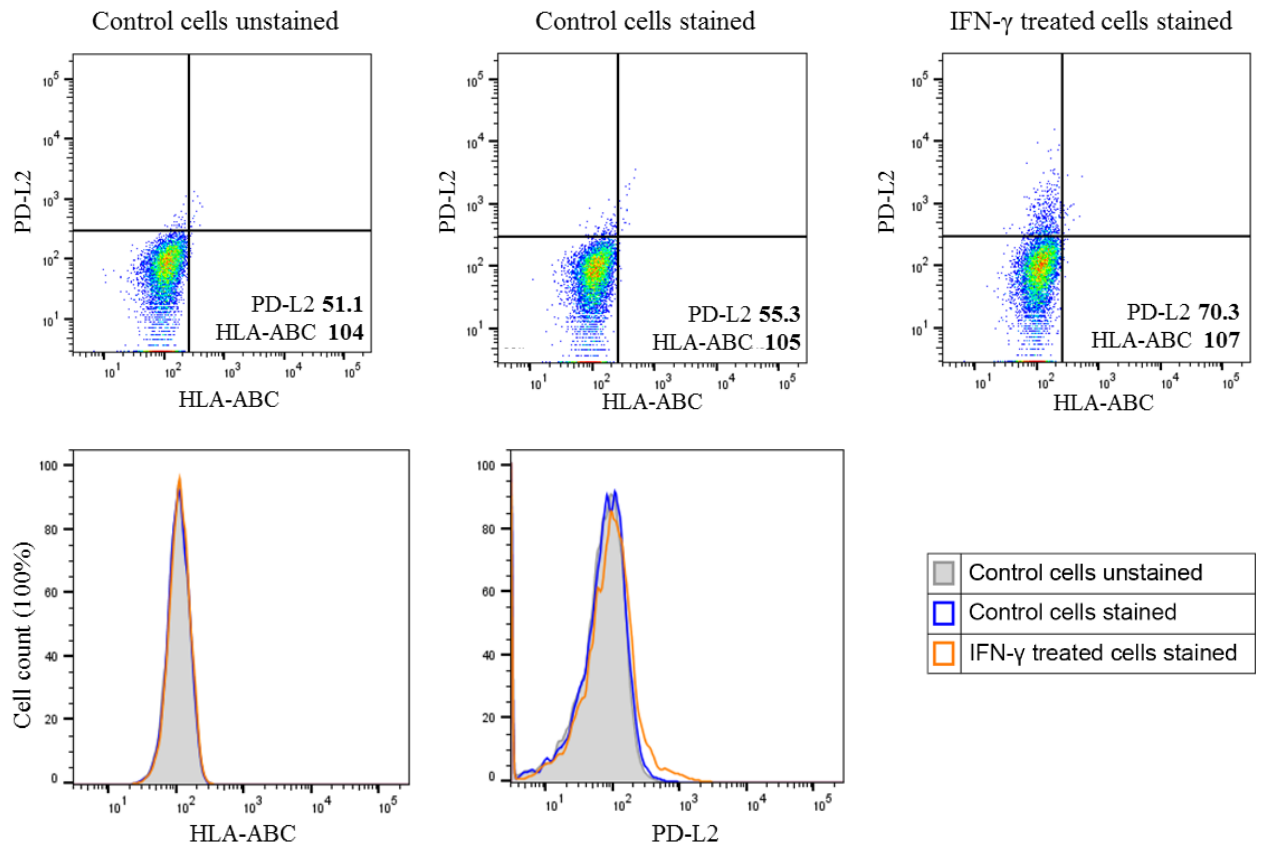


Figure 9. Expression of HLA-ABC and PD-L2 on SMU-092 cell line. Top, Scatterplots showing geometric mean expression of HLA-ABC and PD-L2 (values provided in bold) in unstained control cells, stained control cells and stained IFN- γ treated cells. Bottom, Histograms showing the geometric mean expression of HLA-ABC and PD-L2 in stained control cells (blue line) and IFN- γ treated cells (orange line) compared to the unstained control cells (coloured grey).

The expression levels of PD-L2 and HLA-ABC at baseline (0.1% BSA-treated control cells) and after IFN- γ treatment were collected for all cell lines. The geometric mean fluorescent intensity (MFI) expression of the stained samples were divided by the corresponding unstained samples to obtain a geometric fold change value for all 16 PD-1 PROG melanoma cells lines (Supplementary Table 1 in Appendix). It is also important to mention that the flow cytometry data for 10 of the 16 PD-1 PROG cell lines were acquired on an updated model of the BD LSRFortessa X20 machine (BD Biosciences). Data acquired on the old and new flow cytometers are presented separately because the laser configurations were different and expression data were not directly comparable. For example, HLA-ABC and PD-L2 expression data for the SCC16-0016 cell line was acquired using the old machine and new machine and compared.

Although the cells were treated, and the data was acquired in the same manner, there is obvious differences in fold change value (stained/unstained) between the machines. Fold change expression of HLA-ABC and PD-L2 was much lower on the old machine compared to the new machine (Figure 10). This may be attributed to the detection range and sensitivity of the new lasers,

which may have given higher fluorescence intensity readings. Due to the apparent differences shown in Figure 10, expression data are separated based on which machine the data was acquired on.

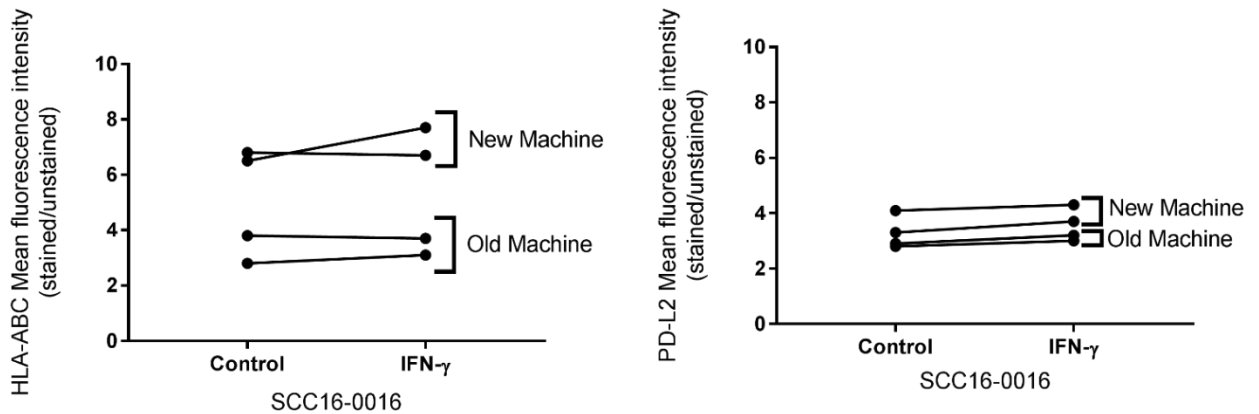


Figure 10. Comparison of flow cytometry expression data acquired on the old compared to new machine. HLA-ABC and PD-L2 expression data for the same cell line, SCC16-0016, was acquired on the old BD LSRFortessa (BD Biosciences) and the new BD LSRFortessa (BD Biosciences) machine. The geometric mean fluorescence intensity (MFI) fold change values were higher when data was acquired on the new machine compared to the old machine for HLA-ABC (left) and PD-L2 (right).

The expression of PD-L2 and HLA-ABC in control cells revealed that 2/16 cells (SCC13-0156 and SMU-092) showed no expression (geometric MFI fold change <1.5) of HLA-ABC (coloured in red, Figure 11). The remaining 14 melanoma cell lines expressed similar levels of HLA-ABC expression levels. PD-L2 expression was more variable. Four cell lines (SCC13-0156, SMU-092, SCC11-0270 and SMU11-0376 M4) showed no expression of PD-L2. Eight cell lines displayed high baseline expression of PD-L2 (MFI fold change > 10) while four had low expression (MFI fold change < 5).

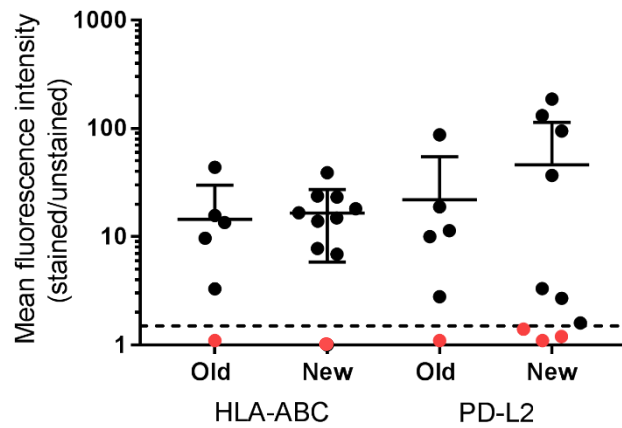


Figure 11. Baseline expression of HLA-ABC and PD-L2 on the 16 PD-1 PROG cell lines. Scatterplot graph showing the fold change expression (geometric mean fluorescence intensity of stained cells/unstained cells) of HLA-ABC and PD-L2, separated based on acquisition on the old or new machine. Cell lines that had a fold change expression lower than 1.5 (shown in red) were considered as having no PD-L2 or HLA-ABC expression.

The impact of IFN- γ induction on HLA-ABC and PD-L2 expression was also evaluated in our 16 PD-1 PROG melanoma cells. Comparison of the MFI fold change values in IFN- γ treated cells to their baseline values (control cells) indicated that the majority of the cell lines showed induction of both markers (Figure 12). Only three cell lines showed no induction of HLA-ABC after treated with IFN- γ and these included the SCC13-0156, SCC16-0016 and SMU-092 cell lines. The SCC15-0534 cell line showed a slight induction in HLA-ABC while the remaining 12 cell lines showed approximately a 2-fold induction. PD-L2 was not induced in five cell lines including SCC16-0016, SCC11-0270, SMU-092, SMU11-0376 M4 and SMU11-0376 M2 while the remaining 11 cell lines showed at least a 2-fold induction. Only the SCC16-0016 and SMU-092 cell lines showed no induction of both HLA-ABC and PD-L2.

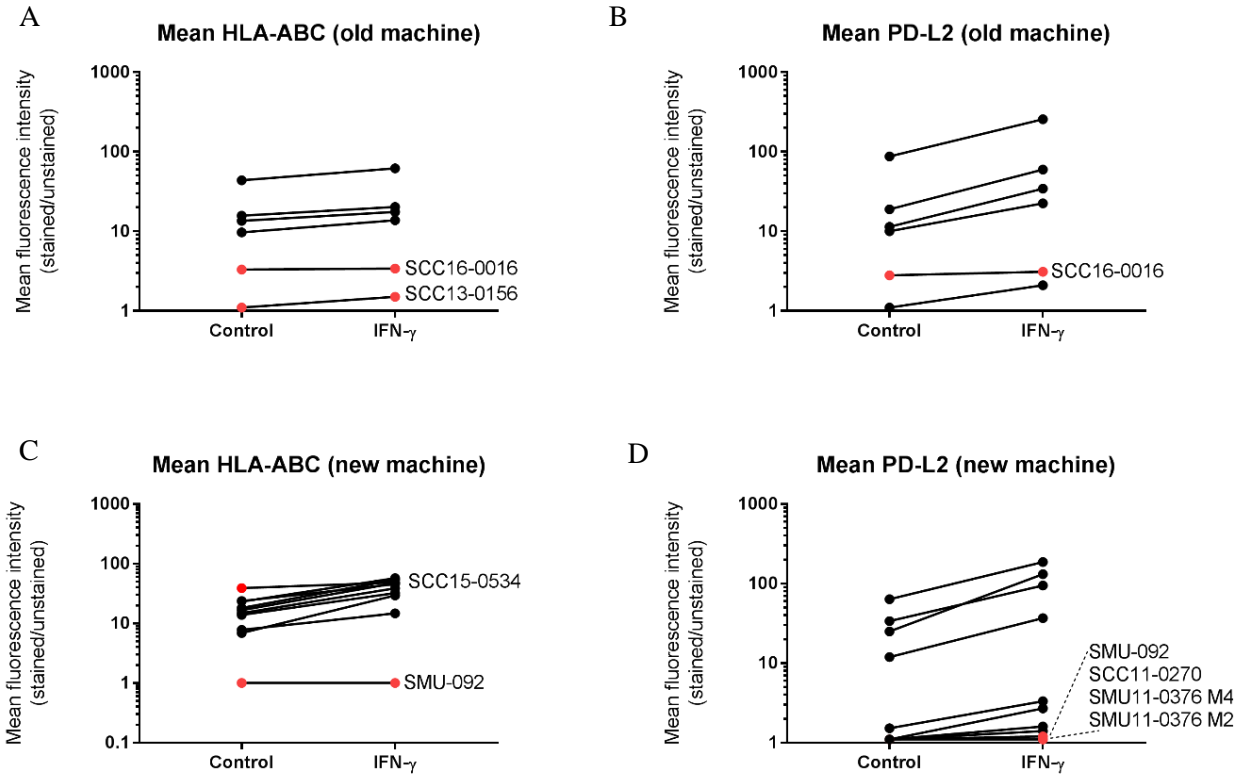


Figure 12. Induction of HLA-ABC and PD-L2 on the 16 PD-1 PROG cells after treatment with IFN- γ . Mean fluorescence intensity fold change expression of HLA-ABC (A and C) and PD-L2 (B and D) at baseline (in control cells) and the matched fold change expression after treatment with IFN- γ are shown. Data acquired on the old (6 cell lines) and new (10 cell lines) machines are presented separately. Cell lines that showed no induction of HLA-ABC or PD-L2 are highlighted in red.

3.3 Discussion

Several studies have reported that IFN- γ regulates cell proliferation and survival in tumour cells (Asao and Fu, 2000; Ivashkiv, 2018). IFN- γ has an inhibitory effect on cell growth, and cell arrest often occurs at the G0/G1 phase of the cell cycle. Cyclin dependant kinase inhibitors are induced by IFN- γ , and this in turn inhibits cyclins which causes downregulation in phosphorylation of proteins responsible for cell cycle progression (Kirch et al., 1997; Yamaguchi et al., 2018). However, in order for IFN- γ to inhibit cell growth, the JAK/STAT1 pathways must be fully functional, as cells that lack STAT1 activity are not capable of undergoing growth inhibition (Bromberg et al., 1996). In contrast, other studies have shown that tumours cells do not undergo cell inhibition in the presence of IFN- γ , even though they have a fully functional JAK/STAT pathway (Chawla-Sarkar et al., 2003; Hiroi et al., 2009; Yamaguchi et al., 2018). This discrepancy in findings may be due to distinct molecular mechanisms underlying cell proliferation and survival in different tumour cell lines, which are currently not well understood (Hiroi et al., 2009).

In our study, we found that IFN- γ had little or no effect on melanoma cell growth (Figure 6). This may be due to a defect in STAT1 activity in our cell lines and dysfunctional JAK/STAT pathway

activity has been reported in tumour cells, often due to truncated or mutated components of the pathway (Zaretsky et al., 2016). IFN- γ suppresses melanoma cell growth, but we have found no data on melanoma cells progressing on immunotherapy, and perhaps their failure to respond may reflect resistance to IFN- γ effects on proliferation. As we could not see a significant effect of IFN- γ on growth of the three selected PD-1 PROG cell lines, we did not continue to assay effects of IFN- γ on melanoma growth for the remaining cell lines but instead chose to focus on expression of immune markers that are known to contribute to resistance to immunotherapy.

IFN- γ stimulates MHC class I, PD-L1 and PD-L2 expression on tumour cells to enable and regulate immune stimulation and recognition (Maio et al., 2015). We found that most of our melanoma cell lines derived from patients who have failed PD-1 based therapy (PD-1 PROG) expressed both HLA-ABC and PD-L2 at baseline (Figure 11). We noted high variability of PD-L2 and HLA-ABC expression in these cell lines, which is expected as it is well-known that tumours exhibit high heterogeneity. However, it does indicate that there does not appear to be an expression level for these molecules that predict tumour evasion of immunotherapy. These results correlate with a study that found high variation in surface expression of immune markers HLA-ABC and PD-L1 at baseline on melanoma cells (Garcia-Diaz et al., 2017; Neubert et al., 2017).

Baseline expression of immune markers may have important implications on immunotherapy response. For example, melanoma patients expressing more than 5% PD-L1 have a better outcome when treated with PD-1 blockade therapy, with a 36% response rate (Topalian et al., 2015). The 5% expression threshold was established by another study (Thompson et al., 2006), which used immunohistochemistry staining to determine level of PD-L1 expression, and association of PD-L1 with better immunotherapy response was consistently shown in several other studies (Taube et al., 2012; Topalian et al., 2015). It is important to mention that two of the 16 PD-1 PROG cells had no expression of HLA-ABC (Figure 11) at baseline, and this could be a potential mechanism of resistance to immunotherapy as T-cells may no longer be able to recognise these melanoma cells (Concha-Benavente et al., 2016).

Four cell lines had no PD-L2 expression at baseline while eight cell lines had relatively high expression. Expression of PD-L2 (and PD-L1) on tumour cells has been shown to contribute to anti-tumour response by inhibiting T-cell activity (Sharma et al., 2017), and high PD-L2 expression on the PD-1 PROG cells at baseline may cause immunotherapy failure by inhibiting adaptive immune response (Sharma et al., 2017). In contrast, cell lines that showed low PD-L2 expression may use a different mechanism to escape treatment. This suggests that although PD-L1, and perhaps PD-L2, may be used as biomarkers of immunotherapy response (Patel and

Kurzrock, 2015; Zou et al., 2016), they may not be entirely reliable as biomarkers because different cell lines show variable expression at baseline.

When treated with IFN- γ , the majority of the PD-1 PROG cell lines showed induction of PD-L2 and HLA-ABC compared to baseline expression (Figure 12). About a two-fold induction is evident in most cells, although seven cell lines showed little (less than 1.5 MFI fold change) or no induction of HLA-ABC or PD-L2. Cell lines that showed induction of PD-L2 and/or HLA-ABC suggest that these cells respond to IFN- γ . We expected to see induction as IFN- γ typically upregulates HLA-ABC and PD-L1 expression, and in some studies, PD-L2 expression as well (Garcia-Diaz et al., 2017; Mojic et al., 2017; Rodig et al., 2003; Sharma et al., 2017). IFN- γ induced expression of PD-L1 correlated with an increase in STAT1 and IFGR1, and in the JAK/STAT pathway activity (Garcia-Diaz et al., 2017), indicating response to IFN- γ treatment.

However, seven cell lines showed little or no induction, suggesting incomplete response to IFN- γ . It was found that patients with no upregulation of PD-L1 had high tumour progression (Herbst et al., 2014) and these patients additionally showed defect in antigen presentation or had non-functional immune activity (Herbst et al., 2014). Lack of induction in the seven cell lines suggest an incomplete immune response and as such may contribute to immunotherapy failure.

It is also important to point out that induction of HLA-ABC and PD-L2 is not co-ordinated, meaning that induction of HLA-ABC in response to IFN- γ does not guarantee induction of PD-L2. For example, the SCC13-0156 cell lines showed an increase in PD-L2 expression after treatment with IFN- γ but not in HLA-ABC expression. Similarly, the SCC11-0270 cell line showed induction of HLA-ABC but not PD-L2. This suggests that HLA-ABC and PD-L2 induction by IFN- γ may involve common and distinct mechanisms (Grenga et al., 2014; Liang et al., 2003). Only SCC16-0016 and SMU-092 cell lines showed no induction of both HLA-ABC and PD-L2, and this could suggest a defect in the JAK/STAT pathway. Different levels of induction of these surface markers reflect heterogeneity in cancer cells, their oncogenic driver mutations, the possible differences in IFN- γ signalling pathway and the regulation involved in each cell line (Alavi et al., 2018).

4. Post-translational modifications of immune effector molecules

4.1 Introduction

IFN- γ regulates PD-L1 and PD-L2 expression via activation of the JAK/STAT signaling pathway, and the induction of these ligands leads to immune suppression and evasion. Multiple studies have now shown that resistance to immunotherapy is partly due to overexpression of these

immune suppressive molecules (Li et al., 2018). However, in addition to overexpression, the activity and stability of these molecules may also affect immunotherapy response. For instance, it was recently demonstrated that post-translational modification of PD-L1 contributes to immunosuppressive activity and stability (Li et al., 2016). *N*-glycosylation and ubiquitination are two types of post-translational modifications previously reported for PD-L1. *N*-glycosylation of PD-L1 allows for stabilization of this ligand, and is also essential for PD-L1 and PD-1 interaction (Li et al., 2016). However more work is required in order to delineate how PD-L1 and PD-1 are affected by glycosylation (Li et al., 2018).

Glycogen synthase kinase 3 β (GSK3 β) is an enzyme responsible for induction of protein degradation, on the other hand, it has been shown that GSK3 β cannot degrade glycosylated PD-L1, therefore assisting in stabilizing PD-L1 and suppressing immune activity (Li et al., 2018). Phosphorylation by GSK3 β creates a motif for the E3-ubiquitin ligase complex to bind, thus targeting proteins for ubiquitination and subsequent degradation (Ding et al., 2007). However, glycosylation can influence the role of GSK3 β . A recent study showed that GSK3 β cannot bind *N*-glycosylated PD-L1, therefore it cannot initiate phosphorylation and protein degradation, leading to a more stable PD-L1 protein (Li et al., 2016). In contrast, GSK3 β can bind non-glycosylated PD-L1 and target it for degradation (Li et al., 2016).

The process of *N*-glycosylation occurs in the endoplasmic reticulum, with the assistance of glycotransferases (Asano, 2003). An oligosaccharyl transferase (OST) complex transfers a standard premade oligosaccharide, Glc₃Man₉GlcNAc₂ for *N*-glycans, onto the glycosylation site of a protein which includes an asparagine (Asn) residue followed by any amino acid (X) excluding proline and continues with serine or threonine (Asn-X-Ser/Thr)(Sun and Zhang, 2015; Wild et al., 2018). Glycosidases then cleave off certain parts of the oligosaccharide as a way of ensuring the protein is folded correctly and ready to be transported. The modified proteins enter the Golgi apparatus where further modifications occur (Asano, 2003). Glycosylation is important for a range of biological activities including cell proliferation, survival and signalling (Cerliani et al., 2017). However, changes during the synthesis of glycans can modify the final glycan structure, thus affecting expression of ligands and receptors on the cell surface (Partridge et al., 2004). This in turn causes changes in cell signalling and modifies the stimulatory or inhibitory function of the protein (Partridge et al., 2004; Salatino et al., 2018).

In this section of the study we looked at expression of PD-L1 and PD-L2 in PD-1 PROG cells after IFN- γ treatment by western blotting to assess its post translational modifications. Because PD-L1 was previously reported to be *N*-glycosylated (Li et al., 2018; Li et al., 2016), we also treated PD-1 PROG cell lysates with PNGaseF to remove *N*-glycans and looked for changes in protein size.

4.2 Results

4.2.1 PD-L1 detection by western blotting

PD-1 PROG cells, collected after treatment with IFN- γ or 0.1% BSA (as control) were lysed in either RIPA buffer or by sonication. Lysis by RIPA buffer disrupts membrane structures to release membrane-bound and intracellular proteins while lysis by sonication physically breaks up cellular membranes (Goldberg, 2008). Lysis by sonication was performed to emulate the method of sample preparation used for the liquid chromatography-mass spectrometry (LC-MS) analysis (to be discussed in Chapter 5). For sonication, PD-1 PROG cell pellets were resuspended in a mild buffer containing 50 mM Tris-HCl (pH 7.4), 1 mM EDTA, 0.1 M NaCl and protease inhibitor cocktail (Roche Diagnostics, Mannheim, Germany) with no detergent-based reagents, as this might interfere with the LC-MS processing.

Cell lysates were resolved on 10% SDS-polyacrylamide gel, transferred onto membranes and blotted for PD-L1 and PD-L2. When cells were lysed with RIPA buffer, the western blot of PD-L1 (Figure 13) showed a band at approximately 40 kDa in most PD-1 PROG cell lines, which is consistent with the reported molecular weight of PD-L1. This band is more prominent after IFN- γ treatment, indicative of IFN- γ -mediated induction. No PD-L1 band was detected in the SCC16-0016 melanoma cell line, in control and IFN- γ treated cells. Expression of PD-L1 in control SCC15-0111 was also low but the 40kDa band was detected in the IFN- γ treated SCC15-0111 cells.

For most of these cell lines, a second band of lower molecular weight (~35-37 kDa) was also observed, especially after IFN- γ treatment, suggesting the possibility of novel isoforms or alternate splice variants. Expression of PD-L1 is very high in some cell lines such as SCC15-0534, WMD15-083 and SMU16-0150, resulting in a thick dark band on the western blot, thus making it difficult to distinguish whether there are multiple bands at 35-37 kDa present.

We additionally compared western blot PD-L1 expression to those obtained by flow cytometry. We found expression levels to be comparable with the two methods. For example, cell lines with geometric MFI mean fold change values of < 1.5 by flow cytometry (which we previously categorised as no expression in Section 3.2.3) also lacked the 40 kDa band on the western blot. These included SCC13-0156, SMU16-0150, SMU11-0376 M2, SMU11-0376 M4, SCC11-0270, SCC16-0016, SCC15-0111, SMU-092 and SMU-059 cell lines in the absence of IFN- γ (control cells), indicating that these cells have no PD-L1 expression at baseline. In contrast, after treatment with IFN- γ , some cell lines including SCC15-0534, WMD15-083 and SCC16-0150, SMU13-0183, SMU11-0376 M4, WMD-084, SMU15-0404 and SMU-092 showed MFI fold change values

of > 2.5 and these cell lines correspondingly showed presence of a thick dark band at 40 kDa, indicating high expression levels.

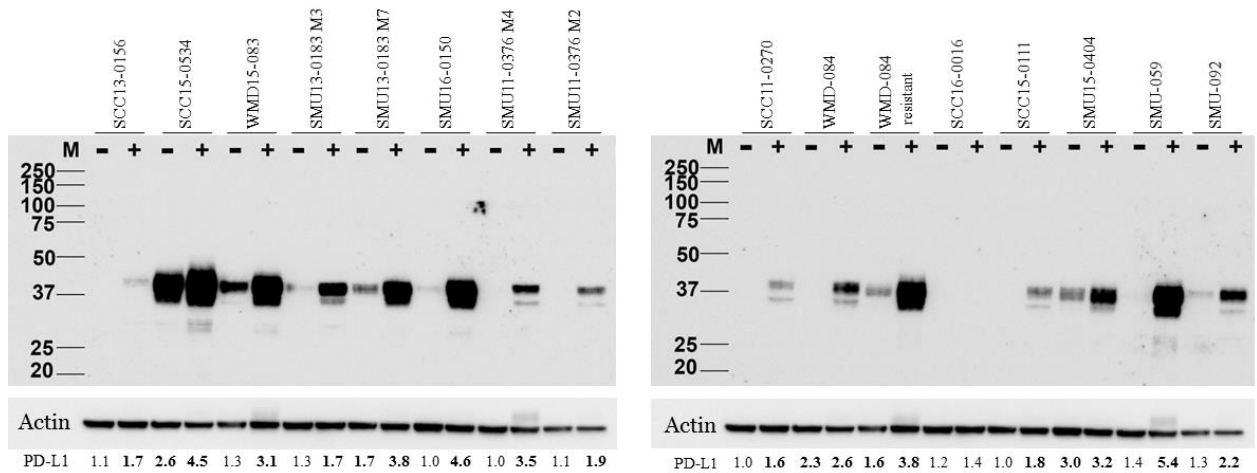


Figure 13. Western blot of 16 PD-1 PROG cell lines lysed using RIPA buffer and probed for PD-L1. Cells were treated with 1000U/ml IFN- γ (+) or 0.1% BSA as control (-) and 40 μ g of total protein was loaded into each well. The molecular weight markers (M) are shown in kDa on the left. β -actin was used as a loading control and is shown in the lower panel. PD-L1 expression was also analysed by flow cytometry and expression levels (calculated from geometric mean of stained samples/unstained samples) are shown directly under the actin blots (expression >1.5 is shown in bold). Analysis of PD-L1 expression levels by flow cytometry were performed by Ms. Sara Alavi (Alavi et al., 2018).

When cells were lysed by sonication, the western blot of PD-L1 (Figure 14) also showed a band at approximately 40 kDa in most PD-1 PROG cell lines, similar to Figure 13. As with the cells lysed with RIPA, in most cell lines treatment with IFN- γ treatment, induced the accumulation of PD-L1. Induction was seen in the following cell lines SCC15-0534, WMD15-083, SMU13-0183 M3, SMU13-0183 M7, SMU16-0150, SMU11-0376 M4, SMU11-0376 M2, SCC11-0270, WMD-084, WMD-084 resistant, SCC15-0111, SMU-059 and SMU-092.

We noted that PD-L1 band was absent in control and IFN- γ treated SCC16-0016 cells. The band was also absent in cell line SCC13-0156, which does not correspond to the data shown in Figure 13 (i.e a faint PD-L1 band was noted after IFN- γ induction in the RIPA-lysed cells). We applied a ratio of greater than 1.5 (stained/unstained MFI) to indicate PD-L1 expression by flow cytometry, and SCC13-0156 displayed PD-L1 MFI ratio of 1.7, suggestive of low expression. Expression of PD-L1 in control SCC15-0111, SMU11-0376 M4, SMU11-0376 M2, SCC11-0270 and WMD-084 M3 was also low according to the flow cytometry data, and showed no bands, but the 40 kDa band was detected in the IFN- γ treated these cell lines.

For almost all of the cell lines in Figure 14, a second band of lower molecular weight (~35-37kDa) was also observed, especially after IFN- γ treatment, suggesting that this protein is truncated in

some way. Expression of PD-L1 was very high in some cell lines post RIPA treatment (e.g SCC15-0534 cells relative to other the cell lines), however the relative level of PD-L1 expression in the sonicated SCC15-0534 sample was not as high (Figure 14). WMD15-083, SMU16-0150, and WMD-084 resistant also has a similar pattern of expression SCC15-0534 with expression being high but not as high as the cells lysed with RIPA. These results suggest that RIPA buffer is more effective than sonication in releasing proteins, including membrane proteins.

The expression levels between the western blot data and the flow cytometry data are also comparable. Cell lines with MFI fold change values of < 1.5 by flow cytometry did not show bands at 40 kDa, indicating that these cells had no PD-L1 expression at baseline. However, in the cell line WMD15-083, although the MFI expression value was < 1.5, there was an extremely faint band visible. The MFI fold change expression for this cell line was 1.4, which is close to the cut-off value and may reflect very low PD-L1 expression. Cells that showed MFI fold change values of > 2.5 showed thicker and darker bands at 40 kDa, suggesting high expression levels, these cells included SCC15-0534, WMD15-083, SCC16-0150, WMD-084, SMU15-0150, SMU13-0183, SMU11-0376 M4, SMU15-0404, SMU-059 and SMU-092.

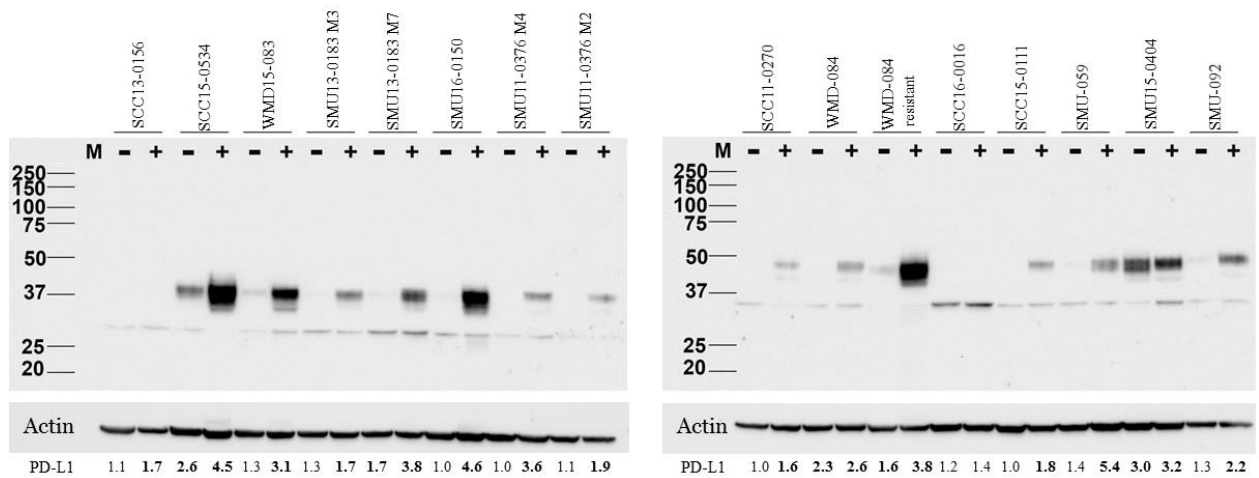


Figure 14. Western blot of 16 PD-1 PROG cell lines lysed by sonication and probed for PD-L1. Cells were either treated with 1000U/ml IFN- γ (+) or 0.1% BSA as control (-) and 40 μ g of total protein was loaded into each well. The molecular weight markers (M) are shown in kDa on the left. β -actin was used as a loading control and this is shown in the lower panel. PD-L1 expression was also analysed by flow cytometry and expression levels (calculated from geometric mean of stained samples/unstained samples) are shown directly under the actin blots corresponding to the cell line (expression >1.5 is shown in bold).

4.2.2 PD-L2 detection by western blotting

Cells lysed by RIPA buffer and probed for PD-L2 showed protein bands at around 40 kDa, however this was not the case for all cells. Cell lines SCC13-0156, SCC15-0534, WMD15-0183, SMU13-0183 M3, SMU13-0183 M7 and SMU16-0150 showed the 40 kDa band in the control and IFN- γ treated samples. This band was absent in the control SCC16-0016 and SMU15-0404

cell lines but was apparent after IFN- γ treatment, while the same band was not detected in cell lines SCC11-0270, WMD-084 M3, SCC15-011, SMU-059 and SMU-092 in either IFN- γ treated or control samples. The 40 kDa band were most prominent in the SMU16-0150, SCC16-0016 and SMU15-0404 cell lines. The bands were darker and larger, therefore harder to distinguish whether there were indeed multiple bands around the same molecular weight (Figure 15).

Although PD-L2 immunoreactive bands were detected in some cell lines suggestive of PD-L2 expression, the western blot expression data did not match the flow cytometry data. For example, we noted presence of a band in the SCC13-0156 control and IFN- γ treated cells, however their corresponding MFI fold change value was 1.1 and 1.2 respectively. This suggests that MFI fold change values of < 1.5 did not correspond to no PD-L2 expression. In addition, the immunoreactive bands in cell lines SCC13-0156, SCC15-0534, WMD-084 and SMU13-0183 were of similar intensity, despite having very different MFI fold change expression ranging from 10 to 187. The inconsistency between the western blot data and flow cytometry data could be attributed to the PD-L2 antibody used. The antibodies used for flow cytometry may have different sensitivity and specificity compared to antibodies used in western blotting. If this is the case, the sensitivity of the antibodies used in flow cytometry may be higher as the relative expression values are higher compared to the levels detected by the PD-L2 western blot antibodies.

Another indication that the western blot PD-L2 antibodies have poor sensitivity is the presence of the spots all over the membrane. This western blot was performed exactly as in the westerns for PD-L1 (Figure 13). To reduce background the blocking reagent (5% skim milk powder) was filtered, and membranes thoroughly washed after the antibody incubation steps. Nevertheless, PD-L2 western analysis produced high levels of background 'spotting' which may be due to the non-specific binding of the PD-L2 antibody.

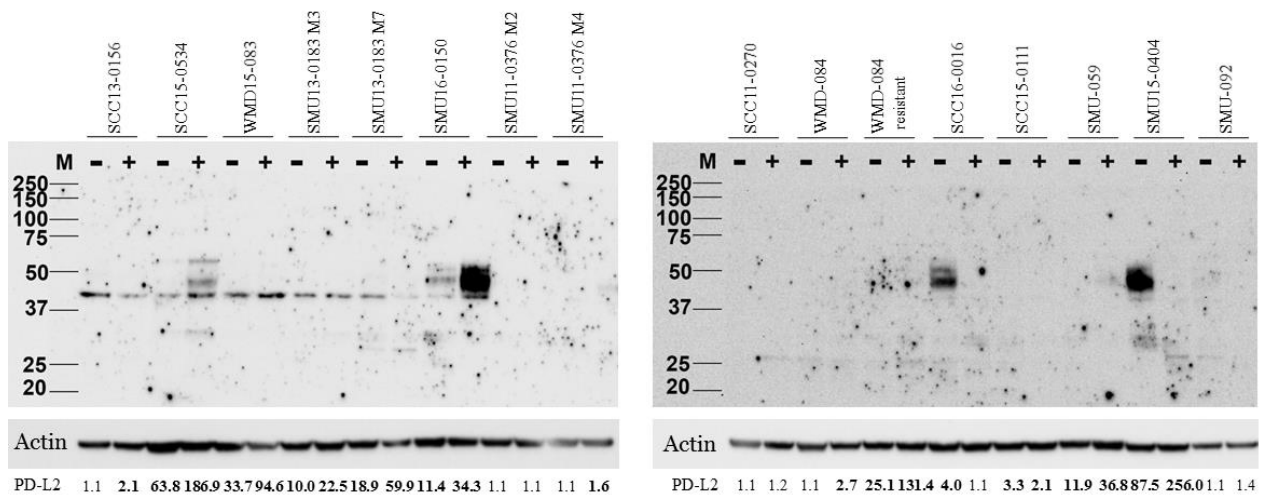


Figure 15. Western blot of 16 PD-1 PROG cell lines lysed using RIPA buffer and probed for PD-L2. Cells were treated with 1000U/ml IFN- γ (+) or 0.1% BSA as control (-) and 80 μ g of total protein was loaded into each well. The molecular weight markers (M) are shown in kDa on the left. β -actin was used as a loading control and this is shown in the lower panel. PD-L2 expression was also analysed by flow cytometry and expression levels (calculated from geometric mean of stained samples/unstained samples) are shown the area directly under the actin blots corresponding to the cell lines written at the top, (expression >1.5 is shown in bold).

Figure 16 shows the PD-L2 western blot for samples lysed by sonication. Similar to the comparison in Figure 13 and 14, the different lysis methods produced slightly different results. Immunoreactive bands were more obvious when cells were lysed by sonication compared to when they were treated with RIPA buffer. The bands were visually darker, suggesting that detection with the PD-L2 antibodies may be more compatible with sonication as it yields clearer and more abundant bands. However, this is not always the case. For example, no bands were evident in the SCC13-0156 cell line when lysed by sonication but a thin band at 40 kDa was observed in the control and IFN- γ treated cells when they were lysed by RIPA buffer. The 40 kDa band corresponding to PD-L2 was detected in cell lines WMD15-0183, SMU13-0183 M3, SMU13-0183 M7 and SMU16-0150 in both the RIPA buffer-lysed and sonicated samples. However, the PD-L2 band was detected in cell lines SMU11-0376 M4, SMU11-0376 M2, SCC11-0270, WMD-084, WMD-084 resistant, SCC15-0111 and SMU-059 only when sonicated, but not when lysed with RIPA buffer.

Regardless of the lysis method, the PD-L2 accumulation as determined by western analysis were still not comparable with the flow data. For instance, cell lines WMD15-0183, SMU13-0183 M3, SMU13-0183 M7, SMU16-0150, WMD-084 resistant, SMU-059, SMU15-0404 and SCC15-0534 all showed high expression in the flow cytometry data but only a faint 40 kDa band was detected in these cell lines. Bands were also detected in cell lines that had geometric mean fold change expression of < 1.5. Of note, even though the fold change expression for PD-L2 was 63.8 (control)

and 186.9 (IFN- γ treated) by flow cytometry in the SCC15-0534 cell line, it was marginally detected in both the IFN- γ treated and control cells when lysed by RIPA buffer sample, and not detected when cells were lysed by sonication.

It is important to mention that only 40 μ g of total proteins were loaded for the sonicated samples (in Figure 16) as opposed to 80 μ g loaded for RIPA buffer-lysed samples (in Figure 15) as there was not enough total proteins. Despite having two-fold less total proteins, it seems that PD-L2 detection was still better in the sonicated samples. It would have been beneficial to repeat and optimise the western blot experiments for PD-L2 using different antibody clones but due to time constraints, more experiments could not be performed. However, because the PD-L2 antibodies showed inconsistent expression data, we did not use it in further experiments.

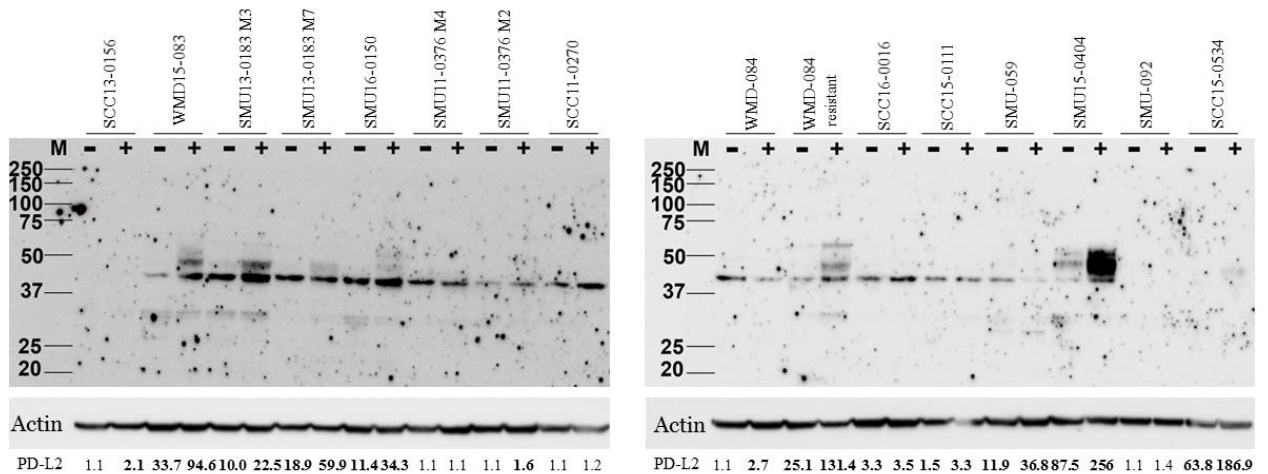


Figure 16. Western blot of 16 PD-1 PROG cell lines lysed by sonication and probed for PD-L2. Cells were either treated with 1000U/ml IFN- γ (+) or 0.1% BSA as control (-) and 40 μ g of total protein was loaded into each well. The molecular weight markers (M) are shown in kDa on the left. β -actin was used as a loading control and this is shown in the corresponding blots in the lower panel. PD-L2 expression was also analysed by flow cytometry and expression levels (calculated from geometric mean of stained samples/unstained samples) are shown directly under the actin blots, (expression >1.5 is shown in bold).

4.2.3 Effect of PNGaseF treatment on PD-L1 detection

Five cell lines (WMD15-083, SMU13-0183 M3, WMD-084 resistant, SMU-059 and SMU15-0404) that showed PD-L1 expression in the western blots (Figures 13 and 14) were chosen to further investigate potential *N*-glycosylation modifications by treating these cell lines with PNGaseF. In the absence of PNGaseF treatment, PD-L1 immunoreactive bands were observed at around 40 kDa, consistent with the previous blots shown in Figures 13 and 14. However, when treated with PNGaseF, bands at 37 kDa or lower were observed. This suggests that the mass of the PD-L1 protein has decreased and confirms that the proteins are in fact *N*-glycosylated. This was expected as we know *N*-glycosylation is a common post-translational protein modification and that PNGaseF cleaves *N*-glycans, therefore the decrease in mass is due to the removal of *N*-glycans.

Cells were either lysed with RIPA buffer or sonicated before treatment with PNGaseF. PD-L1 bands seemed clearer and more visible when cells, either in the absence or presence of PNGaseF treatment, were lysed with RIPA buffer compared to when sonicated (Figure 17). Under both lysis conditions, PD-L1 bands were observed at 40 kDa when not treated, and below 37 kDa when treated with PNGaseF. However, there were some slight differences in the patterns of bands seen pre and post PNGaseF treatment between the RIPA and sonication treatments, but no consistent pattern was observed.

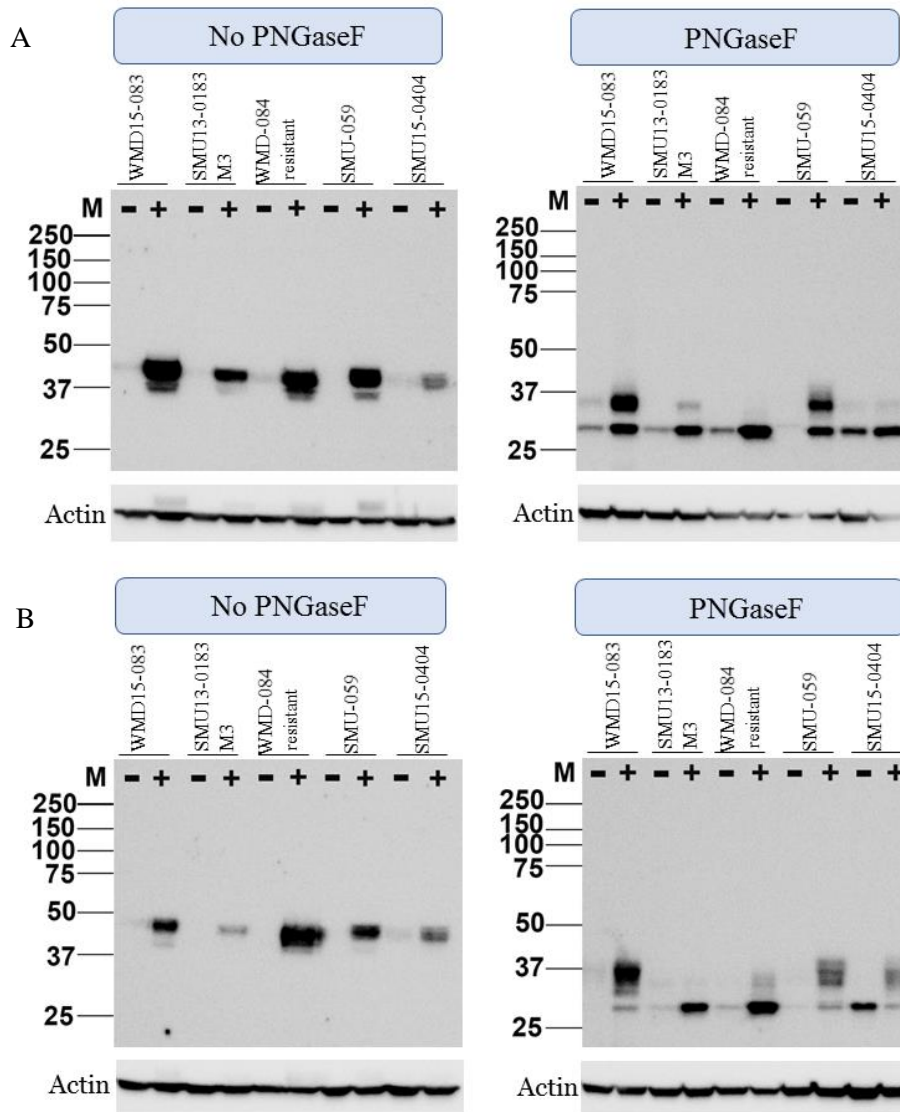


Figure 17. Treatment of control and IFN- γ treated PD-1 PROG cell lines with PNGaseF. Five PD-1 PROG cell lines were treated with IFN- γ (+) or 0.1% BSA as a control (-) and lysed by either RIPA buffer (A) or sonication (B). Lysates were either treated with 1:20 PNGaseF overnight or left untreated. 40 μ g of total proteins were loaded into each well and β -actin was used as a loading control (shown in the corresponding blots in the lower panel).

4.3 Discussion

In this chapter we explored PD-L1 and PD-L2 expression by western blotting. We initially wanted to confirm our flow cytometry results (from Chapter 3), specifically whether the geometric

mean fold change expression data was comparable. As described in Chapter 3, we considered a geometric mean MFI fold change (IFN- γ fold change/baseline fold change) value of <1.5 to be no expression or induction. For the majority of cell lines with MFI fold change of >2 , the PD-L1 western blot also showed strong intense bands. In some cases, band intensity increased as expression level increased such as in cell line SCC15-0534 (Figure 14), which had a MFI fold change of 2.5 for the control and showed a clear band while after treatment with IFN- γ , MFI fold change increased to 4.4 and the band was evidently darker. Overall, the flow cytometry data was consistent with the western blot data for PD-L1.

However, this was not the case for PD-L2 as the western blot expression did not correlate with expression values obtained from flow cytometry. The antibodies used to detect PD-L2 in the western blots were not very reliable as the chemiluminescence exposed images were spotty and the bands were not very clear and consistent. These antibodies were optimized several times (data not shown) to identify an appropriate protein loading concentration as well as antibody timing and concentration. However, it was difficult to improve on the specificity and sensitivity of the results. It is possible that the spots in the background are due to a high antibody concentration thus increasing non-specific binding on the PVDF membrane or the blocking agent (Mahmood and Yang, 2012). The 5% skim milk used for blocking was filtered to remove contaminants and decrease aggregation (Mahmood and Yang, 2012), but the membranes remained spotty.

Although, we expected concordance between the flow cytometry and western blot data (Maguire et al., 2011), it is not uncommon for western blot data and flow cytometry data to show poor correlation. Although both techniques are used to detect protein expression, they differ in sensitivity and reactivity. Western blotting for example shows the combined result from a population of cells, while flow cytometry uses a range of parameters to collect data for each single cell (Krutzik et al., 2004). Because flow cytometry is more sensitive (detecting single cell expression), this could explain why the values from our flow cytometry data was relatively higher than what could be detected on the western blot for PD-L2. The data are also represented in different ways, i.e MFI vs abundance ratio relative to the β -actin loading control. It could also be due to the fact that the antibodies used in flow cytometry may have different sensitivity and specificity compared to antibodies used in western blotting.

Even though there were obvious differences in PD-L1 and PD-L2 expression on the western blots, in the majority of cell lines, expression of both molecules was increased after treatment with IFN- γ compared to the control cells. This is expected as IFN- γ has been shown to induce PD-L1 and PD-L2 on the surface of tumour cells, a response which is mediated by the JAK/STAT pathway (Mimura et al., 2018). Several studies have found that different cells have variable response to

IFN- γ , resulting in variable PD-L1 and PD-L2 expression (Garcia-Diaz et al., 2017). This correlates with our data that the majority of our cell lines showed induction after IFN- γ treatment but expression levels were heterogeneous between cell lines (Gupta et al., 2018; Tang and Zheng, 2018). Our results show that the majority of PD-1 PROG melanoma cell lines exposed to IFN- γ can upregulate PD-L1 and PD-L2 expression, and as PD-L1 and PD-L2 expression is associated with immune evasion and suppression, this may contribute to immune escape of these cells.

Some cancer cell lines have also been shown to be non-responsive to IFN- γ , with no induction of PD-L1 or PD-L2 (Mimura et al., 2018). We similarly found that a few cell lines including SCC16-0016 showed no PD-L1 induction while SMU-092 showed no PD-L2 induction. A recent study by Mimura et al. (2018) showed that cells resistant to IFN- γ did not increase p-STAT and p-JAK expression following IFN- γ treatment, suggesting defective pathway signaling (Mimura et al., 2018). It is possible that SCC16-0016 and SMU-092 may also have defective IFN- γ signaling, hence the lack of induction in PD-L1 or PD-L2. Dysfunctional IFN- γ signaling has been implicated in immunotherapy resistance. For example, a loss of function mutation in JAK1 was identified in a patient who have progressed on anti-PD-1 immunotherapy (Zaretsky et al., 2016). Thus, defective IFN- γ signaling in the SCC16-0016 and SMU-092 cell lines may similarly play a role in immunotherapy resistance.

The PD-L1 protein presents as an immunoreactive band between 37 kDa and 50 kDa, typically around 45 kDa on western blots (Li et al., 2016). Our western blotting data for PD-L1 (Figure 13 and 14) also showed presence of a band at this molecular weight in cell lines that express PD-L1. An additional band at around 30 kDa was also observed in some cell lines. Li et al (2016) reported a similar finding when they investigated PD-L1 expression in different cancer cell lines, including melanoma. They were able to confirm that the band at the higher molecular weight was the glycosylated form of PD-L1 while the lower thinner band was non-glycosylated PD-L1. They treated the sample with PNGaseF to remove the *N*-glycans and found that the mass of the non-glycosylated PD-L1 was about 33 kDa (Li et al., 2016).

Due to all the remodelling that glycans undergo, the mass of each glycan can vary. The molecular weight of *N*-glycans is about 1.5-2.2 kDa, therefore a change in 1 *N*-linked chain will be apparent (Freeze and Kranz, 2010). As our western blotting data show a predominant band of higher molecular weight (around 40 kDa) and an additional faint band at 30 kDa, this suggests that the majority of PD-L1 expressed by our melanoma cell lines may also be glycosylated. Figure 17 confirms PD-L1 glycosylation, as treatment with PNGaseF, an enzyme that cleaves *N*-glycans, increased the mobility of PD-L1. In the absence of PNGaseF, bands were visible around 40 kDa, while after PNGaseF treatment, bands were observed at 37kDa or below. However, it is difficult

to make further conclusions as these samples (Figure 17: PNGaseF vs no PNGaseF) were run on separate gels. Ideally this experiment should have been repeated with PNGaseF and no PNGaseF-treated cell lysates being run on the same gel, to determine the exact shift in molecular weight. However due to time limitations this was not possible.

In this chapter, we also compared two different methods of cell lysis. Cells were lysed by sonication or with RIPA buffer and lysates used to probe for PD-L1 and PD-L2 expression. We observed different expression patterns on the western blot membranes for the two cell lysis method. While it is possible that this difference may be due to different exposures when developing the membrane (Alegria-Schaffer et al., 2009; Mahmood and Yang, 2012), it is more likely because of the lysis process.

RIPA is the most optimal lysis process for western blotting as it preserves protein stability, morphology and integrity, it reduces non-specific binding of proteins and allows us to obtain membrane, nuclear and cytoplasmic proteins (Ngoka, 2008). However, sonication was also used because we wanted to treat our cells with PNGaseF, and as ionic detergents inactivate PNGaseF (Freeze and Kranz, 2010), we had to use a lysis method that does not include detergents. Sonication relies on ultrasonic waves creating cycles of low and high pressure which shears the cells due to cavitation, thus releasing the proteins (Brown and Audet, 2008). The longer the cells are exposed to the ultrasonic pressures the increased likelihood of protein denaturation (Zhang and Jin, 2006). Although we only exposed our cells to sonication for 15 s intervals, some protein denaturation may have occurred and may account for the difference in expression patterns on the western blots. It is difficult to determine which cell lysis method is superior, as the appropriate lysis process depends on the application (Brown and Audet, 2008). Based on our results, both seem suitable for PD-L1 and PD-L2 expression however, lysis by sonication seems to produce more bands while lysis by RIPA buffer (Figure 13 and 15, respectively) shows clearer and darker bands.

Although PD-L1 and PD-L2 both bind the same PD-1 receptor, they may have distinct and overlapping functions (Latchman et al., 2001). For example, binding of PD-L1 or PD-L2 to PD-1 has been shown to inhibit T-cell proliferation and activation. PD-L2 additionally downregulates CD4⁺ T cell cytokines while PD-L1 causes cell cycle arrest in the G0 /G1 phase (Latchman et al., 2001; Loke and Allison, 2003). Their difference in function is supported by their difference in expression pattern; expression of PD-L1 and PD-L2 do not always correlate (Gao et al., 2009). For example, cell lines SMU-092 expresses PD-L1 but not PD-L2 (Figures 13, 14, 15 and 16) is evident while PD-L2 expression in that same cell line is absent. This is not unusual as several other studies have also found that although some cell lines express high levels of PD-L1 after IFN- γ treatment, they do not always express PD-L2 (Alavi et al., 2018; Blank et al., 2004; Gao et al.,

2009; Keir et al., 2006). It is tempting to speculate that the distinct expression patterns of PD-L1 and PD-L2 may be indicative of independent and distinct functions.

5. Mass spectrometry of released *N*-glycans from melanoma cells

5.1 Introduction

Glycosylation is a post-translational modification process involving glycans that occurs on a majority of cellular proteins, particularly those found on the cell membrane. This process occurs in the endoplasmic reticulum (ER) and Golgi apparatus. It requires glycotransferases, which are enzymes used to assemble and build glycans onto the protein as well as glycosidases, enzymes that degrade glycans (Sweeney et al., 2018). Glycans are responsible for a range of biological activities, including the maintenance of protein integrity, contributing to the folding and trafficking of proteins, regulation of the immune response, cell growth and differentiation. Amongst the glycans, *N*-linked glycans have predominantly been found to be responsible for these processes, and additionally regulate intracellular signalling and protein interactions within and between cells (Agthe et al., 2018; Fan et al., 1997).

N-glycans are oligosaccharides binding to the amide nitrogen present on an asparagine (Asn) side chain in a Asparagine-X-Serine/Threonine sequence, where 'X' residue cannot be a proline (Cheung and Reithmeier, 2007; Wang, 2005). *N*-glycans are also involved in signalling and interaction between cells and proteins, as well as intracellular signalling (Chen et al., 2018; Cheung and Reithmeier, 2007). Glycosylation patterns and profiles are distinct in cancer compared to non-cancerous tissues suggesting that changes in glycosylation may contribute to tumour progression (Pocheć et al., 2003). It is currently understood that these changes in glycans support growth and survival of cancerous cells and promote metastasis (Marsico et al., 2018).

Glycosylation has also been found to play a crucial part in immunotherapy response and resistance through its effects on PD-1/PD-L1 interaction. In order for the PD-L1 ligand to bind to its PD-1 receptor, glycosylation is mandatory; glycosylation helps stabilise PD-L1 and contributes to its suppressive activity (Li et al., 2018; Li et al., 2016). PD-L1, which is induced via transcriptional activation upon IFN- γ binding to the IFN- γ receptor 1 (IFNGR1), suppresses effector T-cell function (Zaretsky et al., 2016). However, glycogen synthase kinase 3b (GSK3b) cannot phosphorylate and degrade glycosylated PD-L1, indicating that glycosylation of PD-L1 may influence its immunosuppressive activity (Li et al., 2016)

This chapter focuses on the initial characterisation of *N*-glycans on melanoma cells due to their association with tumour progression. Liquid chromatography-mass spectrometry (LC-MS)

analysis of *N*-glycans was performed on three melanoma cell lines, SMU-0404, SMU-092 and SMU-059, to explore the impact of IFN- γ stimulation on the profile of *N*-glycans. These melanoma cell lines were selected as they showed variable responses to IFN- γ stimulation. As shown in Chapters 3 and 4, at baseline and post IFN- γ induction SMU15-0404 had high PD-L2 and HLA-ABC expression while SMU-092 showed no induction of these markers and SMU-059 showed slight induction of both PD-L1 and HLA-ABC (Supplementary Table 1 in Appendix). We investigated differences in *N*-glycan expression between cell lines and in response to IFN- γ .

5.2 Results

5.2.1 Liquid Chromatography – mass spectrometry (LC-MS) spectral analysis of released glycans

Mass spectrometry was performed on three melanoma cell lines to determine the amount and type of *N*-glycans expression, at baseline and after treatment with IFN- γ . These cell lines included SMU15-0404, a cell line that expressed relatively high levels of PD-L2 and HLA-ABC, SMU-092, a cell line that had low expression of HLA-ABC and PD-L2 and SMU-059, a cell line that showed intermediate levels of HLA-ABC and PD-L2 (Supplementary Table 1 in Appendix). To ensure that only *N*-glycans were analysed, samples were treated with PNGaseF, an endoglycosidase that specifically cleaves and removes mammalian *N*-linked glycans from proteins before separation using LC-MS/MS.

Glycan peaks generated from the mass spectrometry were manually analysed by examining the retention time and mass to charge (m/z) ratio. The glycan peaks were observed in different charged states such as carrying a single, double or triple charge (Figure 18).

Glycan peaks were first identified based on retention time (Figure 18A, x axis). When the retention profiles of the control- and IFN- γ -treated samples were compared, we observed similar peak patterns and relative abundance of each peak. The m/z ratio was then used to further separate the glycan peaks (Figure 18B, enlarged peak area between 28 to 35 min), and this allowed more precise comparison of relative abundance. For example, while both control and IFN- γ treated samples showed glycans with identical m/z , such as 893.36, 1038.94 and 1057.4, the relative intensities of these glycans differ between the samples.

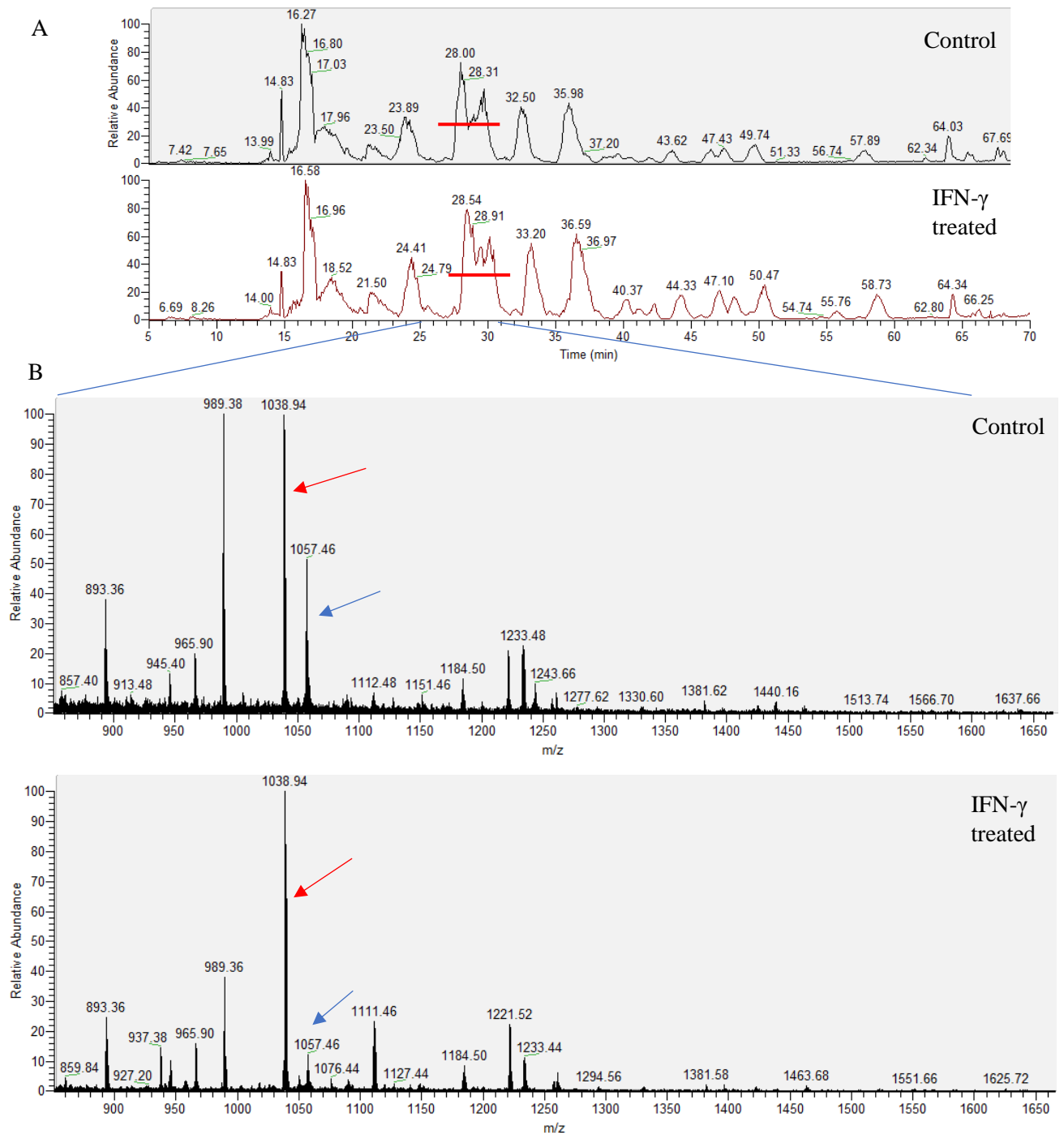
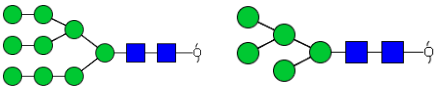
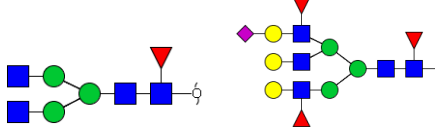
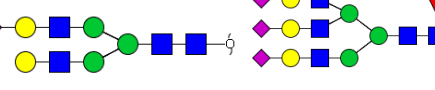
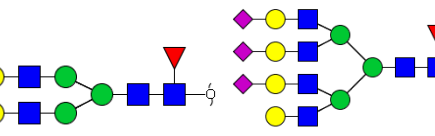


Figure 18. Identification of glycan peaks in the SMU15-0404 cell line in control- and IFN- γ treated samples on Thermo Xcalibur software. A) Base peak chromatogram showing the retention time of each peak (from 5 to 70 min of Liquid Chromatography (LC) elution time; retention time written above each peak) and relative abundance in control (top) and IFN- γ treated (bottom) samples. Mass spectra at retention time of 27 to 32 min were averaged and the glycan the mass to charge ratio determined. (B) The glycans mass to charge ratio (written above each peak) and relative abundance in control (top) and IFN- γ treated (bottom) samples is shown. The glycan with m/z 1057.4 (blue arrow) had a much lower abundance in both samples, compared to the glycan with m/z 1038.9 peak (red arrow).

5.2.2 Glycan composition and abundance of released glycans

To convert the masses seen into possible glycan compositions, the masses of the peaks shown on the m/z spectra were entered into Glycomod (Expasy; <https://web.expasy.org/glycomod/>) to deduce the composition of each glycan. This allowed the generation of potential glycan structures, as shown in Supplementary Table 2 (Appendix) along with their corresponding m/z ratio and relative abundance, drawn using the GlycoWorkbench2 program (Ceroni et al., 2008). Relative abundance of each glycan was calculated using the Skyline software (Figure 19), which required the retention time and m/z data obtained from the Thermo Xcalibur software. The Skyline software provides the relative abundance of each glycan by calculating the area under the curve for each peak. The transition results were then exported to Microsoft Excel to generate a list of glycans organised into categories based on their types and composition. Table 4 gives information on the four main classes of glycans used to group the data and shows the structures using the standard sugar symbols used for each sugar residue (Harvey et al., 2009).

Table 4: Classes used to group glycans in this work

	Description	Example structures
Oligomannose	Glycans are grouped into oligomannose if they consist of only the core <i>N</i> -glycan (Man3GlcNAc2) and only have mannose residues attached (Varki and Schauer, 2009)	 <p>Glycan containing nine mannose residues (left) and glycan containing five mannose residues (right).</p>
Deoxyhexose	Fucose is the most common type of deoxyhexose. It attaches to <i>N</i> -acetylglucosamine and galactose residues in <i>N</i> -glycans. Expression of core-fucose is often elevated in cancer tissue (Staudacher et al., 1999)	 <p>Structures showing one deoxyhexose (left) and showing three deoxyhexose residues (right), respectively.</p>
NeuAc	<i>N</i> -Acetyl-neuraminic Acid (NeuAc) is more commonly known as sialic acid. NeuAc are monosaccharides often found at the terminus of a glycan chain. They attach to <i>N</i> -acetylgalactosamine and galactose residues (Varki and Schauer, 2009)	 <p>Structures showing one NeuAc (left) and three NeuAc residues (right), respectively.</p>
Antennary HexNAc	HexNAc represent two isomers, <i>N</i> -Acetylglucosamine (GlcNAc), a derivative of glucose and <i>N</i> -Acetylgalactosamine (GalNAc), which is derived from galactose. These residues attach to the mannose of the <i>N</i> -glycan core making known as antennary HexNAc (Ren et al., 2007); (Stanley et al., 2009)	 <p>Structures showing two antennary HexNAc (left) and four antennary HexNAc residues, respectively.</p>

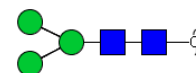
 = mannose residue;

 = *N*-Acetylglucosamine (GlcNAc) residue;

 = *N*-Acetylneuraminic Acid (NeuAc) residue;

 = deoxyhexose residue.

All *N*-glycan structures in images show the common *N*-glycan core (two GlcNAc and three mannose).



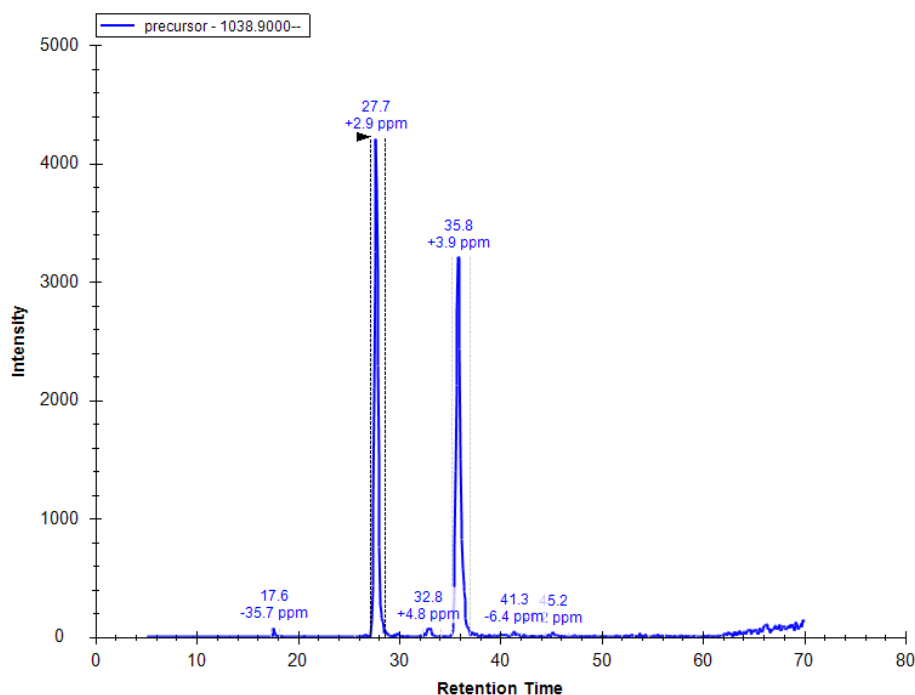


Figure 19. Extracted ion chromatogram of the m/z 1038.9 glycan, and peak area quantitation using the Skyline software. Relative abundance of each peak is calculated by entering the list of potential glycans (from Supplementary Table 2 in Appendix) into the Skyline software. The retention time spectrum shows peaks corresponding to two isoforms of the same composition, (Hex)₂ (HexNAc)₂ (Deoxyhexose)₁ (NeuAc)₁ + (Man)₃(GlcNAc)₂, with retention times of 27.7 min and 35.8 min, and the area under the curve of each peak is calculated to determine relative abundance (intensity).

5.2.3 Comparison of glycan abundance after treatment and across melanoma cell lines

Abundance of glycans relative to total glycans available are shown as a percentage across the four main glycan classes (Table 4) and compared to determine the effects of IFN- γ . In the SMU15-0404 cell line, the relative abundance of oligomannose glycans were very similar between control and IFN- γ treated cells (Figure 20A). The relative abundance of deoxyribose-containing glycans were also similar between control and IFN- γ treated cells. The SMU15-0404 cells showed high levels of 1x deoxyhexose glycans, and low levels of 2x, 3x and 4x deoxyhexose (Figure 20B). The relative abundance of antennary HexNAc- and NeuAc-containing glycans were also similar in IFN- γ treated and control cells (Figure 20C and 3D). Amongst the antennary HexNAc glycans, 2xHexNAc was most abundant, while the abundance of 3x, 4x, 5x and 6x antennary HexNAc, gradually decreases. NeuAc containing glycans, 1x, 2x, 3x and 4x NeuAc were expressed at similar levels regardless of IFN- γ treatment in the SMU15-0404 cell line. Overall, IFN- γ treatment appeared to have little effect on the abundance and composition of *N*-glycans in the SMU15-0404 cell line.

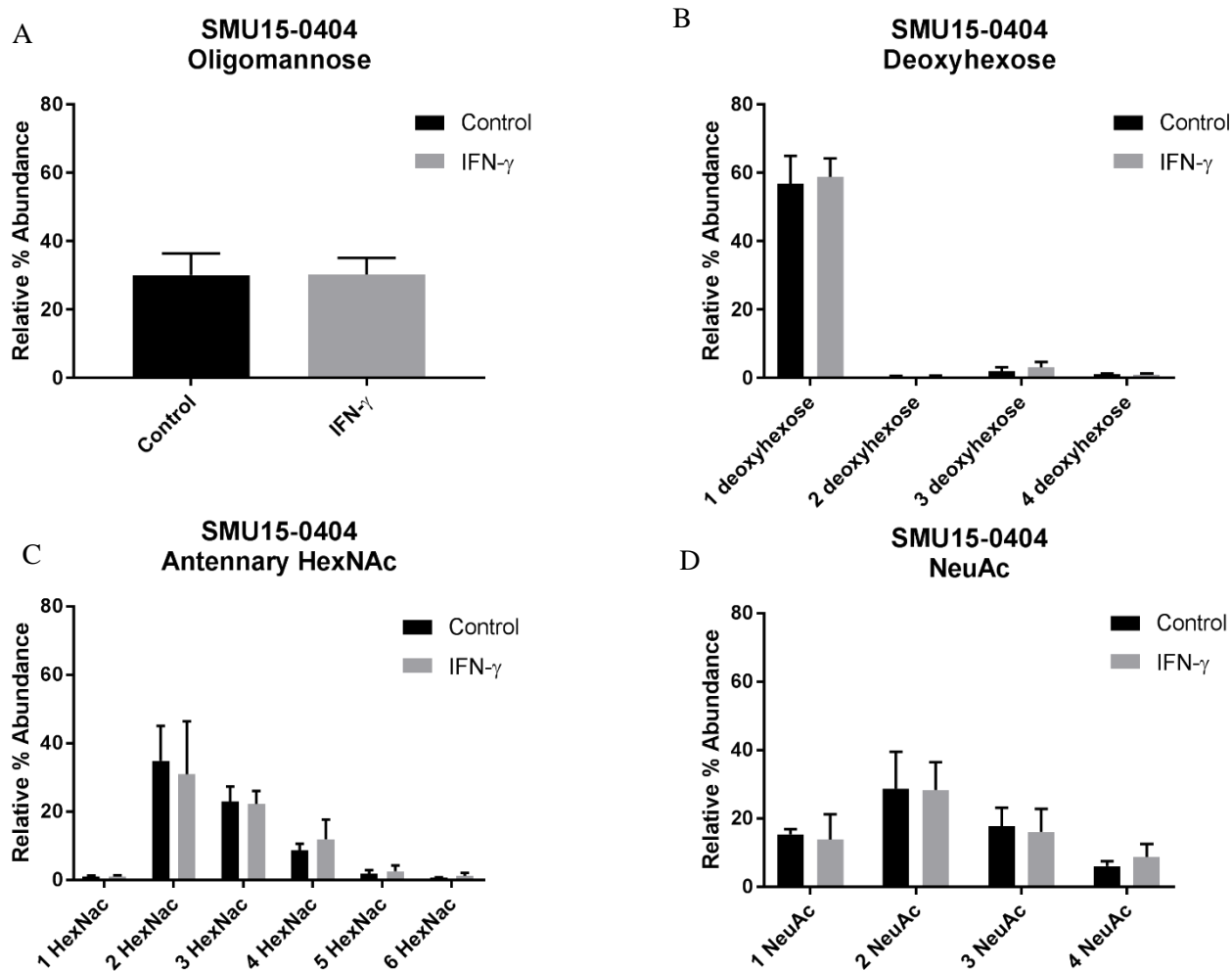


Figure 20. Relative abundance of glycans in SMU15-0404 melanoma cells at baseline and after IFN- γ treatment. A) The relative abundance of oligomannose glycans, B) deoxyribose-containing glycans (including 1x, 2x, 3x and 4x deoxyhexose), C) Antennary HexNAc (1x, 2x, 3x, 4x, 5x and 6x HexNAc) and D) NeuAc-containing glycans (1x, 2x, 3x and 4x NeuAc) in control-and IFN- γ treated SMU15-0404 cells are shown. Data represent three biological replicates and the graph depicts mean \pm standard deviation. Significant was determined using a paired t-test ($*p < 0.05$).

The relative abundance of oligomannose in cell line SMU-092, was very similar between control and IFN- γ treated cells (Figure 21A). The relative abundance of deoxyribose-containing glycans were also similar between control and IFN- γ treated cells. The abundance of deoxyhexose in the SMU-092 cell line decreases as deoxyhexose residues increase. For example, this cell line shows high levels of 1x deoxyhexose glycans at around 80% and a level of 5% or lower in 2x and 3x deoxyhexose and 4x deoxyhexose (Figure 21B). The relative abundance of antennary HexNAc- and NeuAc-containing glycans were also similar in IFN- γ treated and control cells (Figure 21C and 21D). Amongst the HexNAc glyans, 2x antennary HexNAc was most abundant, similarly the 2x NeuAc was also the most abundant in the NeuAc category. These results suggest that IFN- γ

treatment does not have obvious effects on abundance and composition of *N*-glycans in the SMU-092 cell line.

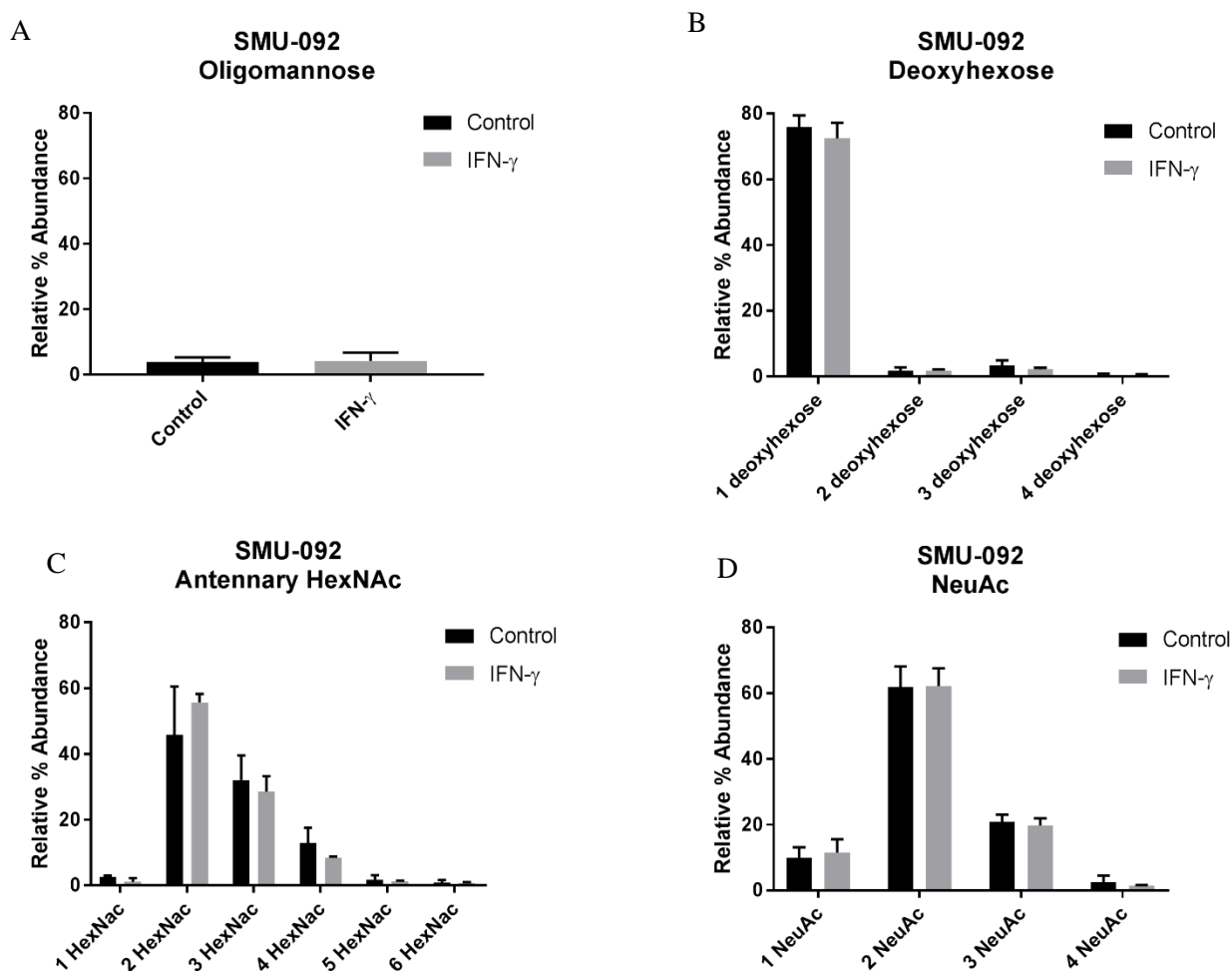


Figure 21. Relative abundance of glycans in SMU-092 melanoma cells at baseline and after IFN- γ treatment. A) The relative abundance of oligomannose glycans, B) deoxyribose-containing glycans (including 1x, 2x, 3x and 4x deoxyhexose), C) HexNAc-containing glycans (1x, 2x, 3x, 4x, 5x and 6x HexNAc) and D) NeuAc-containing glycans (1x, 2x, 3x and 4x NeuAc) in control and IFN- γ treated SMU-092 cells are shown. Data represents three biological replicates and the graph depicts mean \pm standard deviation. Significant was determined using a paired t-test (* $p < 0.05$).

In the SMU15-059 cell line, the relative abundance of oligomannose glycans were very similar between control and IFN- γ treated cells, although there was approximately a 10% increase in cells treated with IFN- γ (Figure 22A). The relative abundance of deoxyribose-containing glycans is highest in 1x deoxyhexose at around 23-30% compared to the 2x or 3x deoxyhexoses which have relative abundance below 5%, however there is no 4x deoxyhexose monosaccharides present in both the control or IFN- γ treated samples (Figure 22B). The abundance of the antennary HexNAc monosaccharide in SMU-059 is lowest in the glycans containing 1x, 4x, 5x and 6x antennary HexNAc and highest in the glycans containing 2x antennary HexNAc (Figure 22C). The abundance of NeuAc monosaccharides is slightly higher in the control samples compared to the

IFN- γ treated samples in glycans with the 1x, 2x and 3x NeuAc, however the glycans containing 4x NeuAc are similar between the control and IFN- γ treated cell, these monosaccharides also have the least abundance at around 3% (Figure 22D). This suggests that although there are slight changes in relative abundance between IFN- γ and control cells, overall IFN- γ treatment appears to have little to no effect on abundance and composition of *N*-glycans in the cell line SMU-059.

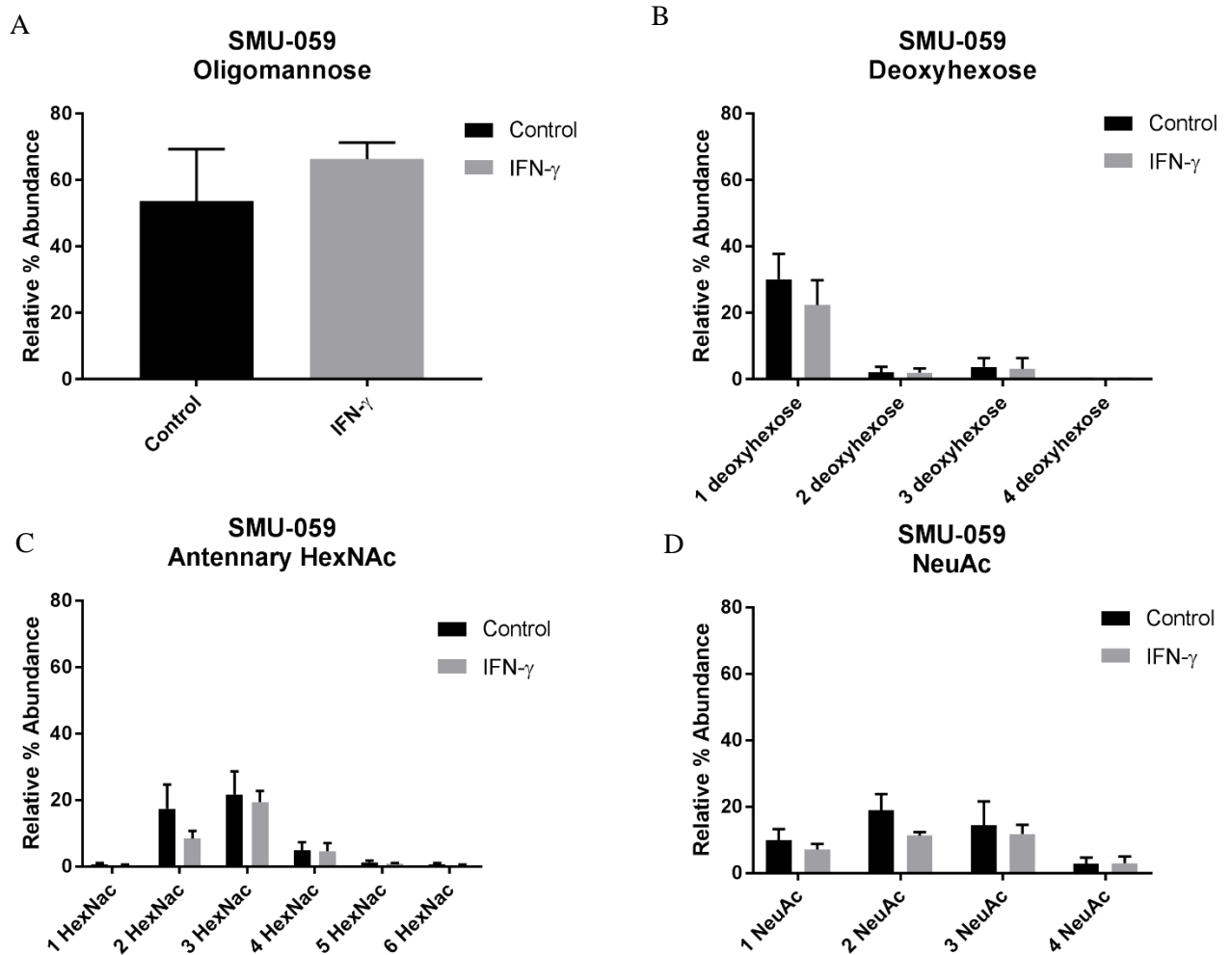


Figure 22. Relative abundance of glycans in SMU-059 melanoma cells at baseline and after IFN- γ treatment. A) The relative abundance of oligomannose glycans, B) deoxyribose-containing glycans (including 1x, 2x, 3x and 4x deoxyhexose), C) Antennary HexNAc-containing glycans (1x, 2x, 3x, 4x, 5x and 6x HexNAc) and D) NeuAc-containing glycans (1x, 2x, 3x and 4x NeuAc) in control (BSA-treated) and IFN- γ treated SMU-059 cells are shown. Data represents three biological replicates and the graph depicts mean \pm standard deviation. Significant was determined using a paired t-test (* p <0.05).

Because IFN- γ treatment had minimal effects on glycan expression in our melanoma cell models, we compared glycan abundance and composition across the different cell lines in the absence of IFN- γ (in control cells). Each cell line showed distinct expression and abundance of *N*-glycans. As shown in Figure 23A, SMU-059 cells had visibly higher expression of oligomannose glycans

(55%) compared to SMU-092, which showed very low expression (4%) while SMU15-0404 had intermediate expression (30%). The number of deoxyhexoses also shows distinct expression between the cell lines (Figure 23B), for example the 1x deoxyhexose is around 30% in SMU-059, but over 50% in SMU15-0404 and SMU-092. The 2x HexNAc (Figure 23C) is highest in cell line SMU-092 at 50%, while it is around 30% and 17% for SMU15-0404 and SMU-059, respectively. Comparing NeuAc, SMU-092 also has the highest 2x NeuAc, consistent with the high 2x HexNAc, as the NeuAc is capping the glycan antennae.

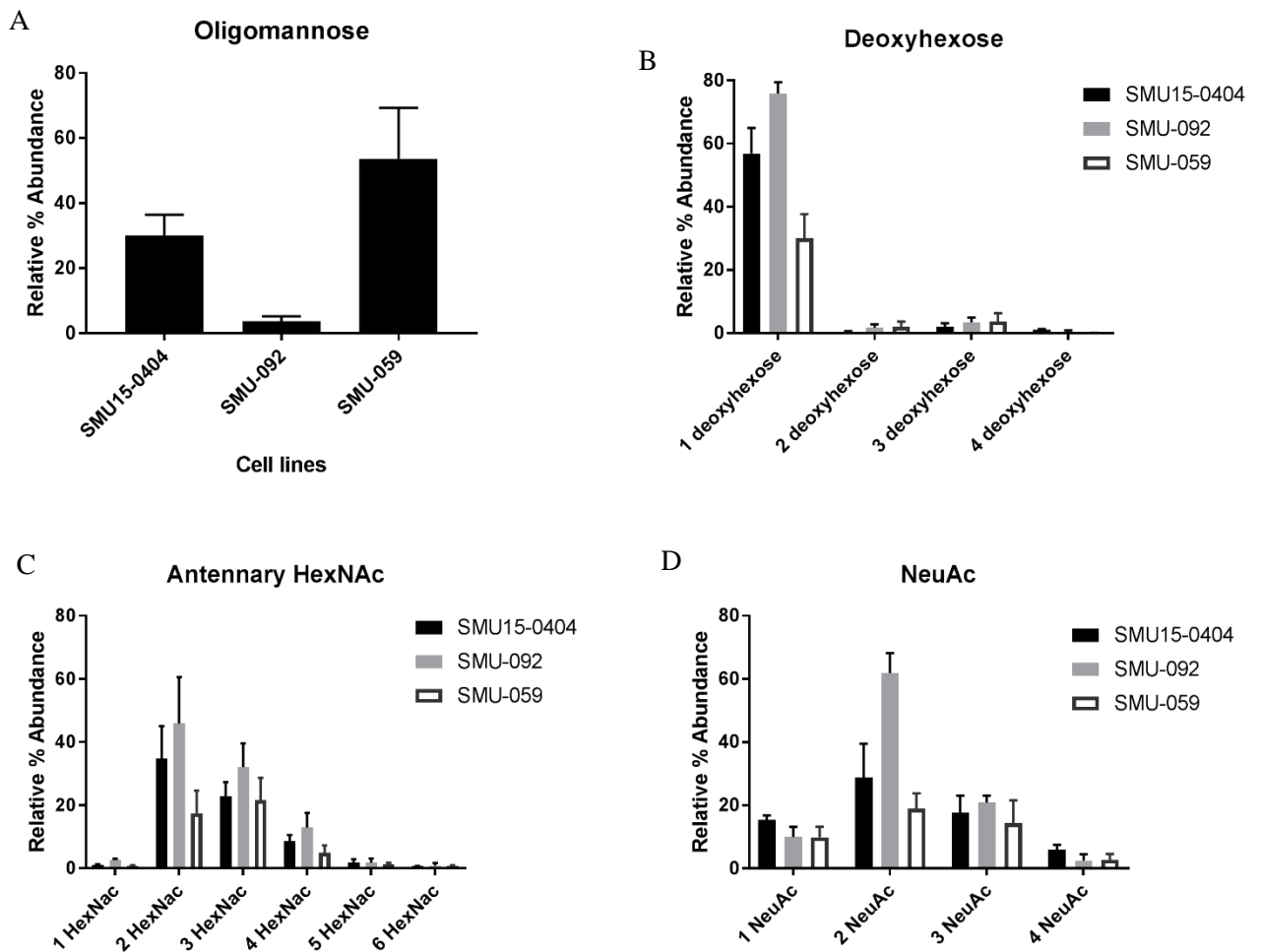


Figure 23. Relative abundance of glycans in melanoma cell lines. All data shown is obtained from control-treated cells. The abundance of A) oligomannose B) deoxyribose C) antennary HexNAc and D) NeuAc varies between all three cell lines. X axis of B, C and D represent the number of the specific glycan residues.

5.3 Discussion

In this study, we investigated whether IFN- γ treatment affected expression and composition of *N*-glycans using liquid chromatography-mass spectrometry. We selected three melanoma cell lines from our panel of 16 PD-1 PROG cell lines that we have previously screened for PD-L2 and HLA-ABC expression (Chapter 3). Our results showed that in each cell model the control and IFN- γ treated samples were similar for the expression and diversity of *N*-glycans. Thus, IFN- γ had little effects on global *N*-glycan expression in these cell lines.

It has been demonstrated that expression of PD-L1 (Dong et al., 2002) and PD-L2 (Wang et al., 2017) in cancer cells is regulated by IFN- γ and stabilised by glycosylation (Shi, 2018). Therefore, we expected to see higher induction of PD-L1 and PD-L2 following IFN- γ treatment and correspondingly higher levels of glycosylation, as PD-L1 is reported to be glycosylated (Li et al., 2018; Li et al., 2016). Thus far, there have been no studies looking at changes in glycosylation levels due to IFN- γ treatment. According to our results (Figure 20, 23, 24) the global glycosylation profile that was carried out does not reflect a significant difference in glycosylation, although this does not preclude protein-specific glycosylation changes. In future analysis, analysis of individual proteins such as PD-L1 and PD-L2 will be necessary to reveal potential effects of glycosylation in the regulation of these immune checkpoint inhibitors. Treatment of tumour cells with tunicamycin, a drug which suppresses *N*-linked glycosylation, significantly decreases PD-L2 expression. The molecular weight of PD-L2 was also reduced following tunicamycin treatment, suggesting that the higher molecular weight isoform may be a result of post-translational glycosylation (Wang et al., 2017). This study highlighted that PD-L2 is glycosylated on tumour cells, and that this modification may be important for its stabilisation and expression, and consequently, its immunosuppressive activity.

N-linked glycosylation has been reported on tumour cells and have been shown to contribute to tumour malignancy. For example, fucosylation is the addition of fucose, a deoxyhexose type monosaccharide, to glycan structures and proteins (Moriwaki and Miyoshi, 2010). Deoxyhexose addition to the core *N*-glycan (Man3GlcNAc2) by fucosyltransferase 8 is termed 'core fucose' (Guo et al., 2018) and the presence and high abundance of core fucosylation is often associated with cancer and inflammation. The level of deoxyhexose in glycans is dramatically high in a range of tumour tissues including breast, colon, liver, pancreatic and non-small cell lung cancer (Guo et al., 2018; Miyoshi et al., 2008). In our results, deoxyhexose was detected in all three melanoma cell lines, with 1x deoxyhexoses (fucose) being most abundant and 4x deoxyhexoses as least abundant (Figure 23B). Similar to a previous study, we detected glycans containing 4x deoxyhexose which have been linked to tumour progression in gastrointestinal cancer as it affects

signalling pathways which impacts immune surveillance (Moriwaki and Miyoshi, 2010). However, the abundance that we observe of these big structures can be under-represented as the method we applied is quantitatively biased against large and highly branched glycans (Abrahams et al., 2015). Although IFN- γ treatment did not change the level of fucosylation across all three samples, the presence of fucosylation may be associated with melanoma progression. However, to confirm this, further experiments are needed to compare expression to those in normal melanocyte tissues.

In addition to deoxyhexose, we examined expression of other *N*-glycans including oligomannose, antennary HexNAc and NeuAc across the three cell lines. The relative abundance of these glycans differed between the cells, thus prompting comparison of oligomannose between all the cell lines. Figure 23 shows that there are in fact differences in total abundance of oligomannose structures between each cell line. The cell lines used in this project for LC-MS glycan analysis were specifically chosen. Cell line SMU15-0404 expresses high PD-L2 and HLA-ABC at baseline (-) and when treated with IFN- γ (+) (MFI fold change for HLA (-) = 43.9; HLA-ABC (+) = 61.9; PD-L2 (-) = 87.5; PD-L2 (+) = 256.0), while cell line SMU-092 expresses low PD-L2 and HLA-ABC at baseline and when treated with IFN- γ with the MFI fold change of less than 1.5 for all categories. Cell line SMU-059 expresses intermediate levels of PD-L2 and HLA-ABC at baseline (-) and when treated with IFN- γ (+) (MFI fold change for HLA (-) = 6.9; HLA-ABC (+) = 29.3; PD-L2 (-) = 11.9; PD-L2 (+) = 36.8), all data is shown in Supplementary Table 1 (Appendix).

The differences in oligomannose structure and abundance across the three cell lines shown in Figure 23, may be explained by the fact that different cell lines are known to display high levels of glycan heterogeneity (Rudd and Dwek, 1997). Heterogeneity can be attributed to the synthesis and degradation of the glycans that occur via glycotransferases and glycosidases, as all proteins undergo different post-translational modification processing steps (Rudd and Dwek, 1997). It is common to find differences in glycans between different samples (Li et al., 2018; Li et al., 2016). Glycan modifications are also affected by differences at the protein level (Kong 2017). It has been shown that PD-L1 expression in tumour tissue is heterogenous (Kong, 2017; McLaughlin et al., 2016). Glycan heterogeneity between the samples is evident in my results as displayed in Supplementary Table 2 (Appendix), there are many isoforms of the glycans present in our samples, which increases the glycan pool and thus heterogeneity.

Although we were able to make sufficient conclusions from the results, it is important to note that there was high variability between and within our three biological replicates (Figure 23). The samples were processed identically following the exact same method and practice (detailed in the Methods section, chapter 2.3); however, there are several steps throughout the cell culture process

that may have caused this variation. The variability in our data may have been due to our use of biological replicates, rather than technical replicates. Although there are studies that have successfully performed mass spectrometry on biological replicates and found little variance (Behrens et al., 2018), there are several other papers that mentioned technical replicates providing higher robustness compared to separate biological samples (Dotz 2018; Shubhakar 2018).

There are many things that affect the process of cell metabolism and glycosylation, and growing cells *in-vitro* are susceptible to more change in glycosylation (Kim et al., 2018). Culture conditions, such as changes in temperature or pH are often associated with glycosylation diversity, as cell metabolism and activity are altered, thus having an effect on post-translation modification processes (Ahn et al., 2008; Kim et al., 2018). The carbon source of cells, which is the medium, also causes changes in glycosylation. Although glucose is an essential source for glycosylation to occur, an increase of glucose cause lactate accumulation in media, therefore affecting glycan profiles (Hossler et al., 2009). Passage number also alters glycosylation; higher passage numbers as well as cells in the late stationary growth phase cause modification in cellular activity (Kim et al., 2018).

Variation can also be attributed to the instrumentation and current technologies used. The field of glycomics is one of the most recent and emerging ‘omics’ platforms (North et al., 2009). However due to its current nature it is associated with many challenges, such as the lack of analytical software, the databases available and the approached towards the analysis(North et al., 2009). Analysis of mass peaks is done manually, and often described as ‘performed by an expert’; this is an issue as most peaks are identified by presumption (von der Lieth et al., 2006). Specific glycan peaks may be easily noticeable by an expert eye; however, it is difficult for an inexperienced individual to efficiently perform peak analysis.

Time consumption, inconsistency and incorrect glycan assignments are some of the most common issues associated with glycan peaks analysis, and this has prompted several researchers to attempt to automate the process. However, several tools still had high ambiguity and still required manual assignment of each mass and glycan (Gotz et al., 2014) or did not work on complex samples such as those found melanoma cells, only simple structures (Walsh et al., 2018). SimGlycan (Apte and Meitei, 2010), a more advanced tool created for automating glycan peak assignment and determining structure. It also gives information on glycan composition, mass, fragments and pathways and enzymes involved (Apte and Meitei, 2010). Similarly another platform, MultiGlycan (Yu et al., 2013), was created with the same aim of advancing and automating the glycan analysis process (Yu et al., 2013). However, it was not possible for us to use these tools as they were not designed for glycan MS data acquired in the negative mode, which is our method of choice (Tsai

and Chen, 2017). Negative-mode was used as it provides a MS spectra which is not as complicated as a positive mode and has been shown that it is more useful for structural identification (Snyder et al., 2017).

The abundance of databases available for glycans and glycoproteins also pose a problem in analysis. There are over 50 glyco-related tools and databases, and the information deposited in each is not robust. Glyco-specific data bases are also not consistent between each other as each is independently archived (Campbell et al., 2013; von der Lieth et al., 2006). This is an issue as each databank has its own standards and in some cases information is deposited in different languages, making it difficult to get consistent results among different databases (North et al., 2009). Another issue with Glyco-databases is that some rely on information found in another database. For example Glycobase (Royle et al., 2008), which has data on over 350 *N*-glycan structures relies on the framework and algorithms of EUROCarbDB (von der Lieth et al., 2010), however this database has been discontinued, therefore affecting data obtained from glycobase (Campbell et al., 2014; Zhao et al., 2018). However, a more recent database, GlycoStore (Zhao et al., 2018), has been created to ensure all past data from across different databases is preserved and integrated in one place and that it is easily accessible (Zhao et al., 2018).

Using technical replicates reduces variation (Ashwood et al., 2018), but may not reveal robust signatures that are important in melanoma development and progression. In summary, this is the first detailed global *N*-glycosylation analysis of melanoma cells treated with IFN- γ and derived from patients progressing on immune checkpoint inhibition. Another significant feature of this study is that the analysis was done at the global total protein level which masks specific glycosylation changes at the protein level such as on PD-L1, however further purification of the protein would allow us to identify the specific proteins. Despite the global glycosylation analysis, differences were seen in the level of oligomannose structures between the cell lines, which may be explained as described above, but it may also give us a new clue to investigate further as to the difference between these melanoma cell lines.

6. General Discussion & Future Directions

Tumour cells expressing PD-L1 and PD-L2 ligands have been associated with the suppression of immune response and evasion of immune attack (Hamanishi et al., 2007; Ma et al., 2016; Marzuka et al., 2015). Typically, PD-L1 expression is important for preventing overactivation of the immune response thus regulating self-tolerance (Ma et al., 2016). However, in cancer cells, the binding of this ligand to its receptor contributes to immune evasion and immune suppression by inhibiting T-cell proliferation and cytokine production (Li et al., 2016). The biological activity and role of PD-L1 is well established (Karachaliou et al., 2018; Mojic et al., 2017), however PD-L2 is not as well researched, making it a point of interest in this study although PD-L2 has been similarly implicated in suppression of T-cell immunity.

Monoclonal antibodies have been developed to block the inhibitory interaction between PD-L1 and PD-L2 with the PD-1 receptor on T-cells. These antibodies, known as immune checkpoint inhibitors, include anti-PD-L1 and anti-PD-1 antibodies. Clinical trials using immune checkpoint inhibitors have shown promising outcomes and have revolutionised the treatment of advanced melanoma (Marzuka et al., 2015). Although immune checkpoint inhibition has been shown to extend the life of patients, not all patients respond to immune checkpoint inhibition. For example, using anti-PD-1 antibodies to block the PD-1 receptor on T-cells initially showed a 40% response rate, and a proportion of patients also progressed after initial response (Postow et al., 2015; Sharma et al., 2017). Several mechanisms of resistance to PD-1 inhibition have been identified, including diminished response to IFN- γ via alterations in the JAK1 downstream effector kinase, altered expression of PD-L1 and PD-L2, and loss of MHC class I expression (Garcia-Diaz et al., 2017; Zaretsky et al., 2016).

Both PD-L1 and PD-L2 are induced by the cytokine IFN- γ , which regulates their expression via the JAK/STAT pathway (Zaretsky et al., 2016). Activation of the JAK/STAT pathway also upregulates the expression of other immune modulating molecules such as the MHC class I antigen presenting molecules, HLA-A, -B and -C. For this study, we examined expression of HLA-ABC and PD-L2 on melanoma cell lines derived from patients who have failed immunotherapy, in order to investigate their expression in immunotherapy resistance.

Most of the 16 cell lines examined in this study expressed PD-L2 and HLA-ABC at baseline, in the absence of IFN- γ . Expression (>1.5 MFI fold change) of PD-L2 at baseline in some cell lines such as SMU15-0404, SMU13-0183 M3, SMU13-0183 M7, SMU16-0150, SCC16-0016, SMU11-0376 M2, SCC15-0111, WMD-084, WMD-084 resistant, SMU-059, SCC15-0534 and

WMD15-083 suggests that it may be a potential immunotherapy resistance mechanism. Elevated expression of PD-L2 (and PD-L1) on tumour cells has been shown to contribute to immune suppression (Mojic et al., 2017).

Patients with high PD-L2 levels are more likely to have tumour recurrence and tumour vascular invasion (Gao et al., 2009). This is in contrast to PD-L1 where expression levels over 5% in melanoma patients was associated with a 36% response rate when treated with PD-1 blockade therapy (Topalian et al., 2015) (Taube et al., 2012; Topalian et al., 2015). Cell lines SCC13-0156 and SMU-092 did not express HLA-ABC at baseline and cell lines SCC13-0156, SMU-092, SCC11-0270 and SMU11-0376 M4 showed no expression of PD-L2 at baseline. Reduced levels of HLA-ABC may diminish recognition of melanoma cells by T cells thus inferring a potential mechanism of resistance to immunotherapy (Concha-Benavente et al., 2016).

Expression of the MHC class I structural component β -2-microglobulin (β 2m) (Figure 3), is also essential for T-cell receptor binding. Consequently, mutations or loss of β 2m expression is linked with immune evasion as antigen presentation for T-cell receptor recognition is abrogated (Cabrera et al., 2003). Patients with no MHC class I expression often display resistance to immune checkpoint blockade, indicating that these molecules are essential for immune recognition of tumour cells (Cabrera et al., 2003). The cell lines that showed low PD-L2 expression at baseline may use a different mechanism to escape treatment. Identifying baseline expression of immune markers may be important for immunotherapy response as expression of these molecules may affect T cell activity.

Melanoma cell lines were also treated with IFN- γ in this study. IFN- γ treatment did not affect melanoma cell growth but did induce HLA-ABC and PD-L2 expression in the majority of cell lines. However, some cell lines did not show any induction when treated with IFN- γ , such as SCC13-0156, SCC16-0016, SMU-092 and SCC15-0534 which showed no HLA-ABC induction and SCC16-0016, SCC11-0270, SMU-092, SMU11-0376 M4 and SMU11-0376 M2 which showed no PD-L2 induction. The level of PD-L2 and HLA-ABC induction was variable amongst cell lines indicating heterogeneity in expression and response to IFN- γ . The difference in response may be due to distinct intracellular signalling mechanisms regulating HLA-ABC and PD-L2 expression in these cell lines (Grenga et al., 2014; Liang et al., 2003). Decreased IFN- γ signalling is associated with diminished adaptive immune response (Sharma et al., 2017) and may be a potential cause of immunotherapy failure (Sharma et al., 2017).

We additionally explored expression of PD-L1 and PD-L2 in these cell lines by western blotting. This detection technique allowed assessment of the protein molecular weight and amount based

on the size and amount of the immunoreactive bands. The relative expression levels of PD-L1 on western blot correlated with levels detected by flow cytometry as cell lines showing MFI fold change over 1.5 by flow cytometry were detected on the western blot. However, expression levels of PD-L2 did not correlate well; some cell lines showing MFI fold change over 1.5 were detected on the western blot but others were not. The inconsistency in PD-L2 expression levels could be due to the different antibody clones used in the two detection methods (flow cytometry vs Western analysis) as they may have non-specific reactivity or may have low detection sensitivity. Due to time constraints, further experiments to explore this discrepancy in PD-L2 accumulation could not be performed, however, it would have been ideal to repeat and optimise the western blot experiments for PD-L2 using different antibody clones.

Regardless, the western blot results did allow us to confirm expression levels of PD-L1 at baseline and after IFN- γ induction in these cell lines, and to some extent, expression levels of PD-L2. In addition, the western blot data also revealed several isoforms of PD-L1 and PD-L2, as bands of slightly different molecular weights were detected, suggesting that these proteins may be post-translationally modified, consistent with previous studies (Li et al., 2018; Li et al., 2016). This prompted us to investigate whether the proteins are glycosylated in the subsequent experiments.

N-glycosylation of PD-L1 contributes to its stabilization, and is also essential for PD-L1 and PD-1 interaction (Li et al., 2016). This may in part contribute to immunotherapy resistance as high levels of glycosylated PD-L1 in the PD-1 PROG cell lines may be indicative of more stable PD-L1 and hence, more immunosuppressive activity. Glycogen synthase kinase 3 β (GSK3 β), the enzyme responsible for induction of protein degradation, plays a role in stabilizing PD-L1 (Li et al., 2018). GSK3 β phosphorylates proteins and this creates a motif for an E3-ubiquitin ligase complex to bind, which initiates protein degradation, thus inhibiting tumour growth (Ding et al., 2007). However, GSK3 β cannot bind glycosylated PD-L1, and it cannot initiate phosphorylation to cause protein degradation. The glycosylated, stable form of PD-L1 (Li et al., 2016), can therefore exert its immunosuppressive activity and promote tumorigenesis (Li et al., 2018; Li et al., 2016). However more work needs to be done on understanding how PD-L1, PD-L2 and PD-1 are affected by glycosylation (Li et al., 2018).

We treated the PD-1 PROG cell lysates with PNGaseF, an enzyme that removes and releases *N*-linked oligosaccharides from glycosylated proteins to examine the glycosylation status of PD-L1 and PD-L2. Cells were lysed with RIPA buffer or by sonication to determine the optimal conditions for PNGaseF as it has been shown that the SDS present in RIPA buffer may inactivate PNGaseF (Freeze and Kranz, 2010). However, both sonication and RIPA buffer lysis showed similar results, suggesting that they may both be used for PNGaseF treatment. Compared to the

untreated samples, PNGaseF treatment appeared to generate PD-L1 bands of lower molecular weights, suggesting that PD-L1 may be glycosylated but because the untreated and PNGaseF-treated samples were run on different SDS PAGE gels, a direct comparison is not possible.

An experiment with the untreated and PNGaseF-treated samples run on the same gel and probed for PD-L1 needed to be performed to definitively determine if PD-L1 is glycosylated, and the extent of glycosylation. However, due to time constraints, this was not possible but would be ideal for future studies. Moreover, we were not able to optimise PD-L2 detection with the antibodies available, hence could not perform the western blotting for PD-L2 in untreated and PNGaseF-treated samples. Other future studies include treating the PD-1 PROG cell lines with tunicamycin, an inhibitor of the *N*-glycosylation pathway (Sun et al., 2016), and compare the glycosylation profiles of PD-L1 and PD-L2.

Since PD-L1 is glycosylated and this may contribute to immunotherapy resistance, we explored the glycosylation status of the PD-1 PROG cell lines further using LC-MS. Three PD-1 PROG cell lines were chosen as they had different expression characteristics; SMU15-0404 expressed high levels of PD-L2 and HLA-ABC, SMU-092 had low expression of HLA-ABC and PD-L2 and SMU-059 showed intermediate levels of HLA-ABC and PD-L2 expression (based on flow cytometry data derived in Chapter 1). Our LC-MS data showed high variability in the expression patterns of glycans among the three cell lines. Several studies have shown that different cell lines expressed specific types of glycans (Guo et al., 2018; Miyoshi et al., 2008) and some specific glycans are linked to tumour malignancy (Moriwaki & Miyoshi, 2010). For example, high abundance of core fucosylation is often associated with cancer and inflammation as it has been observed that the level of core fucose in glycans is dramatically high in a range of tumour tissues (Guo et al., 2018; Miyoshi et al., 2008).

Different levels of deoxyhexoses (fucose) were detected in all three of our melanoma cell lines, 1x deoxyhexoses were the most abundant in all samples and 4x deoxyhexoses were the least abundant. High expression of the enzyme responsible for synthesising deoxyhexose often correlates with the size of the tumour and the level of metastasis (Miyoshi et al., 2008; Zhao et al., 2006). It has been demonstrated that core deoxyhexose on *N*-glycans affects cellular functions and signalling as it increases cell adhesion between cells. These activities may be responsible for metastasis and tumour proliferation (Moriwaki and Miyoshi, 2010; Osumi et al., 2009). This suggests that the deoxyhexoses present on our PD-1 PROG cell lines may alter cell signalling and cell adhesion, and may contribute to tumour proliferation and possibly immunotherapy resistance.

Other *N*-glycosylation residues such as *N*-Acetylglucosamine (GlcNAc) and *N*-Acetylgalactosamine (GalNAc), which are two isoforms of antennary HexNAc (Table 4), are also associated with immune regulation (Pinho and Reis, 2015). In our samples we found that antennary HexNAc was abundant in all three cell lines with 2x, 3x and 4x HexNAc being the most abundant. Specific proteins that bind to HexNAc residues are able to regulate T-cell survival via intracellular signalling, and signalling is dependent on the glycans present on the membrane (Rabinovich and Toscano, 2009). Alteration of these glycans affects signalling and therefore may allow tumours to evade the immune response (Pinho and Reis, 2015). This suggests that the presence of antennary HexNAc in our samples may be target sites for proteins involved in T cell regulation and may have play a role in immunotherapy resistance.

Surprisingly, we found that IFN- γ treatment did not alter the level of *N*-glycosylation across all three PD-1 PROG cells (Figures 3, 4, 5), even though IFN- γ has been shown to upregulate many immune and inflammatory molecules, such as PD-L1 and PD-L2 (Sharma et al., 2017) which have been shown to be glycosylated (Li et al., 2018; Li et al., 2016). However, it is important to note that our LC-MS data looks at global glycosylation levels, and it possible that the levels of PD-L1, PD-L2 and HLA-ABC may be relatively low compared to other proteins, therefore minute glycosylation changes due to IFN- γ treatment may not be detected. Currently there are limited studies on the IFN- γ treatment effects on glycosylation levels and according to what we have found in this study, it appears that IFN- γ may not have dominant effects on global glycosylation levels.

Nevertheless, identifying the glycosylation profiles of the PD-1 PROG cell lines and associating them to treatment response and failure will increase our understanding on the role of glycans in tumour immunity. Currently there are studies using anti-tumour vaccines that target altered glycosylation which may help boost immune response to counteract immunotherapy resistance (Dalziel et al., 2014; Li et al., 2010; Pinho and Reis, 2015).

Due to the complexity of glycan analysis and the time required to manually process the data, we were not able to perform the LC-MS experiments on more cell lines. Ideally it would have been beneficial to perform LC-MS on additional cell lines with similar PD-L2 and HLA-ABC surface marker expression to validate our data. For example, using three different cell lines with high PD-L1, PD-L2 and HLA-ABC expression and three with low expression of these markers. That way we could confirm if the glycosylation profiles of these cell lines are related to the expression of PD-L1, PD-L2 and HLA-ABC.

The LC-MS in this study was used to identify glycosylation profiles, in order to give us a detailed global *N*-glycosylation analysis of the melanoma cells. However, in future studies it would be

interesting to perform glycoproteomic analysis, as opposed to glycomic analysis used in this study, on these cell lines. Glycoproteomic analysis would give us information on exactly which proteins the glycan is attached to, and this would allow us to further investigate the mechanisms involved and answer additional question based on why these patients failed immunotherapy.

6.1 Conclusion

In this study, we sought to identify mechanisms of immunotherapy resistance in PD-1 PROG cell lines derived from melanoma patients who have failed immunotherapy. We showed that majority of the cell lines expressed PD-L1, PD-L2 and HLA-ABC at baseline, and their expression can be upregulated after treatment with IFN- γ . However, some cell lines lacked HLA-ABC expression, showed poor induction of PD-L1, PD-L2 or HLA-ABC, or showed overexpression of PD-L2, and these could be potential resistance mechanisms. By performing LC-MS, we were also able to show differences in the patterns of glycosylation between some PD-1 PROG cell lines. Even though IFN- γ treatment did not alter glycosylation patterns in these cell lines, glycosylation of specific proteins may still contribute to immunotherapy resistance and further studies to investigate this may help improve immunotherapy efficacy and prevent the emergence of resistance.

7. References

- Abbas, A. K., Lichtman, A. H., and Pillai, S. (2014). *Basic immunology: functions and disorders of the immune system*, Elsevier Health Sciences).
- Abrahams, J., Packer, N., and Campbell, M. (2015). Relative quantitation of multi-antennary N-glycan classes: combining PGC-LC-ESI-MS with exoglycosidase digestion. *Analyst* *140*, 5444-5449.
- Adams, J. J., Narayanan, S., Birnbaum, M. E., Sidhu, S. S., Blevins, S. J., Gee, M. H., Sibener, L. V., Baker, B. M., Kranz, D. M., and Garcia, K. C. (2016). Structural interplay between germline interactions and adaptive recognition determines the bandwidth of TCR-peptide-MHC cross-reactivity. *Nature immunology* *17*, 87.
- Agthe, M., Garbers, Y., Grötzinger, J., and Garbers, C. (2018). Two N-Linked Glycans Differentially Control Maturation, Trafficking and Proteolysis, but not Activity of the IL-11 Receptor. *Cellular Physiology and Biochemistry* *45*, 2071-2085.
- Ahn, W. S., Jeon, J. J., Jeong, Y. R., Lee, S. J., and Yoon, S. K. (2008). Effect of culture temperature on erythropoietin production and glycosylation in a perfusion culture of recombinant CHO cells. *Biotechnology and bioengineering* *101*, 1234-1244.
- Ajithkumar, T., Parkinson, C., Fife, K., Corrie, P., and Jefferies, S. (2015). Evolving treatment options for melanoma brain metastases. *The Lancet Oncology* *16*, e486-e497.
- Alavi, S., Stewart, A. J., Kefford, R. F., Lim, S. Y., Shklovskaya, E., and Rizos, H. (2018). Interferon signaling is frequently downregulated in melanoma. *Frontiers in immunology* *9*, 1414.
- Alegria-Schaffer, A., Lodge, A., and Vattem, K. (2009). Performing and optimizing Western blots with an emphasis on chemiluminescent detection. In *Methods in enzymology*. Elsevier), pp. 573-599.
- Apte, A., and Meitei, N. S. (2010). Bioinformatics in glycomics: Glycan characterization with mass spectrometric data using SimGlycan™. In *Functional Glycomics*. Springer), pp. 269-281.
- Arrangoiz, R., Dorantes, J., Cordera, F., Juarez, M. M., Paquentin, E. M., and De León, E. L. (2016). Melanoma review: Epidemiology, risk factors, diagnosis and staging. *J Cancer Treat Res* *4*, 1-15.
- Asano, N. (2003). Glycosidase inhibitors: update and perspectives on practical use. *Glycobiology* *13*, 93R-104R.
- Asao, H., and Fu, X.-Y. (2000). Interferon- γ has dual potentials in inhibiting or promoting cell proliferation. *Journal of Biological Chemistry* *275*, 867-874.
- Ashwood, C., Lin, C.-H., Thaysen-Andersen, M., and Packer, N. H. (2018). Discrimination of Isomers of Released N- and O-Glycans Using Diagnostic Product Ions in Negative Ion PGC-LC-ESI-MS/MS. *Journal of The American Society for Mass Spectrometry*, 1-16.
- Beatty, G. L., and Paterson, Y. (2001). Regulation of tumor growth by IFN- γ in cancer immunotherapy. *Immunologic research* *24*, 201-210.
- Behrens, A.-J., Duke, R. M., Petralia, L. M., Harvey, D. J., Lehoux, S., Magnelli, P. E., Taron, C. H., and Foster, J. M. (2018). Glycosylation profiling of dog serum reveals differences compared to human serum. *Glycobiology* *1*, 7.
- Blank, C., Brown, I., Peterson, A. C., Spiotto, M., Iwai, Y., Honjo, T., and Gajewski, T. F. (2004). PD-L1/B7H-1 inhibits the effector phase of tumor rejection by T cell receptor (TCR) transgenic CD8+ T cells. *Cancer research* *64*, 1140-1145.
- Bromberg, J. F., Horvath, C. M., Wen, Z., Schreiber, R. D., and Darnell, J. E. (1996). Transcriptionally active Stat1 is required for the antiproliferative effects of both interferon alpha and interferon gamma. *Proceedings of the National Academy of Sciences* *93*, 7673-7678.
- Brown, R. B., and Audet, J. (2008). Current techniques for single-cell lysis. *Journal of the Royal Society Interface* *5*, S131-S138.
- Cabrera, T., López-Nevot, M., Gaforio, J., Ruiz-Cabello, F., and Garrido, F. (2003). Analysis of HLA expression in human tumor tissues. *Cancer Immunology, Immunotherapy* *52*, 1-9.
- Campbell, M. P., Peterson, R., Mariethoz, J., Gasteiger, E., Akune, Y., Aoki-Kinoshita, K. F., Lisacek, F., and Packer, N. H. (2013). UniCarbKB: building a knowledge platform for glycoproteomics. *Nucleic acids research* *42*, D215-D221.
- Campbell, M. P., Ranzinger, R., Lütteke, T., Mariethoz, J., Hayes, C. A., Zhang, J., Akune, Y., Aoki-Kinoshita, K. F., Damerell, D., and Carta, G. (2014). Toolboxes for a standardised and systematic study of glycans. *BMC bioinformatics* *15*, S9.

- Cancer Australia (2017). Melanoma of the skin statistics.
- Cerliani, J. P., Blidner, A. G., Toscano, M. A., Croci, D. O., and Rabinovich, G. A. (2017). Translating the 'sugar code' into immune and vascular signaling programs. *Trends in biochemical sciences* *42*, 255-273.
- Ceroni, A., Maass, K., Geyer, H., Geyer, R., Dell, A., and Haslam, S. M. (2008). GlycoWorkbench: a tool for the computer-assisted annotation of mass spectra of glycans. *Journal of proteome research* *7*, 1650-1659.
- Chapman, P. B., Hauschild, A., Robert, C., Haanen, J. B., Ascierto, P., Larkin, J., Dummer, R., Garbe, C., Testori, A., and Maio, M. (2011). Improved survival with vemurafenib in melanoma with BRAF V600E mutation. *New England Journal of Medicine* *364*, 2507-2516.
- Chawla-Sarkar, M., Lindner, D., Liu, Y.-F., Williams, B., Sen, G., Silverman, R., and Borden, E. (2003). Apoptosis and interferons: role of interferon-stimulated genes as mediators of apoptosis. *Apoptosis* *8*, 237-249.
- Chen, L., and Flies, D. B. (2013). Molecular mechanisms of T cell co-stimulation and co-inhibition. *Nature Reviews Immunology* *13*, 227.
- Chen, Y., Ding, L., and Ju, H. (2018). In Situ Cellular Glycan Analysis. *Accounts of chemical research* *51*, 890-899.
- Cheung, J. C., and Reithmeier, R. A. (2007). Scanning N-glycosylation mutagenesis of membrane proteins. *Methods* *41*, 451-459.
- Christiansen, M. N., Chik, J., Lee, L., Anugraham, M., Abrahams, J. L., and Packer, N. H. (2014). Cell surface protein glycosylation in cancer. *Proteomics* *14*, 525-546.
- Cole, D. K., Pumphrey, N. J., Boulter, J. M., Sami, M., Bell, J. I., Gostick, E., Price, D. A., Gao, G. F., Sewell, A. K., and Jakobsen, B. K. (2007). Human TCR-binding affinity is governed by MHC class restriction. *The Journal of Immunology* *178*, 5727-5734.
- Coley, W. B. (1893). THE TREATMENT OF MALIGNANT TUMORS BY REPEATED INOCULATIONS OF ERYSIPELAS: WITH A REPORT OF TEN ORIGINAL CASES. 1. *The American Journal of the Medical Sciences (1827-1924)* *105*, 487.
- Colston, K., Colston, M. J., and Feldman, D. (1981). 1, 25-dihydroxyvitamin D3 and malignant melanoma: the presence of receptors and inhibition of cell growth in culture. *Endocrinology* *108*, 1083-1086.
- Concha-Benavente, F., Srivastava, R. M., Trivedi, S., Lei, Y., Chandran, U., Seethala, R. R., Freeman, G. J., and Ferris, R. L. (2016). Identification of the cell-intrinsic and-extrinsic pathways downstream of EGFR and IFN γ that induce PD-L1 expression in head and neck cancer. *Cancer research* *76*, 1031-1043.
- Dalziel, M., Crispin, M., Scanlan, C. N., Zitzmann, N., and Dwek, R. A. (2014). Emerging principles for the therapeutic exploitation of glycosylation. *Science* *343*, 1235681.
- Davies, H., Bignell, G. R., Cox, C., Stephens, P., Edkins, S., Clegg, S., Teague, J., Woffendin, H., Garnett, M. J., and Bottomley, W. (2002). Mutations of the BRAF gene in human cancer. *Nature* *417*, 949.
- Dhomen, N., and Marais, R. (2009). BRAF signaling and targeted therapies in melanoma. *Hematology/Oncology Clinics* *23*, 529-545.
- Dighe, A. S., Richards, E., Old, L. J., and Schreiber, R. D. (1994). Enhanced in vivo growth and resistance to rejection of tumor cells expressing dominant negative IFN γ receptors. *Immunity* *1*, 447-456.
- Ding, Q., He, X., Hsu, J.-M., Xia, W., Chen, C.-T., Li, L.-Y., Lee, D.-F., Liu, J.-C., Zhong, Q., and Wang, X. (2007). Degradation of Mcl-1 by β -TrCP mediates glycogen synthase kinase 3-induced tumor suppression and chemosensitization. *Molecular and cellular biology* *27*, 4006-4017.
- Dong, H., Strome, S. E., Salomao, D. R., Tamura, H., Hirano, F., Flies, D. B., Roche, P. C., Lu, J., Zhu, G., and Tamada, K. (2002). Tumor-associated B7-H1 promotes T-cell apoptosis: a potential mechanism of immune evasion. *Nature medicine* *8*, 793.
- Elliott, T. M., Whiteman, D. C., Olsen, C. M., and Gordon, L. G. (2017). Estimated healthcare costs of melanoma in Australia over 3 years post-diagnosis. *Applied health economics and health policy* *15*, 805-816.
- Erickson, C., and Driscoll, M. S. (2010). Melanoma epidemic: facts and controversies. *Clinics in dermatology* *28*, 281-286.

- Escorcía, F. E., Postow, M. A., and Barker, C. A. (2017). Radiotherapy and immune checkpoint blockade for melanoma: a promising combinatorial strategy in need of further investigation. *Cancer journal (Sudbury, Mass.)* *23*, 32.
- Fan, H., Meng, W., Kilian, C., Grams, S., and Reutter, W. (1997). Domain-specific N-glycosylation of the membrane glycoprotein dipeptidylpeptidase IV (CD26) influences its subcellular trafficking, biological stability, enzyme activity and protein folding. *European journal of biochemistry* *246*, 243-251.
- Feldman, D., Krishnan, A. V., Swami, S., Giovannucci, E., and Feldman, B. J. (2014). The role of vitamin D in reducing cancer risk and progression. *Nature reviews cancer* *14*, 342.
- Flaherty, K. T., Infante, J. R., Daud, A., Gonzalez, R., Kefford, R. F., Sosman, J., Hamid, O., Schuchter, L., Cebon, J., and Ibrahim, N. (2012). Combined BRAF and MEK inhibition in melanoma with BRAF V600 mutations. *New England Journal of Medicine* *367*, 1694-1703.
- Fonkem, E., Uhlmann, E. J., Floyd, S. R., Mahadevan, A., Kasper, E., Eton, O., and Wong, E. T. (2012). Melanoma brain metastasis: overview of current management and emerging targeted therapies. *Expert review of neurotherapeutics* *12*, 1207-1215.
- Franceschini, D., Franzese, C., Navarra, P., Ascolese, A. M., De Rose, F., Del Vecchio, M., Santoro, A., and Scorsetti, M. (2016). Radiotherapy and immunotherapy: Can this combination change the prognosis of patients with melanoma brain metastases? *Cancer treatment reviews* *50*, 1-8.
- Freeze, H. H., and Kranz, C. (2010). Endoglycosidase and glycoamidase release of N-linked glycans. *Current protocols in protein science* *62*, 12.4. 1-12.4. 25.
- Gao, Q., Wang, X.-Y., Qiu, S.-J., Yamato, I., Sho, M., Nakajima, Y., Zhou, J., Li, B.-Z., Shi, Y.-H., and Xiao, Y.-S. (2009). Overexpression of PD-L1 significantly associates with tumor aggressiveness and postoperative recurrence in human hepatocellular carcinoma. *Clinical Cancer Research* *15*, 971-979.
- García-Díaz, A., Shin, D. S., Moreno, B. H., Saco, J., Escuin-Ordinas, H., Rodríguez, G. A., Zaretsky, J. M., Sun, L., Hugo, W., and Wang, X. (2017). Interferon receptor signaling pathways regulating PD-L1 and PD-L2 expression. *Cell reports* *19*, 1189-1201.
- Garrido, F., and Algarra, I. (2001). MHC antigens and tumor escape from immune surveillance.
- Geller, A. C., Swetter, S. M., and Weinstock, M. A. (2015). Focus on early detection to reduce melanoma deaths. *Journal of Investigative Dermatology* *135*, 947-949.
- Godar, D. E., Subramanian, M., and Merrill, S. J. (2017). Cutaneous malignant melanoma incidences analyzed worldwide by sex, age, and skin type over personal Ultraviolet-B dose shows no role for sunburn but implies one for Vitamin D3. *Dermato-endocrinology* *9*, e1267077.
- Goldberg, S. (2008). Mechanical/physical methods of cell disruption and tissue homogenization. In *2D Page: Sample preparation and fractionation*. Springer), pp. 3-22.
- Gotz, L., Abrahams, J. L., Mariethoz, J., Rudd, P. M., Karlsson, N. G., Packer, N. H., Campbell, M. P., and Lisacek, F. (2014). GlycoDigest: a tool for the targeted use of exoglycosidase digestions in glycan structure determination. *Bioinformatics* *30*, 3131-3133.
- Gough, D. J., Levy, D. E., Johnstone, R. W., and Clarke, C. J. (2008). IFN γ signaling—Does it mean JAK–STAT? *Cytokine & growth factor reviews* *19*, 383-394.
- Goyal, P. K., and Jain, M. K. (2018). Computer-Aided Diagnosis of Melanoma Skin Cancer: A Review. In *Advances in Data and Information Sciences*. Springer), pp. 63-73.
- Gray-Schopfer, V., Wellbrock, C., and Marais, R. (2007). Melanoma biology and new targeted therapy. *Nature* *445*, 851.
- Grenga, I., Donahue, R. N., Lepone, L., Bame, J., Schlom, J., and Farsaci, B. (2014). PD-L1 and MHC-I expression in 19 human tumor cell lines and modulation by interferon-gamma treatment. *Journal for immunotherapy of cancer* *2*, P102.
- Grosso, J., Horak, C. E., Inzunza, D., Cardona, D. M., Simon, J. S., Gupta, A. K., Sankar, V., Park, J.-S., Kollia, G., and Taube, J. M. (2013). Association of tumor PD-L1 expression and immune biomarkers with clinical activity in patients (pts) with advanced solid tumors treated with nivolumab (anti-PD-1; BMS-936558; ONO-4538). *American Society of Clinical Oncology*.
- Guo, D., Guo, J., Li, X., and Guan, F. (2018). Enhanced motility and proliferation by miR-10b/FUT8/p-AKT axis in breast cancer cells. *Oncology letters* *16*, 2097-2104.

- Gupta, S., Vanderbilt, C. M., Cotzia, P., Stella Iii, J. a. A., Chang, J. C., Chen, Y., Tang, L. H., Delair, D. F., Yao, J., and Ladanyi, M. (2018). JAK2, PD-L1, and PD-L2 (9p24. 1) Amplification in Metastatic Mucosal and Cutaneous Melanomas with Durable Response to Immunotherapy. *Human pathology*.
- Hamanishi, J., Mandai, M., Iwasaki, M., Okazaki, T., Tanaka, Y., Yamaguchi, K., Higuchi, T., Yagi, H., Takakura, K., and Minato, N. (2007). Programmed cell death 1 ligand 1 and tumor-infiltrating CD8+ T lymphocytes are prognostic factors of human ovarian cancer. *Proceedings of the National Academy of Sciences* *104*, 3360-3365.
- Hang, I., Lin, C.-W., Grant, O. C., Fleurkens, S., Villiger, T. K., Soos, M., Morbidelli, M., Woods, R. J., Gaus, R., and Aebi, M. (2015). Analysis of site-specific N-glycan remodeling in the endoplasmic reticulum and the Golgi. *Glycobiology* *25*, 1335-1349.
- Harvey, D. J., Merry, A. H., Royle, L., P. Campbell, M., Dwek, R. A., and Rudd, P. M. (2009). Proposal for a standard system for drawing structural diagrams of N- and O-linked carbohydrates and related compounds. *Proteomics* *9*, 3796-3801.
- Herbst, R. S., Soria, J.-C., Kowanetz, M., Fine, G. D., Hamid, O., Gordon, M. S., Sosman, J. A., McDermott, D. F., Powderly, J. D., and Gettinger, S. N. (2014). Predictive correlates of response to the anti-PD-L1 antibody MPDL3280A in cancer patients. *Nature* *515*, 563.
- Hino, R., Kabashima, K., Kato, Y., Yagi, H., Nakamura, M., Honjo, T., Okazaki, T., and Tokura, Y. (2010). Tumor cell expression of programmed cell death-1 ligand 1 is a prognostic factor for malignant melanoma. *Cancer* *116*, 1757-1766.
- Hiroi, M., Mori, K., Sekine, K., Sakaeda, Y., Shimada, J., and Ohmori, Y. (2009). Mechanisms of resistance to interferon-gamma-mediated cell growth arrest in human oral squamous carcinoma cells. *Journal of Biological Chemistry*, jbc. M109. 025932.
- Hossler, P., Khattak, S. F., and Li, Z. J. (2009). Optimal and consistent protein glycosylation in mammalian cell culture. *Glycobiology* *19*, 936-949.
- Hyde, M. A. (2017). Melanoma Risk Factors within the Prostate, Lung, Colorectal, and Ovarian Cancer Screening Trial. The University of Utah).
- Ivashkiv, L. B. (2018). IFN γ : signalling, epigenetics and roles in immunity, metabolism, disease and cancer immunotherapy. *Nature Reviews Immunology*, 1.
- Johnson, H. M., Noon-Song, E. N., Dabelic, R., and Ahmed, C. M. (2013). IFN signaling: how a non-canonical model led to the development of IFN mimetics. *Frontiers in immunology* *4*, 202.
- Kaplan, D. H., Shankaran, V., Dighe, A. S., Stockert, E., Aguet, M., Old, L. J., and Schreiber, R. D. (1998). Demonstration of an interferon γ -dependent tumor surveillance system in immunocompetent mice. *Proceedings of the national academy of sciences* *95*, 7556-7561.
- Karachaliou, N., Gonzalez-Cao, M., Crespo, G., Drozdowskyj, A., Aldegue, E., Gimenez-Capitan, A., Teixido, C., Molina-Vila, M. A., Viteri, S., and De Los Llanos Gil, M. (2018). Interferon gamma, an important marker of response to immune checkpoint blockade in non-small cell lung cancer and melanoma patients. *Therapeutic advances in medical oncology* *10*, 1758834017749748.
- Kefford, R., Ribas, A., Hamid, O., Robert, C., Daud, A., Wolchok, J. D., Joshua, A. M., Hodi, F. S., Gangadhar, T. C., and Hersey, P. (2014). Clinical efficacy and correlation with tumor PD-L1 expression in patients (pts) with melanoma (MEL) treated with the anti-PD-1 monoclonal antibody MK-3475. *American Society of Clinical Oncology*).
- Keir, M. E., Liang, S. C., Guleria, I., Latchman, Y. E., Qipo, A., Albacker, L. A., Koulmanda, M., Freeman, G. J., Sayegh, M. H., and Sharpe, A. H. (2006). Tissue expression of PD-L1 mediates peripheral T cell tolerance. *Journal of Experimental Medicine* *203*, 883-895.
- Kim, S.-M., Chang, K.-H., and Oh, D. J. (2018). Effect of Environmental Parameters on Glycosylation of Recombinant Immunoglobulin G Produced from Recombinant CHO Cells. *Biotechnology and Bioprocess Engineering* *23*, 456-464.
- Kirch, H. C., Putzer, B., Brockmann, D., Esche, H., and Kloke, O. (1997). Formation of the Early-Region-2 Transcription-Factor-1-Retinoblastoma-Protein (E2F-1-RB) TransRepressor and Release of the Retinoblastoma Protein from Nuclear Complexes Containing Cyclin A is Induced by Interferon α in U937V Cells but not in Interferon- α -Resistant U937VR Cells. *European journal of biochemistry* *246*, 736-744.

- Koller, K. M., Mackley, H. B., Liu, J., Wagner, H., Talamo, G., Schell, T. D., Pameijer, C., Neves, R. I., Anderson, B., and Kokolus, K. M. (2017). Improved survival and complete response rates in patients with advanced melanoma treated with concurrent ipilimumab and radiotherapy versus ipilimumab alone. *Cancer biology & therapy* 18, 36-42.
- Kong, T. (2017). *Uncovering A Tumor Intrinsic Role of PD-L1 in Triple Negative Breast Cancer*. McGill University).
- Konieczkowski, D. J., Johannessen, C. M., Abudayyeh, O., Kim, J. W., Cooper, Z. A., Piris, A., Frederick, D. T., Barzily-Rokni, M., Straussman, R., and Haq, R. (2014). A melanoma cell state distinction influences sensitivity to MAPK pathway inhibitors. *Cancer discovery* 4, 816-827.
- Kroon, P., Gadiot, J., Peeters, M., Gasparini, A., Deken, M. A., Yagita, H., Verheij, M., Borst, J., Blank, C. U., and Verbrugge, I. (2016). Concomitant targeting of programmed death-1 (PD-1) and CD137 improves the efficacy of radiotherapy in a mouse model of human BRAFV600-mutant melanoma. *Cancer Immunology, Immunotherapy* 65, 753-763.
- Krutzik, P. O., Irish, J. M., Nolan, G. P., and Perez, O. D. (2004). Analysis of protein phosphorylation and cellular signaling events by flow cytometry: techniques and clinical applications. *Clinical Immunology* 110, 206-221.
- Larkin, J., Chiarion-Sileni, V., Gonzalez, R., Grob, J. J., Cowey, C. L., Lao, C. D., Schadendorf, D., Dummer, R., Smylie, M., and Rutkowski, P. (2015). Combined nivolumab and ipilimumab or monotherapy in untreated melanoma. *New England Journal of Medicine* 373, 23-34.
- Larkin, J., Minor, D., D'angelo, S., Neyns, B., Smylie, M., Miller, W., Gutzmer, R., Linette, G., Chmielowski, B., and Lao, C. D. (2017). Overall survival in patients with advanced melanoma who received Nivolumab versus investigator's choice chemotherapy in checkmate 037: a randomized, controlled, open-label Phase III Trial. *Journal of Clinical Oncology*.
- Latchman, Y., Wood, C. R., Chernova, T., Chaudhary, D., Borde, M., Chernova, I., Iwai, Y., Long, A. J., Brown, J. A., and Nunes, R. (2001). PD-L2 is a second ligand for PD-1 and inhibits T cell activation. *Nature immunology* 2, 261.
- Lee, J., Long, G., Boyd, S., Lo, S., Menzies, A., Tembe, V., Guminski, A., Jakrot, V., Scolyer, R., and Mann, G. (2017). Circulating tumour DNA predicts response to anti-PD1 antibodies in metastatic melanoma. *Annals of Oncology* 28, 1130-1136.
- Li, C.-W., Lim, S.-O., Chung, E. M., Kim, Y.-S., Park, A. H., Yao, J., Cha, J.-H., Xia, W., Chan, L.-C., and Kim, T. (2018). Eradication of triple-negative breast cancer cells by targeting glycosylated PD-L1. *Cancer cell* 33, 187-201. e10.
- Li, C.-W., Lim, S.-O., Xia, W., Lee, H.-H., Chan, L.-C., Kuo, C.-W., Khoo, K.-H., Chang, S.-S., Cha, J.-H., and Kim, T. (2016). Glycosylation and stabilization of programmed death ligand-1 suppresses T-cell activity. *Nature communications* 7, 12632.
- Li, M., Song, L., and Qin, X. (2010). Glycan changes: cancer metastasis and anti-cancer vaccines. *Journal of biosciences* 35, 665-673.
- Liang, S. C., Latchman, Y. E., Buhlmann, J. E., Tomczak, M. F., Horwitz, B. H., Freeman, G. J., and Sharpe, A. H. (2003). Regulation of PD-1, PD-L1, and PD-L2 expression during normal and autoimmune responses. *European journal of immunology* 33, 2706-2716.
- Loke, P. N., and Allison, J. P. (2003). PD-L1 and PD-L2 are differentially regulated by Th1 and Th2 cells. *Proceedings of the National Academy of Sciences* 100, 5336-5341.
- Ma, W., Gilligan, B. M., Yuan, J., and Li, T. (2016). Current status and perspectives in translational biomarker research for PD-1/PD-L1 immune checkpoint blockade therapy. *Journal of hematology & oncology* 9, 47.
- Maguire, O., Collins, C., O'loughlin, K., Miecznikowski, J., and Minderman, H. (2011). Quantifying nuclear p65 as a parameter for NF- κ B activation: Correlation between ImageStream cytometry, microscopy, and Western blot. *Cytometry Part A* 79, 461-469.
- Mahmood, T., and Yang, P.-C. (2012). Western blot: technique, theory, and trouble shooting. *North American journal of medical sciences* 4, 429.
- Maiorano, M., Grob, J.-J., Aamdal, S., Bondarenko, I., Robert, C., Thomas, L., Garbe, C., Chiarion-Sileni, V., Testori, A., and Chen, T.-T. (2015). Five-year survival rates for treatment-naive patients with

- advanced melanoma who received ipilimumab plus dacarbazine in a phase III trial. *Journal of clinical oncology* *33*, 1191-1196.
- Marsico, G., Russo, L., Quondamatteo, F., and Pandit, A. (2018). Glycosylation and Integrin Regulation in Cancer. *Trends in Cancer*.
- Marzuka, A., Huang, L., Theodosakis, N., and Bosenberg, M. (2015). Melanoma treatments: advances and mechanisms. *Journal of cellular physiology* *230*, 2626-2633.
- Mclaughlin, J., Han, G., Schalper, K. A., Carvajal-Hausdorf, D., Pelekanou, V., Rehman, J., Velcheti, V., Herbst, R., Lorusso, P., and Rimm, D. L. (2016). Quantitative assessment of the heterogeneity of PD-L1 expression in non-small-cell lung cancer. *JAMA oncology* *2*, 46-54.
- Meyskens, F. L., Kopecky, K., Samson, M., Hersh, E., Macdonald, J., Jaffe, H., Crowley, J., and Coltman, C. (1990). Recombinant human interferon γ : adverse effects in high-risk stage I and II cutaneous malignant melanoma. *JNCI: Journal of the National Cancer Institute* *82*, 1071-1071.
- Meyskens, F. L., Kopecky, K. J., Taylor, C. W., Noyes, R. D., Tuthill, R. J., Hersh, E. M., Feun, L. G., Doroshow, J. H., Flaherty, L. E., and Sondak, V. K. (1995). Randomized trial of adjuvant human interferon gamma versus observation in high-risk cutaneous melanoma: a Southwest Oncology Group study.
- Michielin, O., and Hoeller, C. (2015). Gaining momentum: New options and opportunities for the treatment of advanced melanoma. *Cancer treatment reviews* *41*, 660-670.
- Mimura, K., Teh, J. L., Okayama, H., Shiraishi, K., Kua, L. F., Koh, V., Smoot, D. T., Ashktorab, H., Oike, T., and Suzuki, Y. (2018). PD-L1 expression is mainly regulated by interferon gamma associated with JAK-STAT pathway in gastric cancer. *Cancer science* *109*, 43-53.
- Miyoshi, E., Moriwaki, K., and Nakagawa, T. (2008). Biological function of fucosylation in cancer biology. *Journal of biochemistry* *143*, 725-729.
- Mojic, M., Takeda, K., and Hayakawa, Y. (2017). The Dark Side of IFN- γ : Its Role in Promoting Cancer Immuno-evasion. *International journal of molecular sciences* *19*, 89.
- Moriwaki, K., and Miyoshi, E. (2010). Fucosylation and gastrointestinal cancer. *World journal of hepatology* *2*, 151.
- Neubert, N. J., Tillé, L., Barras, D., Sonesson, C., Baumgaertner, P., Rimoldi, D., Gfeller, D., Delorenzi, M., Marraco, S. a. F., and Speiser, D. E. (2017). Broad and conserved immune regulation by genetically heterogeneous melanoma cells. *Cancer research*.
- Ngoka, L. C. (2008). Sample prep for proteomics of breast cancer: proteomics and gene ontology reveal dramatic differences in protein solubilization preferences of radioimmunoprecipitation assay and urea lysis buffers. *Proteome science* *6*, 30.
- North, S. J., Hitchen, P. G., Haslam, S. M., and Dell, A. (2009). Mass spectrometry in the analysis of N-linked and O-linked glycans. *Current opinion in structural biology* *19*, 498-506.
- Nozawa, H., Oda, E., Ueda, S., Tamura, G., Maesawa, C., Muto, T., Taniguchi, T., and Tanaka, N. (1998). Functionally inactivating point mutation in the tumor-suppressor IRF-1 gene identified in human gastric cancer. *International journal of cancer* *77*, 522-527.
- Osumi, D., Takahashi, M., Miyoshi, E., Yokoe, S., Lee, S. H., Noda, K., Nakamori, S., Gu, J., Ikeda, Y., and Kuroki, Y. (2009). Core fucosylation of E-cadherin enhances cell-cell adhesion in human colon carcinoma WiDr cells. *Cancer science* *100*, 888-895.
- Pamer, E., and Cresswell, P. (1998). Mechanisms of MHC class I-restricted antigen processing. *Annual review of immunology* *16*, 323-358.
- Parker, B. S., Rautela, J., and Hertzog, P. J. (2016). Antitumour actions of interferons: implications for cancer therapy. *Nature Reviews Cancer* *16*, 131.
- Partridge, E. A., Le Roy, C., Di Guglielmo, G. M., Pawling, J., Cheung, P., Granovsky, M., Nabi, I. R., Wrana, J. L., and Dennis, J. W. (2004). Regulation of cytokine receptors by Golgi N-glycan processing and endocytosis. *Science* *306*, 120-124.
- Patel, S. P., and Kurzrock, R. (2015). PD-L1 expression as a predictive biomarker in cancer immunotherapy. *Molecular cancer therapeutics* *14*, 847-856.
- Pinho, S. S., and Reis, C. A. (2015). Glycosylation in cancer: mechanisms and clinical implications. *Nature Reviews Cancer* *15*, 540.

- Pocheć, E., Lityńska, A., Amoresano, A., and Casbarra, A. (2003). Glycosylation profile of integrin $\alpha 3\beta 1$ changes with melanoma progression. *Biochimica et Biophysica Acta (BBA)-Molecular Cell Research* 1643, 113-123.
- Postow, M. A., Chesney, J., Pavlick, A. C., Robert, C., Grossmann, K., Mcdermott, D., Linette, G. P., Meyer, N., Giguere, J. K., and Agarwala, S. S. (2015). Nivolumab and ipilimumab versus ipilimumab in untreated melanoma. *New England Journal of Medicine* 372, 2006-2017.
- Queen, L. (2017). *Skin Cancer: Causes, Prevention, and Treatment*.
- Rabinovich, G. A., and Toscano, M. A. (2009). Turning'sweet'on immunity: galectin–glycan interactions in immune tolerance and inflammation. *Nature Reviews Immunology* 9, 338.
- Rastrelli, M., Tropea, S., Rossi, C. R., and Alaibac, M. (2014). Melanoma: epidemiology, risk factors, pathogenesis, diagnosis and classification. *In vivo* 28, 1005-1011.
- Ren, J. M., Rejtar, T., Li, L., and Karger, B. L. (2007). N-Glycan structure annotation of glycopeptides using a linearized glycan structure database (GlyDB). *Journal of proteome research* 6, 3162-3173.
- Robert, C., Long, G. V., Brady, B., Dutriaux, C., Maio, M., Mortier, L., Hassel, J. C., Rutkowski, P., Mcneil, C., and Kalinka-Warzocha, E. (2015a). Nivolumab in previously untreated melanoma without BRAF mutation. *New England journal of medicine* 372, 320-330.
- Robert, C., Schachter, J., Long, G. V., Arance, A., Grob, J. J., Mortier, L., Daud, A., Carlino, M. S., Mcneil, C., and Lotem, M. (2015b). Pembrolizumab versus ipilimumab in advanced melanoma. *New England Journal of Medicine* 372, 2521-2532.
- Rock, K. L., Reits, E., and Neefjes, J. (2016). Present yourself! By MHC class I and MHC class II molecules. *Trends in immunology* 37, 724-737.
- Rodig, N., Ryan, T., Allen, J. A., Pang, H., Grabie, N., Chernova, T., Greenfield, E. A., Liang, S. C., Sharpe, A. H., and Lichtman, A. H. (2003). Endothelial expression of PD-L1 and PD-L2 down-regulates CD8+ T cell activation and cytotoxicity. *European journal of immunology* 33, 3117-3126.
- Rossjohn, J., Gras, S., Miles, J. J., Turner, S. J., Godfrey, D. I., and Mccluskey, J. (2015). T cell antigen receptor recognition of antigen-presenting molecules. *Annual review of immunology* 33, 169-200.
- Royle, L., Campbell, M. P., Radcliffe, C. M., White, D. M., Harvey, D. J., Abrahams, J. L., Kim, Y.-G., Henry, G. W., Shadick, N. A., and Weinblatt, M. E. (2008). HPLC-based analysis of serum N-glycans on a 96-well plate platform with dedicated database software. *Analytical biochemistry* 376, 1-12.
- Rudd, P. M., and Dwek, R. A. (1997). Glycosylation: heterogeneity and the 3D structure of proteins. *Critical reviews in biochemistry and molecular biology* 32, 1-100.
- Salatino, M., Girotti, M. R., and Rabinovich, G. A. (2018). Glycans Pave the Way for Immunotherapy in Triple-Negative Breast Cancer. *Cancer cell* 33, 155-157.
- Saper, M., Bjorkman, P., and Wiley, D. (1991). Refined structure of the human histocompatibility antigen HLA-A2 at 2.6 Å resolution. *Journal of molecular biology* 219, 277-319.
- Sharma, P., Hu-Lieskovan, S., Wargo, J. A., and Ribas, A. (2017). Primary, adaptive, and acquired resistance to cancer immunotherapy. *Cell* 168, 707-723.
- Sharpe, A. H., Wherry, E. J., Ahmed, R., and Freeman, G. J. (2007). The function of programmed cell death 1 and its ligands in regulating autoimmunity and infection. *Nature immunology* 8, 239.
- Shi, Y. (2018). Regulatory mechanisms of PD-L1 expression in cancer cells. *Cancer Immunology, Immunotherapy*, 1-9.
- Shin, D. S., Zaretsky, J. M., Escuin-Ordinas, H., Garcia-Diaz, A., Hu-Lieskovan, S., Kalbasi, A., Grasso, C. S., Hugo, W., Sandoval, S., and Torrejon, D. Y. (2017). Primary resistance to PD-1 blockade mediated by JAK1/2 mutations. *Cancer discovery* 7, 188-201.
- Snyder, C. M., Zhou, X., Karty, J. A., Fonslow, B. R., Novotny, M. V., and Jacobson, S. C. (2017). Capillary electrophoresis–mass spectrometry for direct structural identification of serum N-glycans. *Journal of Chromatography A* 1523, 127-139.
- Stanley, P., Schachter, H., and Taniguchi, N. (2009). *Essentials of glycobiology*, (Cold Spring Harbor, NY, Cold Spring Harbor Laboratory Press).
- Staudacher, E., Altmann, F., Wilson, I. B., and März, L. (1999). Fucose in N-glycans: from plant to man. *Biochimica et Biophysica Acta (BBA)-General Subjects* 1473, 216-236.

- Sun, S., Shah, P., Eshghi, S. T., Yang, W., Trikannad, N., Yang, S., Chen, L., Aiyetan, P., Höti, N., and Zhang, Z. (2016). Comprehensive analysis of protein glycosylation by solid-phase extraction of N-linked glycans and glycosite-containing peptides. *Nature biotechnology* 34, 84.
- Sun, S., and Zhang, H. (2015). Identification and validation of atypical N-glycosylation sites. *Analytical chemistry* 87, 11948-11951.
- Sweeney, J. G., Liang, J., Antonopoulos, A., Giovannone, N., Kang, S., Mondala, T. S., Head, S. R., King, S. L., Tani, Y., and Brackett, D. (2018). Loss of GCNT2/I-branched glycans enhances melanoma growth and survival. *Nature communications* 9, 3368.
- Tang, F., and Zheng, P. (2018). Tumor cells versus host immune cells: whose PD-L1 contributes to PD-1/PD-L1 blockade mediated cancer immunotherapy? *Cell & bioscience* 8, 34.
- Taube, J. M., Anders, R. A., Young, G. D., Xu, H., Sharma, R., Mcmillan, T. L., Chen, S., Klein, A. P., Pardoll, D. M., and Topalian, S. L. (2012). Colocalization of inflammatory response with B7-h1 expression in human melanocytic lesions supports an adaptive resistance mechanism of immune escape. *Science translational medicine* 4, 127ra37-127ra37.
- Thompson, R. H., Kuntz, S. M., Leibovich, B. C., Dong, H., Lohse, C. M., Webster, W. S., Sengupta, S., Frank, I., Parker, A. S., and Zincke, H. (2006). Tumor B7-H1 is associated with poor prognosis in renal cell carcinoma patients with long-term follow-up. *Cancer research* 66, 3381-3385.
- Topalian, S. L., Drake, C. G., and Pardoll, D. M. (2015). Immune checkpoint blockade: a common denominator approach to cancer therapy. *Cancer cell* 27, 450-461.
- Tsai, P.-L., and Chen, S.-F. (2017). A brief review of bioinformatics tools for glycosylation analysis by mass spectrometry. *Mass Spectrometry* 6, S0064-S0064.
- Varki, A., and Lowe, J. B. (2009). Biological roles of glycans. In *Essentials of Glycobiology*. 2nd edition. Cold Spring Harbor Laboratory Press, pp.
- Varki, A., and Schauer, R. (2009). Chapter 14. Sialic acids. *Essentials of glycobiology*, 2nd ed. Cold Spring Harbor Laboratory Press, Cold Spring Harbor, NY.
- Veness, M. J., Morgan, G. J., Palme, C. E., and Gebski, V. (2005). Surgery and adjuvant radiotherapy in patients with cutaneous head and neck squamous cell carcinoma metastatic to lymph nodes: combined treatment should be considered best practice. *The Laryngoscope* 115, 870-875.
- Von Der Lieth, C.-W., Freire, A. A., Blank, D., Campbell, M. P., Ceroni, A., Damerell, D. R., Dell, A., Dwek, R. A., Ernst, B., and Fogh, R. (2010). EUROCarbDB: an open-access platform for glycoinformatics. *Glycobiology* 21, 493-502.
- Von Der Lieth, C.-W., Lütteke, T., and Frank, M. (2006). The role of informatics in glycobiology research with special emphasis on automatic interpretation of MS spectra. *Biochimica et Biophysica Acta (BBA)-General Subjects* 1760, 568-577.
- Walsh, I., Nguyen-Khuong, T., Wongtrakul-Kish, K., Tay, S. J., Chew, D., Tasha, J., Taron, C. H., Rudd, P. M., and Valencia, A. (2018). GlycanAnalyzer: software for automated interpretation of N-glycan profiles after exoglycosidase digestions. *Bioinformatics*.
- Wang, H., Yao, H., Li, C., Liang, L., Zhang, Y., Shi, H., Zhou, C., Chen, Y., Fang, J.-Y., and Xu, J. (2017). PD-L2 expression in colorectal cancer: Independent prognostic effect and targetability by deglycosylation. *Oncoimmunology* 6, e1327494.
- Wang, P.-H. (2005). Altered glycosylation in cancer: sialic acids and sialyltransferases. *J Cancer Mol* 1, 73-81.
- Wild, R., Kowal, J., Eyring, J., Ngwa, E. M., Aebi, M., and Locher, K. P. (2018). Structure of the yeast oligosaccharyltransferase complex gives insight into eukaryotic N-glycosylation. *Science* 359, 545-550.
- Wolchok, J. D., Kluger, H., Callahan, M. K., Postow, M. A., Rizvi, N. A., Lesokhin, A. M., Segal, N. H., Ariyan, C. E., Gordon, R.-A., and Reed, K. (2013). Nivolumab plus ipilimumab in advanced melanoma. *New England Journal of Medicine* 369, 122-133.
- Yamaguchi, H., Hiroi, M., and Ohmori, Y. (2018). Silencing of the interferon-inducible gene Ifi204/p204 induces resistance to interferon- γ -mediated cell growth arrest of tumor cells. *Cytokine*.
- Young, H. A., and Hardy, K. J. (1995). Role of interferon- γ in immune cell regulation. *Journal of Leukocyte biology* 58, 373-381.

- Yu, C.-Y., Mayampurath, A., Hu, Y., Zhou, S., Mechref, Y., and Tang, H. (2013). Automated annotation and quantification of glycans using liquid chromatography–mass spectrometry. *Bioinformatics* 29, 1706-1707.
- Zaidi, M. R., and Merlino, G. (2011). The two faces of interferon- γ in cancer. *Clinical cancer research* 17, 6118-6124.
- Zaretsky, J. M., Garcia-Diaz, A., Shin, D. S., Escuin-Ordinas, H., Hugo, W., Hu-Lieskovan, S., Torrejon, D. Y., Abril-Rodriguez, G., Sandoval, S., and Barthly, L. (2016). Mutations associated with acquired resistance to PD-1 blockade in melanoma. *New England Journal of Medicine* 375, 819-829.
- Zhang, H., and Jin, W. (2006). Single-cell analysis by intracellular immuno-reaction and capillary electrophoresis with laser-induced fluorescence detection. *Journal of chromatography A* 1104, 346-351.
- Zhao, S., Walsh, I., Abrahams, J. L., Royle, L., Nguyen-Khuong, T., Spencer, D., Fernandes, D. L., Packer, N. H., Rudd, P. M., and Campbell, M. P. (2018). GlycoStore: a database of retention properties for glycan analysis. *Bioinformatics* 1, 2.
- Zhao, Y., Itoh, S., Wang, X., Isaji, T., Miyoshi, E., Kariya, Y., Miyazaki, K., Kawasaki, N., Taniguchi, N., and Gu, J. (2006). Deletion of core fucosylation on $\alpha 3\beta 1$ integrin down-regulates its functions. *Journal of Biological Chemistry*.
- Zhao, Y. Y., Takahashi, M., Gu, J. G., Miyoshi, E., Matsumoto, A., Kitazume, S., and Taniguchi, N. (2008). Functional roles of N-glycans in cell signaling and cell adhesion in cancer. *Cancer science* 99, 1304-1310.
- Zitelli, J. A., Brown, C., and Hanusa, B. H. (1997). Mohs micrographic surgery for the treatment of primary cutaneous melanoma. *Journal of the American Academy of Dermatology* 37, 236-245.
- Zou, W., Wolchok, J. D., and Chen, L. (2016). PD-L1 (B7-H1) and PD-1 pathway blockade for cancer therapy: Mechanisms, response biomarkers, and combinations. *Science translational medicine* 8, 328rv4-328rv4.

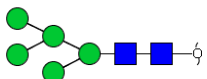
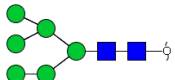
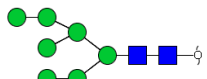
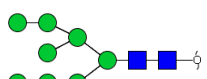
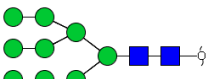
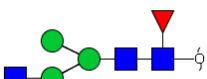
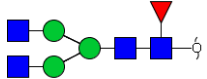
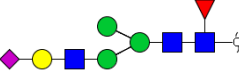
8. Appendix

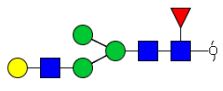
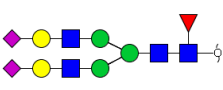
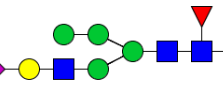
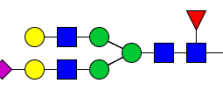
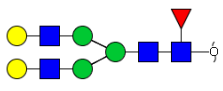
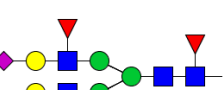
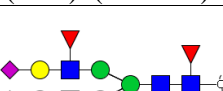
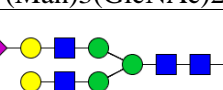
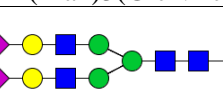
Supplementary Table 1: Mean fluorescent intensity of cells that underwent flow cytometry analysis. Table shows mean of triplicates of each cell line, analysis performed on FlowJo software (TreeStar, Ashland, OR). CU=control unstained; IFNU= IFN- γ unstained.

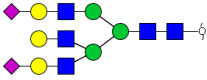
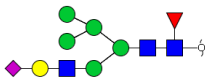
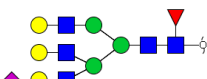
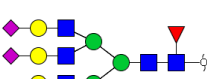
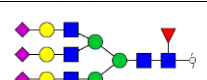
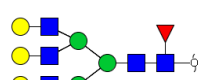
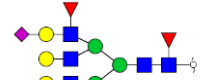
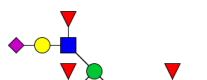
	Mean fluorescent intensity for HLA-ABC							Mean fluorescent intensity for PD-L2						
					Baseline HLA-ABC Fold Δ	IFN- γ treated HLA-ABC Fold Δ	Level of HLA-ABC induction Fold Δ					Baseline PD-L2 Fold Δ	IFN- γ treated PD-L2 Fold Δ	Level of PD-L2 induction Fold Δ
	Control unstained	Control stained	IFN- γ stained	IFN- γ unstained	Control / CU	IFN/IFNU	(IFN/IFNU)/(Control /CU)	Control unstained	Control stained	IFN- γ stained	IFN- γ unstained	Control / CU	IFN/IFNU	(IFN/IFNU)/(Control /CU)
NEW MACHINE														
SCC13-0156 mean	300.3	320.7	407.7	314.0	1.1	1.5	1.4	302.1	316.0	501.7	316.0	1.1	2.1	1.9
SMU15-0404 M3 mean	204.3	8403.7	13380.0	234.0	43.9	61.9	1.4	138.9	11820.7	36437.7	149.1	87.5	256.0	2.9
SMU13-0183 M3 mean	529.1	6779.3	9233.7	569.0	13.5	17.5	1.3	361.3	3405.0	9001.0	406.7	10.0	22.5	2.3
SMU13-0183 M7 mean	161.3	2557.3	3658.7	180.7	15.7	20.2	1.3	153.3	2857.0	10329.3	177.3	18.9	59.9	3.2
SMU16-0150 mean	274.3	2252.3	3086.3	245.0	9.7	13.8	1.1	259.3	2592.3	8122.3	270.0	11.4	34.3	3.1
SCC16-0016 mean	277.0	847.5	884.5	270.5	3.3	3.4	1.0	203.0	574.0	617.0	201.5	2.8	3.1	1.1
OLD MACHINE														
SCC16-0016 mean	224.0	894.5	923.7	216.9	6.7	7.2	1.1	135.0	488.0	479.5	121.0	3.7	4.0	1.1
SMU-092 M2 mean	239.0	244.1	238.3	241.0	1.0	1.0	1.0	52.8	57.4	75.1	54.0	1.1	1.4	1.3

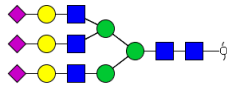
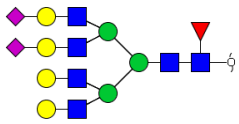
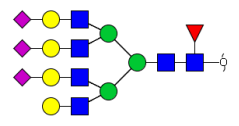
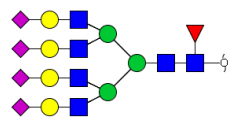
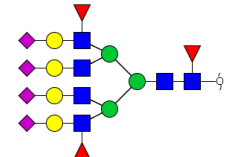
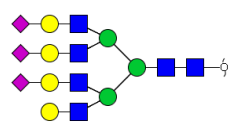
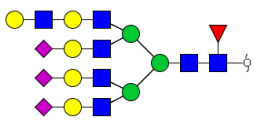
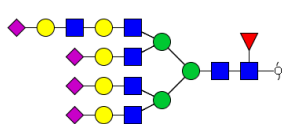
SMU11-0376 M4 mean	142.0	2128.3	5731.0	146.3	14.9	38.9	2.8	106.9	110.5	136.7	120.7	1.1	1.1	1.1
SMU11-0376 M2 mean	184.3	4421.3	8860.3	193.0	23.8	45.4	1.9	156.7	171.7	279.3	177.3	1.1	1.6	1.4
SCC15-0111 M3 mean	133.7	2418.7	7014.0	130.3	18.2	53.8	3.0	93.2	142.3	324.0	97.9	1.5	3.3	2.2
WMD-084 M3 mean	150.0	2057.3	5148.7	160.3	13.9	32.2	2.4	147.3	153.3	411.0	152.7	1.1	2.7	2.5
SCC-0270 mean	86.8	678.0	1291.3	87.5	7.8	14.7	1.9	77.1	82.8	100.4	85.7	1.1	1.2	1.1
SMU-059 mean	87.4	608.3	2508.7	85.9	6.9	29.3	4.2	74.9	886.3	2693.7	73.2	11.9	36.8	3.1
SCC15-0534 mean	71.5	2736.7	3674.3	77.0	39.1	48.4	1.3	64.1	4012.0	11212. 3	65.4	63.8	186.9	2.8
WMD-15-083 mean	60.5	1403.7	3493.3	61.0	23.2	57.3	2.5	50.5	1700.7	5082.0	54.1	33.7	94.6	2.8
WMD-084 resistant mean	90.0	1469.3	4315.7	93.0	16.6	47.2	2.8	84.2	2114.0	11577. 3	88.0	25.1	131.4	5.2

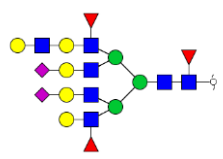
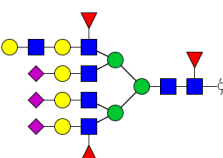
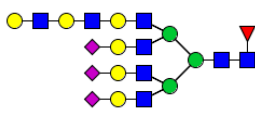
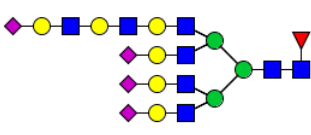
Supplementary Table 2: Representative glycan structures based on composition analysis and relative abundance for each melanoma cell line.

	Observed m/z			Possible Structure	Averaged Relative abundance (n=3)					
	Charge:				SMU15-0404		SMU-092		SMU-059	
	-1	-2	-3		BSA	IFN	BSA	IFN	BSA	IFN
OLIGOMANNOSE	1235.4			 (Hex)2 + (Man)3(GlcNAc)2	3.6	2.5	1.1	0.8	3.4	20
	1397.5	698.2		 (Hex)3 + (Man)3(GlcNAc)2	4.2	3.7	0.2	0.1	8.5	5.8
	1559.6	779.3		 (Hex)4 + (Man)3(GlcNAc)2	9.2	8.1	1.9	2.8	10.3	7.5
	1721.6	860.3		 (Hex)5 + (Man)3(GlcNAc)2	9.2	10.6	0.3	0.2	2.0	7.2
		941.3		 (Hex)6 + (Man)3(GlcNAc)2	5.7	6.5	1.1	0.9	30.0	26.1
COMPLEX STRUCTURES	1260.5			 (HexNAc)1 (Deoxyhexose)1 + (Man)3(GlcNAc)2	0.1	0.2	0.6	0.2	0.1	0.1
	1463.6			 (HexNAc)2 (Deoxyhexose)1 + (Man)3(GlcNAc)2	0.2	0.2	0.2	0.2	0.1	0.2
	1713.7			 (Hex)1 (HexNAc)1 (Deoxyhexose)1 (NeuAc)1 + (Man)3(GlcNAc)2	0.1	0.2	1.2	0.3	0.0	0.0

1422.5				0.1	0.0	0.0	0.3	0.1	0.1
	1184.4			19.6	16.3	39.2	47.2	10.4	3.4
1875.9				0.1	0.2	0.4	0.1	0.0	0.1
	1038.9			5.0	4.1	0.2	0.2	0.7	0.1
1787.7	893.3			1.1	1.6	0.0	0.0	0.0	0.1
	1111.9			0.2	0.2	1.1	1.6	1.9	0.7
	1257.4			0.4	0.5	1.7	1.8	2.0	1.9
	965.8	1932.6		0.3	0.3	0.5	1.9	0.7	0.2
	1111.4			0.6	0.8	0.7	0.1	0.3	0.2

	1294.0		 <p>(Hex)3 (HexNAc)3 (NeuAc)2 + (Man)3(GlcNAc)2</p>	0.2	0.2	0.6	1.2	0.2	0.1
	1018.3		 <p>(Hex)3 (HexNAc)1 (Deoxyh exose)1 (NeuAc)1 + (Man)3(GlcNAc)2</p>	0.3	0.3	0.1	0.0	0.2	0.1
	1221.4		 <p>(Hex)3 (HexNAc)3 (Deoxyh exose)1 (NeuAc)1 + (Man)3(GlcNAc)2</p>	1.7	2.7	1.1	3.3	0.8	0.7
	1367.0		 <p>(Hex)3 (HexNAc)3 (Deoxyh exose)1 (NeuAc)1 + (Man)3(GlcNAc)2</p>	0.7	1.0	2.2	1.4	0.9	0.2
	1512.6		 <p>(Hex)3 (HexNAc)3 (Deoxyh exose)1 (NeuAc)3 + (Man)3(GlcNAc)2</p>	8.4	9.8	6.3	5.7	6.2	1.4
	1075.9		 <p>(Hex)3 (HexNAc)3 (Deoxyh exose)1 + (Man)3(GlcNAc)2</p>	0.7	0.8	0.1	0.2	0.0	0.1
	1367.5		 <p>(Hex)3 (HexNAc)3 (Deoxyh exose)3 (NeuAc)1 + (Man)3(GlcNAc)2</p>	0.9	1.4	1.8	1.4	3.0	2.8
	1731.2		 <p>(Hex)3 (HexNAc)3 (Deoxyh exose)4 (NeuAc)3 + (Man)3(GlcNAc)2</p>	0.1	0.1	0.5	0.4	0.0	0.0

	1439.5		 (Hex)3 (HexNAc)3 (NeuAc) 3 + (Man)3(GlcNAc)2	6.3	2.7	8.8	10. 6	6.5	4.4
	1549.6		 (Hex)4 (HexNAc)4 (Deoxyh exose)1 (NeuAc)2 + (Man)3(GlcNAc)2	1.9	2.6	7.0	5.4	2.2	1.6
	1695.2	1129.7	 (Hex)4 (HexNAc)4 (Deoxyhex ose)1 (NeuAc)3 + (Man)3(GlcNAc)2	1.3	1.3	2.8	1.2	0.6	0.4
	1840.8	1226.8	 (Hex)4 (HexNAc)4 (Deoxyh exose)1 (NeuAc)4 + (Man)3(GlcNAc)2	5.0	7.0	1.6	0.9	1.9	2.4
		1324.2	 (Hex)4 (HexNAc)4 (Deoxyh exose)3 (NeuAc)2 + (Man)3(GlcNAc)2	0.3	0.8	0.6	0.2	0.1	0.0
	1622.2		 (Hex)4 (HexNAc)4 (NeuAc) 3 + (Man)3(GlcNAc)2	0.1	0.1	0.4	0.4	0.0	0.1
		1251.4	 (Hex)5 (HexNAc)5 (Deoxyh exose)1 (NeuAc)3 + (Man)3(GlcNAc)2	0.2	0.3	0.9	0.7	0.1	0.1
		1348.5	 (Hex)5 (HexNAc)5 (Deoxyh exose)1 (NeuAc)3 + (Man)3(GlcNAc)2	0.5	1.2	0.5	0.3	0.4	0.2

			(Hex)5 (HexNAc)5 (Deoxyhexose)1 (NeuAc)4 + (Man)3(GlcNAc)2							
	1877.9		 <p>(Hex)5 (HexNAc)5 (Deoxyhexose)3 (NeuAc)2 + (Man)3(GlcNAc)2</p>	0.0	0.0	0.2	0.3	0.0	0.1	
		1348.8	 <p>(Hex)5 (HexNAc)5 (Deoxyhexose)3 (NeuAc)3 + (Man)3(GlcNAc)2</p>	0.8	0.9	0.7	0.3	0.7	0.2	
		1373.2	 <p>(Hex)6 (HexNAc)6 (Deoxyhexose)1 (NeuAc)3 + (Man)3(GlcNAc)2</p>	0.1	0.6	0.5	0.4	0.1	0.1	
		1470.2	 <p>(Hex)6 (HexNAc)6 (Deoxyhexose)1 (NeuAc)4 + (Man)3(GlcNAc)2</p>	0.5	0.5	0.4	0.3	0.5	0.2	